

THE UNIVERSITY OF ZAMBIA
SCHOOL OF MINES

Department of Mining Engineering

**AN IMPROVED SUPPORT SYSTEM FOR SAFE AND ECONOMICAL
UNDERGROUND EXCAVATION; A CASE STUDY OF MINDOLA
DEEPS SECTION, ZAMBIA**

By

Noble Chifwaila

**A dissertation submitted to the University of Zambia in partial fulfilment of
the requirement for the award of Master of Mineral Sciences Degree in
Mining Engineering (M. Min. Sc.)**

November 2017

Declaration

I, **Noble Chifwaila**, do hereby declare that this work was produced by me, with valuable assistance from various people from Mopani Copper Mines Plc., and the University of Zambia, School of Mines. I, therefore, declare that, to the best of my knowledge, this document ably supervised by Professor Mutale. W, Chanda, assisted by Professor Radhe Krishna has never been submitted anywhere else except to the University of Zambia for the award of the degree of Master of Mineral Science (M. Min. Sc.). All works of other researchers have been duly acknowledged.

Signature:

Date:

Approval

This dissertation of Noble Chifwaila is approved as a partial fulfilment of the requirement for the award of the degree of Master of Mineral Science in Mining Engineering by the University of Zambia.

Supervisor: Professor Mutale Chanda

Signature:

Date:

Co-Supervisor: Professor Radhe Krishna

Signature:

Date:

Internal Examiner:

Signature:

Date:

Internal Examiner:

Signature:

Date:

External Examiner:

Signature:

Date:

Dedication

This work is dedicated to my wife Mercy Kaenga Chifwaila, my son Noble Chifwaila and my daughter Mercy Mapalo Chifwaila. Without their input and assistance, it would not have been possible with the existing challenges we have had to undergo. Your input has yielded fruit and will always be appreciated. Thank you so much.

I would further and most importantly acknowledge our father, God almighty for guiding me through the journey and his endless provision during this study. It is clear that a workman can work but without the lord, it's in vain, (**Psalms 127: 1**) **“Except the Lord builds the house, they that labour in vain that build it: except the Lord keep the city, the watchman watches but in vain.”** Thank you Lord.

Abstract

Mopani Copper Mines Plc. (MCM) is sinking a vertical rock and man shaft. The rock hoisting winder will handle 2.0 million tonnes of ore per annum. The project will significantly boost the current productivity of Mindola Mine, as it will enable the company to increase ore production from 800 thousand tonnes to 1.4 million tonnes in the Deeps section. Currently, the Deeps mining method employs up dip Vertical Crater Retreat method with waste rock as back fill material. The method has posed huge challenges in as far as excavation stability problems are concerned. Stability problems range from rock falls between support units to collapse of Vertical Crater Retreat chambers and Ventilation drives. These problems lead to equipment damage, injuries, loss of reserves, loss of tipping space, loss of ore production and disturbance in the ventilation network. The methodology used in this research work involved geotechnical data acquisition, Data analysis and Geotechnical designs. Geotechnical raw data was collected by conducting underground joint survey and core logging. Underground joint survey involved line mapping of joints and window mapping. The output of this exercise was joint spacing, joint orientation and joint condition. Rock samples collected were tested for Point load Index using a Point Load Equipment for the calculation of Intact Rock Strength. Other tools used in data collection were a 30m measuring tape, a Geotechnical compass, a Schmidt hammer, a Clino rule and a Point Load machine. The raw data was evaluated to obtain inputs into geotechnical designs. The methods of analysis included Joint analysis, Rock mass classification and Rock mass stability number. During Joint analysis, the dip and dip direction of joints from mapping were entered into the DIPS Program to determine the number of joint sets and their dip and dip directions. The rock mass quality was determined by using the Rock Mass Rating and the Q system. The Rock Mass Stability number was also determined using the raw data. Geotechnical designs were then carried out for the purpose of

establishing the loads that were induced on excavations and determine the support required to counter the loads so as to ensure stability of the excavations. The design methods involved the use of empirical and numerical methods. The empirical methods included Potvin's stability graph method for the estimating the stable span of Vertical Crater Retreat chambers and Grinstad/Barton graph method for estimating the support requirements. Mining simulations using Phase 2 and Examine tab numerical modelling programs were carried out. The research recommends measures to improve the stability of Vertical Crater Retreat chambers and Ventilation drives. Among them are, mining the Ventilation drives at not less than 48 meters from the geological footwall contact, mining the Vertical crater retreat chambers at 25.25 meters strike length and supporting them with 6 meters cable bolts and fibre reinforced shotcrete. Furthermore, adopting of a steeper stoping echelon is also recommended. This research gives the details of the problems of excavation instability, research methodology used to combat them and finally the way forward for better stability with economic benefits.

Acknowledgement

It is with heartfelt gratitude and pleasure that I acknowledge all the people who contributed to the successful completion of this dissertation. Without their effort, this work could not have been completed successfully.

Special thanks go to individuals who particularly took their time to ensure that all information and data provided was up to the required standards. It would be impractical to list all of them but the most significant contributions were made by my supervisors Professor Mutale W. Chanda and Professor Radhe Krishna. I am very grateful for the continued encouragement and guidance; I would not have accomplished this work without you. I am very grateful to you Professors.

I would also like to acknowledge Mr Beza Mwanza Chief Engineer (Mining Eng.) from the University of Zambia for his contributions and comments he provided to improve this dissertation.

Further acknowledgement goes to the Mopani Copper Mines Plc. Management; Mr Andrew Phiri, Mr Harry Yashini, Mr Yudah Mulemi, the entire Nkana Rock Mechanics team and Open House Management Solution Consultants for the assistance and training rendered to me during the study.

Finally, I would like to acknowledge my family for their patience, sacrifice and understanding during this period. The road has been tough through thin and thick but you stood by my side. You have added a dimension to my life and because of this; I guarantee you a special place in my heart.

Table of contents

Declaration / i

Approval / ii

Dedication / ii

Abstract / iv

Acknowledgement / vi

Table of contents / vii

List of Figures / ix

List of Tables / xii

Chapter 1 INTRODUCTION / 1

- 1.1 Preamble / 1
- 1.2 Location and Description of the Research Site / 2
- 1.3 Geology / 3
 - 1.3.1 Regional Setting / 3
 - 1.3.2 Stratigraphy of the Zambian Copperbelt / 4
 - 1.3.3 Katangan Super Group / 6
 - 1.3.4 Copper and Cobalt mineralization / 9
 - 1.3.5 Property Geology / 9
 - 1.3.5.1 Structure / 10
 - 1.3.5.2 Mindola Stratigraphy / 12
 - 1.3.5.3 Mineralization / 15
 - 1.3.5.4 Mineral Zoning / 16
 - 1.3.5.5 Barren Gaps / 18
- 1.4 Problem Statement / 18
- 1.5 Research Questions / 19
- 1.6 Research Objective / 20

- 1.7 Sub Objectives / 20
- 1.8 Methodology / 20
- 1.9 Significance of the Research / 21

Chapter 2 LITERATURE REVIEW / 22

- 2.1 Introduction / 22
- 2.2 Geotechnical designs / 22
 - 2.2.1 Excavations and Structures / 22
- 2.3 Design methods / 23
 - 2.3.1 Empirical methods / 23
 - 2.3.2 Numerical support design methods / 34

Chapter 3 BASICS OF SUPPORT DESIGN / 37

- 3.1 Introduction / 37
- 3.2 Empirical Cable Bolt Design / 38
 - 3.2.1 Cable bolt length / 38
 - 3.2.2 Cable bolt density (bolts/m² of face) and spacing / 39

Chapter 4 geotechnical DATA COLLECTION and analysis / 42

- 4.1 Geotechnical data acquisition / 42
- 4.2 Analysis of Geotechnical data / 42

Chapter 5 geotechnical designs / 47

- 5.1 Stability of the Vertical Crater Retreat chamber / 47
 - 5.1.1 Stable span of the Vertical Crater Retreat chamber / 47
 - 5.1.2 Secondary support requirements / 49
 - 5.1.3 Cable bolt specification / 51
 - 5.1.3.1 Cable bolt length / 51
 - 5.1.3.2 Bolt density / 51
 - 5.1.3.3 Support Patterns and Cost Comparison / 52
 - 5.1.3.3.1 Support Patterns / 52
 - 5.1.3.3.2 Cost comparison / 53
- 5.2 Numerical Modelling / 54

5.2.1	Location of the Ventilation drive in relation to the ore body (Phase 2 – stress analysis) /	56
5.2.2	Stoping echelon (Examine ^{tab} – Stress analysis) /	64
5.2.2.1	Examine ^{tab} Results at no lead/ lag distance /	64
5.2.2.2	Examine ^{tab} Results at 30m lead/ lag distance /	67
5.2.2.3	Examine tab Results at 120m lead/ lag distance /	69

Chapter 6 Conclusions and recommendations / 74

6.1	Conclusions /	74
-----	---------------	----

6.2	Recommendations /	75
-----	-------------------	----

REFERENCES /	77
--------------	----

APPENDICES /	82
--------------	----

Appendix A: Proposed stoping echelon and mining sequence /	82
--	----

Appendix B: Geotechnical and structural data collection log sheets /	83
--	----

Appendix C: Rock Mass Rating System /	89
---------------------------------------	----

Appendix D: Phase 2 analysis information /	91
--	----

Appendix E: Mindola Sub Vertical Shaft Succession /	96
---	----

Appendix F: Procedure for Mining and Supporting the Vertical crater Retreat (VCR) chamber /	97
---	----

Appendix H: Joint Survey collected data /	101
---	-----

List of Figures

Figure 1.1 Location of the new shaft at Mindola Mine /	2
--	---

Figure 1.2 Location map of Kitwe city /	3
---	---

Figure 1.3 Geological map of the Zambian Copperbelt showing the Katangan sedimentary Rocks Exposed on the Flank of the Kafue Anticline and the Major Towns and Mines of the Region /	5
--	---

Figure 1.4 Stratigraphy of the Zambian Copperbelt /	6
---	---

Figure 1.5 Stratigraphic Correlation of the Lower Roan Group of the Katangan Supergroup on the Western Flank of the Kafue Anticline, Including a Comparison with the Mufulira Deposit on the Eastern Side / 8

Figure 1.6 Nkana Mine Site Geology / 11

Figure 1.7 Mindola Stratigraphy / 13

Figure 1.8 Mineralised Argillite at Mindola Mine / 16

Figure 1.9 Banded Ore, light whitish grey on the left in contact with Khaki brown Cherty Ore on the right / 17

Figure 1.10 Showing equipment damaged by a rock in the Vertical Crater Retreat chamber / 19

Figure 2.1 Estimated support categories based on the tunnelling quality index Q / 29

Figure 2.2 Rock Stress Factor 'A' (Potvin, 1988) for Stability Graph analysis / 31

Figure 2.3 Stability graph showing zones of stable ground, caving ground and ground required support / 33

Figure 2.4 UNWEDGE Analysis: (A) Wedges formed surrounding a tunnel; (B) Support installation / 35

Figure 3.1 Bolt lengths in current practice (after Lang and Bischoff, 1984) with adjustment for cable bolt application (relationships are for S.I. units) / 39

Figure 3.2 Potvin/Nickson guidelines for cable bolt density to control local unravelling / 40

Figure 3.3 Guidelines for cable spacing and density - overall stope face stability / 41

Figure 5.1 Mathews/Potvin stability graph /48

Figure 5.2 Grimstad and Barton's graph /50

Figure 5.3 Potvin/Nickson cable bolting graph (Guidelines for cable bolt density to control local unravelling) / 51

Figure 5.4 Section of a Vertical Crater Retreat chamber with cable bolts installed in a ring / 52

Figure 5.5 Section of the proposed cable bolt support pattern / 53

Figure 5.6 Model set up showing mesh, the orebody and location of foot wall developments on various levels / 56

Figure 5.7 Phase2 results showing variation of virgin stress levels with depth (prior to mining out) / 57

Figure 5.8 Section showing stress levels as VCR blasting advances upward at early stages of up dip mining / 58

Figure 5.9 Excessive stress loading around the ventilation drive as stope blasting progresses up dip / 59

Figure 5.10 Levels of strength factors in the early stages of stoping between 5220 FT level and 5045 FT level / 60

Figure 5.11 Strength factor levels in the late stages of stoping between 5220 FT level and 5045 FT level / 61

Figure 5.12 Levels of strength factors in the late stages of stoping on 5045 FT level / 62

Figure 5.13 Strength factor levels in the late stages of stoping between 4881 FT level and 4716 Ft level / 63

Figure 5.14 No lead/lag, contours of stress levels. Note very high stress levels in the corner of the block not mined / 65

Figure 5.15 Volume of stressed ground when there is no lead/lag / 66

Figure 5.16 Contours of normal stress levels at 30m lead/lag / 67

Figure 5.17 Volume of stressed ground with short lead/lag distance / 68

Figure 5.18 Contours of stress levels at 120m lead/lag / 70

Figure 5.19 Volume of stressed ground with long lead/lag distance (120m) / 71

Figure 6.1 Proposed Stopping Echelon (58o) and Mining sequence / 82

Figure 6.2 Geotechnical logging sheet / 83

Figure 6.3 Structural data collection sheet / 88

Figure 6.4 A ring of cable bolt support in a Vertical Crater Retreat (VCR) chamber / 98

Figure 6.5 A ring of cable bolt support in a Vertical Crater Retreat (VCR) chamber / 99

List of Tables

Table 2.1 Rock mass classifications, shear strength estimation and average stand - up time for unsupported excavation / 26

Table 2.2 Rock mass quality types after Q values / 28

Table 2.3 Range of values (for hard rock mining) / 33

Table 4.3 Geotechnical parameters used in the calculation of the Q' value / 45

Table 5.1 Analysis of cable bolt support cost in a ring (Current cable bolt support pattern) / 53

Table 5.2 Analysis of cable bolt support cost in a ring (Proposed cable bolt support pattern) / 54

Table 6.1 Rock Mass Rating System / 89

Table 6.2 Geotechnical parameters of different rock formations at Mindola's Deeps section / 96

CHAPTER 1

INTRODUCTION

1.1 Preamble

Mopani Copper Mines Plc. (MCM) is a Zambian registered company located in the Copperbelt Province of Zambia. The company is owned by Glencore International AG (73.1% shares), First Quantum Minerals Ltd (16.9% shares) and ZCCM Investments Holdings Plc. (10% shares).

Mopani's operations consist of four underground mines, a concentrator and a cobalt plant in the Nkana Mine site and an underground mine, a concentrator, a smelter and refinery in the Mufulira Mine site.

Mopani is sinking one rock and man shaft at Mindola mine in order to increase its productivity and reduce operating costs associated with the existing old infrastructure. The new rock and man shaft, which is located in proximity to the already operational Mindola Mine shaft, has a diameter of 6.1 meters and extends 1,940 meters from surface. In terms of capacity, the rock hoisting winders for the new shaft will handle 2.0 million tonnes per annum. This project will significantly boost the current productivity of Mindola Mine, as it will enable the company to increase ore production from 800 thousand tonnes to 1.4 million tonnes in the Deeps section (Mindola SV Mine, New Shaft Project Report, 2012). Figure 1.1 shows the site location of the new shaft relative to surrounding existing structures.

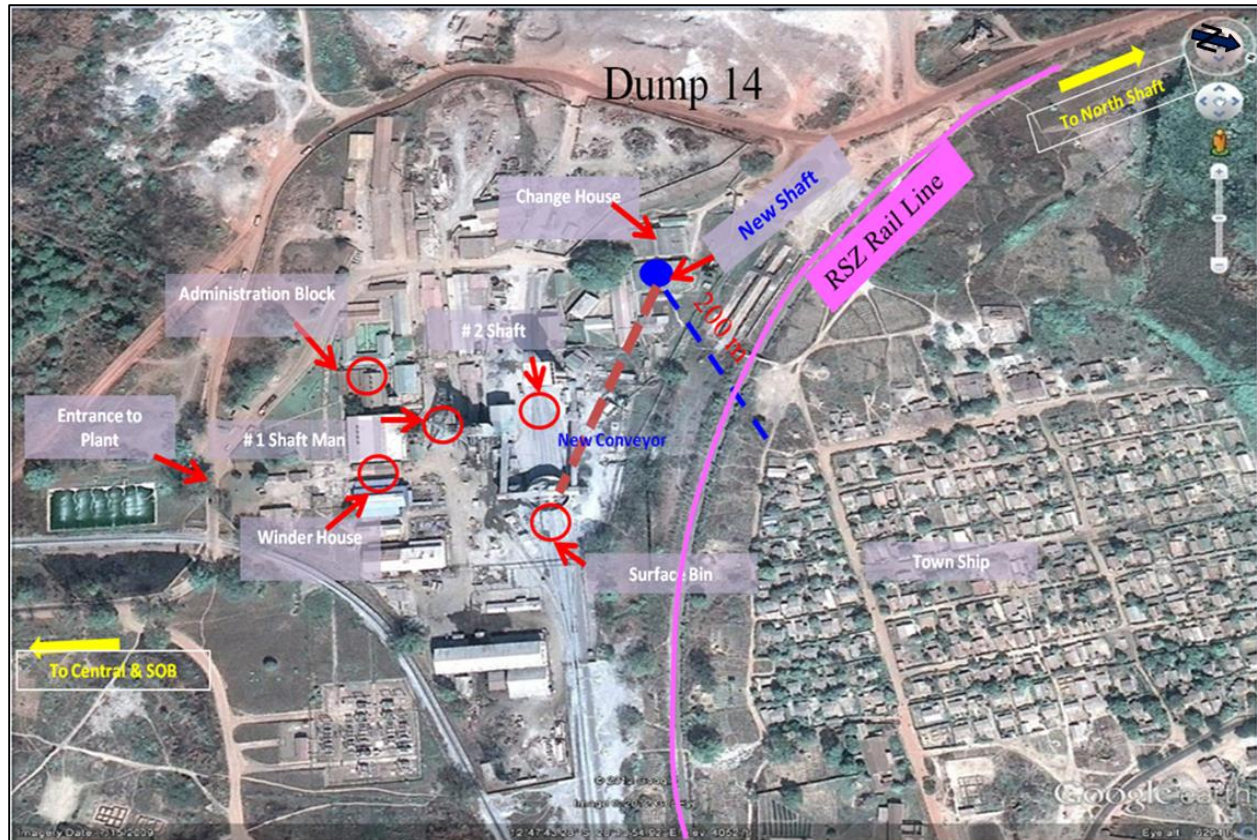


Figure 1.1 Location of the new shaft at Mindola Mine, (Mindola Technical Office, 2012)

The new shaft project is scheduled for completion in 2018 and will extend the life of Mindola Mine by at least 10 years.

Mindola Mine is currently producing from two sections which are the Upper section and the Deeps section. However, the reserves in the Upper section have almost been depleted and the focus now is to produce from the Deeps section, where the mine life lies. The Deeps section is where this project was undertaken.

1.2 Location and Description of the Research Site

Mindola Mine is situated at Nkana Mine site of Mopani Copper Mines Plc., and is located on the Zambian Copperbelt Province in the city of Kitwe as shown in Figure 1.2.



Figure 1.2 Location map of Kitwe city (Mindola Technical Office, 2012).

1.3 Geology

1.3.1 Regional Setting

The Zambian Copperbelt (Figure 1.3) forms the south eastern part of the 900km-long Neoproterozoic Lufilian Arc, a Pan-African fold belt (approximately 550Ma) that extends northwards into the Democratic Republic of Congo (Cahen and Snelling, 1966; Clifford, 1967, Daly et al., 1984; Porada and Berhorst, 2000) and links with the Damara Belt of Namibia (Hunter and Pretorius, 1981; Unrug, 1983; Coward and Daly, 1984). This fold belt contains the Precambrian sediments of the Katangan Super group and the majority of the copper-cobalt deposits

of Zambia and the D.R.C. (Daly et al., 1984). The Lufilian Arc is bounded to the northwest by the Kasai Shield; to the north and northeast by the Kibaran Belt and Bangwelu Block; to the east by the Irumide Belt of Kibaran age (1300-1000Ma); and to the south by the Mwembeshi Shear Zone (Ackermann and Forster, 1960; De Swardt and Drysdall, 1964; Unrug, 1983; Porada and Berhorst, 2000). The western boundary is covered by post-Katangan sediments (Unrug, 1983). The Zambezi Belt was defined by Unrug (1983) as “the region south of the Mwembeshi Shear zone and north of the Zimbabwe Craton not affected by Pan-African tectono-thermal processes.” The Lufilian Arc is reported to have formed during the collision of the Angola-Kalahari and Congo-Tanzania Plates and accompanying NE-directed thrusting at 560-550Ma (Porada and Berhorst, 2000). The Mwembeshi Shear zone has been interpreted by some previous authors as the structure that separates the two plates (Unrug, 1983; Daly, 1986; Kampunzu and Cailteux, 1997), although this is rejected by Porada and Berhorst (2000).

1.3.2 Stratigraphy of the Zambian Copperbelt

The stratigraphy of the Zambian Copperbelt is summarized in Figure 1.4. The Basement Complex consists of the Lufubu System (the oldest rocks of the Copperbelt area), the Muva System (rarely exposed on the Copperbelt) overlying the Basement, and granitic rocks which intrude the Lufubu but are mostly older than the Muva, with the exception of the Nchanga Red Granite (Mendelsohn, 1961; Fleischer et al., 1976). The lowermost units of the Katangan Super group (Lower and Upper Roan Groups of the Mine Series) are exposed in mines and rare outcrops, whereas the Kundulungu sedimentary rocks only occur locally on the Copperbelt (Mendelsohn, 1961). The Lower Roan Group, the dominant ore-bearing sequence, occurs in structural basins, separated by outcropping pre-Katangan basement highs (Cailteux et al., 1994), where the sediments rest with an angular unconformity on the granites and schists of the Basement Complex.

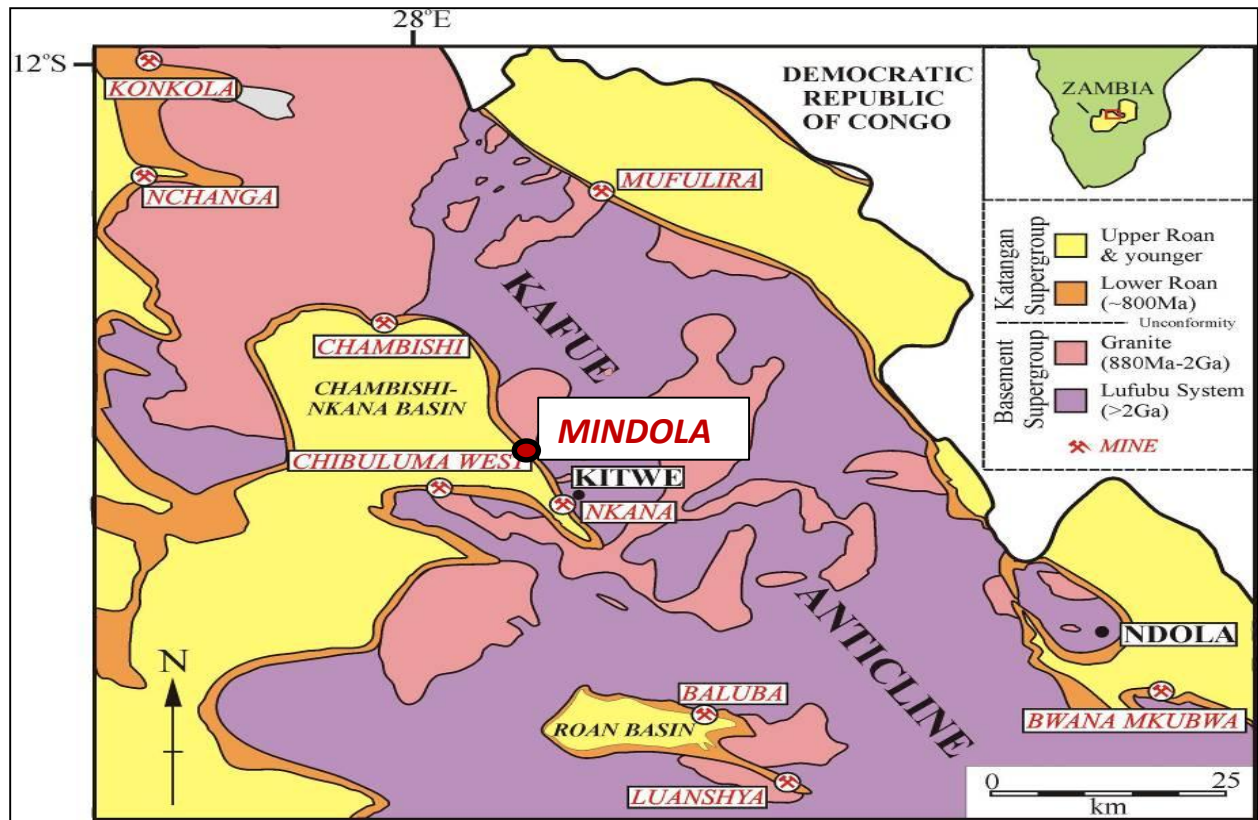


Figure 1.3 Geological map of the Zambian Copperbelt showing the Katangan sedimentary Rocks Exposed on the Flank of the Kafue Anticline and the Major Towns and Mines of the Region (modified from Fleischer et al., 1976).

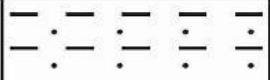
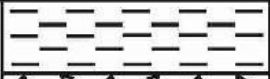

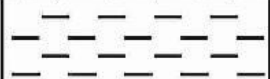
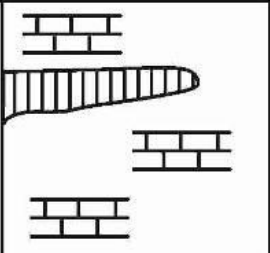
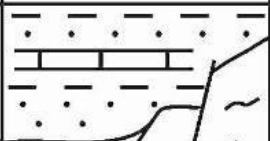
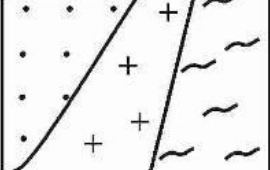
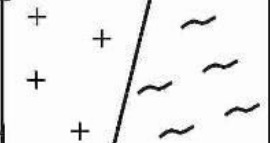

KATANGAN SUPERGROUP	Kundulungu Series	Upper	Shale & quartzite	
		Middle	Shale Tillite	
		Lower	Shale Dolomite & shale Tillite	
	Mine Series	Mwashia	Carbonaceous shale & argillite	
		Upper Roan Group	Dolomite & argillite Argillite & arenite	
		Lower Roan Group	Shales & argillites micaceous, dolomitic arenites footwall arkose Conglomerate	
				Unconformity
BASEMENT COMPLEX	Muva Supergroup		Quartzites & meta-pelitic rocks	
	Granite		Red & grey microcline granites	
	Lufubu System		Quartz-mica schists micaceous quartzites & gneiss (intruded by granites)	

Figure 1.4 Stratigraphy of the Zambian Copperbelt (modified from Fleischer et al., 1976).

1.3.3 Katangan Super Group

The sediments of the Katangan Super group are well described in the available literature compared with the rocks of the Basement Complex, in particular the Lower and Upper Roan Groups of the Mine Series, which are the hosts to all the major occurrences of copper and cobalt. The maximum age for the Katangan is constrained by the U-Pb 877 ± 11 Ma age of the Nchanga Red Granite;

zircons in the overlying basal arkoses have been dated at 880 Ma and 1800-2000 Ma suggesting that the Roan was derived from the Nchanga Red Granite or correlatives as well as from older basement (Armstrong et al., 1999). The Mine Series, ranging in thickness from 800m to 2000m, has a well-defined sequence. This passes upwards from basal continental clastics (deposited in response to marine incursion across a continental landscape) to accumulations of shallow argillaceous marine clastics to mixed carbonate platform sequence (mainly dolomitic units) and finally to the carbonaceous shales of the Mwashia Group (Mendelsohn, 1961; Simmonds, 1998). The trend of palaeo-shorelines has been interpreted as NW-SE from studies at Luanshya and Chambishi (Garlick, 1961b) and Mufulira (Van Eden and Binda, 1972). The upper units of the Katanga Super group, preserved in deeper parts of the basins (away from mines), are less well known.

The Lower Roan Group of rocks that host the copper and cobalt of the Zambian Copperbelt has in the past been subdivided into five formations: the 'Footwall Formation,' the 'Ore Shale,' the 'Hanging wall Formation,' the 'Chingola Dolomite' and the 'Shale with Grit' Formation (based on observations made at Luanshya Mine by Binda and Mulgrew (1974), although recognized at each Copperbelt deposit. The Lower Roan is then conformably overlain by the dolomites and dolomitic shales of the Upper Roan Group and the black carbonaceous shales of the Mwashia Group (Cailteux et al., 1994). It must be kept in mind that these formation names are mining terms and do not necessarily represent the true lithology. Binda (1994) alternatively subdivided the Lower and Upper Roan Groups into three lithostratigraphical divisions and this report uses this subdivision to avoid use of misleading mining terms: the Siliciclastic Unit (equivalent to the 'footwall formation'); the Mixed Unit (equivalent to the 'ore-shale'); and the Carbonate Unit (all units overlying the 'ore-shale' but below the Mwashia Group). In addition to the main lithologies,

anhydrite is common, both as lenses and scattered beds within the Lower Roan sediments (in particular within the Mixed Unit).

Although the stratigraphy has been described in detail for individual deposits, often using different terms to describe units, Binda and Mulgrew (1974) presented a detailed correlation of the Lower Roan units on the western side of the Kafue Anticline, and Binda (1994) and Binda and Mulgrew (1974) correlated these with the Lower Roan at Mufulira on the eastern side (see Figure 1.5). The result is that the inter-deposit sequence of the Lower Roan appears to correlate well, if the stratigraphic classification of units at each deposit is correct. The variable thickness of the Siliciclastic Unit, where near palaeo-highs may be thin and may contain only one conglomerate unit, but further away may be several hundred metres thick and contain up to three conglomerate units.

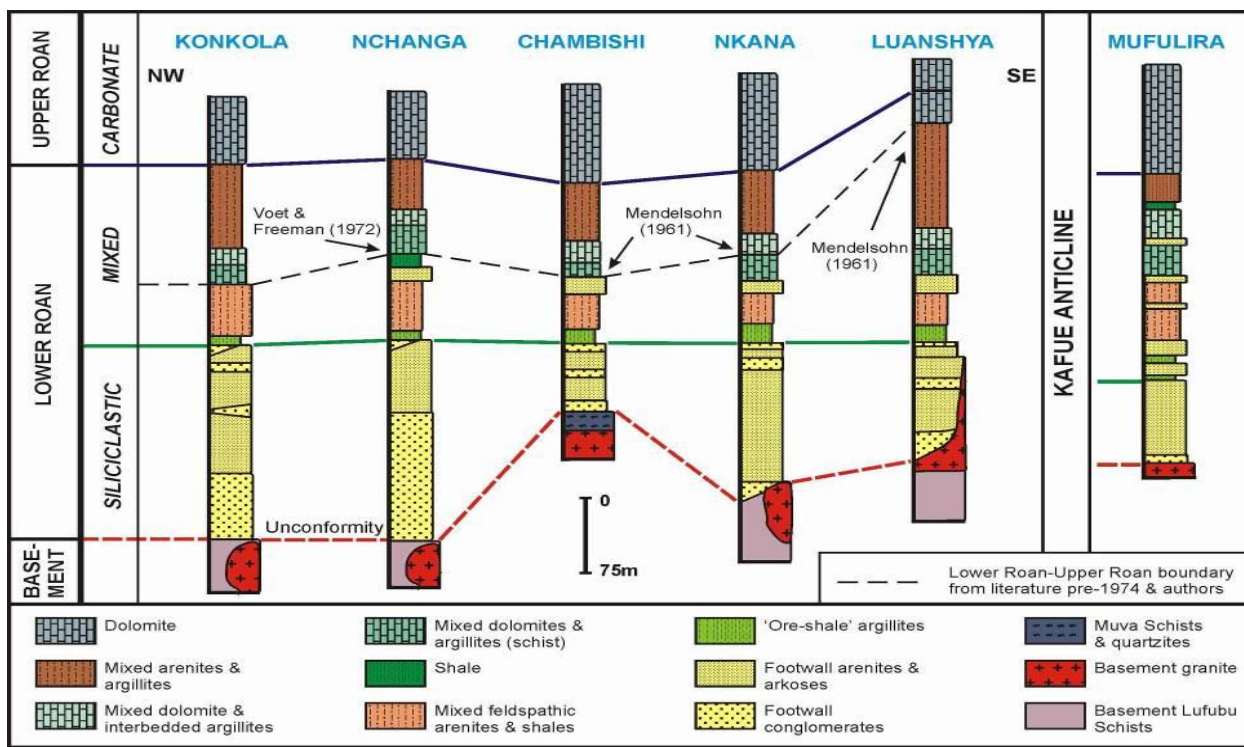


Figure 1.5 Stratigraphic Correlation of the Lower Roan Group of the Katangan Supergroup on the Western Flank of the Kafue Anticline, Including a Comparison with the Mufulira Deposit on the Eastern Side (modified from Binda & Mulgrew, 1974 and Binda, 1994).

1.3.4 Copper and Cobalt mineralization

The Zambian-Congo Copperbelt, one of the world's great copper metallogenes, coincides with the Lufilian Arc, a major fold thrust belt developed between 600 and 500 million years b.p. (Binda and Mulgrew, 1974). This belt contains both Late Proterozoic Katangan meta-sediments and Mid Proterozoic basement, together forming a complex, thrust dominated tectonostratigraphy, perhaps most of which is allochthonous.

The principal ore deposits occur within the Roan Super group of the lower Katangan succession which comprises a basal siliciclastic group, overlain by a mixed siliciclastic and carbonate group, and finally by a carbonate group. The boundary between the siliclastic and mixed groups is the main site of mineralization, with ore occurring in both the clastic rocks (Footwall ore) and the overlying dolomitic schists (Ore Shale Formation). This site represents a high strain zone marked by layer parallel shearing, which in some cases has progressed to decollements, and mineralization is now believed to have been introduced during this shearing event. Most of the major deposits in Zambia occur on one limb of NW plunging synclinal or anticlinal features, presumably representing focusing of ore fluids into favourable structural traps. Mineralization, which is accompanied by carbonate and biotite alteration, occurs as chalcopyrite and bornite disseminations and stringers, and as quartz or dolomite copper sulphide veinlets. Carrollite and Cobaltiferous pyrite are the principal cobalt minerals.

1.3.5 Property Geology

Mindola Shaft is on the eastern part of northwesterly plunging Synclinorium, which is part of the Chambeshi- Nkana basin located on the southwestern flank of the Kafue Anticline. The Kafue Anticline forms part of the southern end of the 800 km long Lufilian fold belt.

The stratigraphic sequence within the syncline comprises shales, arenites and dolomitic horizons of the Lower and Upper Roan groups unconformable overlying the Basement Complex. The Basement is divisible into an assemblage of meta-sediments, assigned to the Lufubu System, and a suite of igneous rocks including granitoid gneisses and intrusive and segregation pegmatites.

Very little of the Mwashia Group which overlies the Roan Super Group is known at the Mine site. Only the lower part is known and consists of conglomerates, argillites, and shaly dolomites. The Post-Katanga intrusive rocks comprise of quartz-carbonate veins, sills, dykes and irregular bodies of metabasic rocks.

Copper and Cobalt mineralization occur within the ore shales of the Lower Roan Group.

The copper mineralization is a mixture of chalcopyrite- bornite, while the cobalt mineralization is Carrolite and cobaltiferous pyrite in approximately equal proportions. Oxides and mixed oxide and sulphides occur near the upper parts of the mine which form the oxide caps. The major oxide minerals are crysocola, malachite and pseudo malachite, cuprite, tenorite, small amounts of azurite and libethenite.

1.3.5.1 Structure

The predominant mega-structure of Nkana Mine Site is the northwest-plunging Nkana syncline (see Figure 1.6). This structure is asymmetric, with a curved axial plane inclined steeply to the northwest in the trough of the syncline but upright to westward dipping at higher structural levels.

As a result of the northwesterly plunge of the Nkana syncline, the present land surface represents a horizontal section through progressively higher structural levels of the syncline from southeast to northwest. Similarly, current underground mining operations at South Orebody Shaft are located along the northeastern edge of the folded axial zone whereas at Central, Mindola and North Shafts

these operations are mainly in the relatively undeformed steep to shallow-dipping northeastern flank of the Nkana syncline.

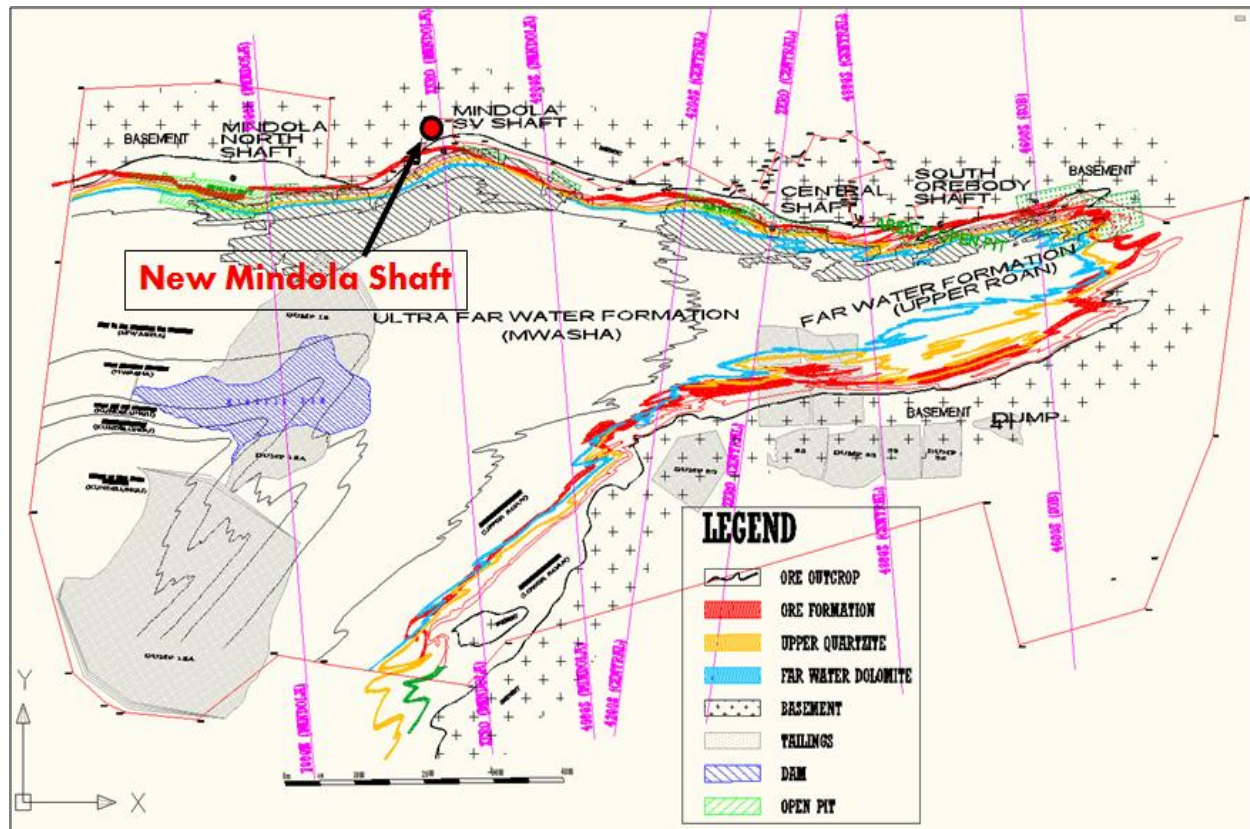


Figure 1.6 Nkana Mine Site Geology (Mindola Technical Office, 2012)

Outside the working areas, surface mapping and diamond drilling from both underground and surface provide the basis for structural interpretation. Even so, the structure of the deeper parts of the syncline, particularly from the Kitwe Barren Gap northwards, is little known.

Within the axial zone of the Nkana syncline, shear folding is characteristic of the deformation style of the Lufilian Orogeny, with transposed bedding attenuated to sheared-out folds limbs, axial swelling and chevron structures being developed. The structures indicate thrusting directed towards the northeast, with decollement present at the Basement/Lower Roan and Footwall

Formation/Ore Formation boundaries. In addition, the Basement Complex adjacent to the Lower Roan cover has been sheared with refoliation developed parallel to the axial planes of the folds in the Katanga rocks. During the early stages of deformation, open symmetrical folds such as the C anticline at South Orebody Shaft and the Zero Anticline at Central Shaft, were formed. As shearing stress built up, these earlier structures were modified; in some cases substantially. Post-shearing effects such as reversals of fold plunges, trans-current movements, faulting and kink zones are probably related to the late-tectonic up-doming of the Kafue anticline as the Katanga cover rocks adjusted themselves to essentially vertical movements between blocks of different competency within the underlying basement. In places, for example at 4800S (SOB), there is evidence to suggest that the late-tectonic vertical movements have accented the pre-Katanga palaeo-topography, which itself has influenced the deformation by the buttressing effect produced by the granite gneiss palaeo-hills.

At Mindola, below 1380L the dip increases to about 45° and increases both southwards to the dyke at 1300N and with increasing depth, locally it reaches about 70°. South of the dyke, the dip becomes steep to over-turn and assumes a maximum reverse value of 75° at 5660S. Dewatering and exploration drilling in the area between 2330S and 5000S have indicated folding of the Hanging wall Beds. This folding and the reversal of dip in the far south of Mindola is probably related to the buttressing effect of the Kitwe Barren Gap combined with the axial zone deformation where it plunges northwards through the barren gap from Central Shaft area.

1.3.5.2 Mindola Stratigraphy

At Mindola and the northern part of Central Shaft, the Ore Formation comprises eight members reflecting three cycles consists of a lower Dolomitic phase and an upper silty phase, as shown in the following table based on the southern part of Mindola Mine. The whole sequence represents a

series of alternating tidal flats and sub tidal regressive and transgressive phases as shown in Figure 1.7.

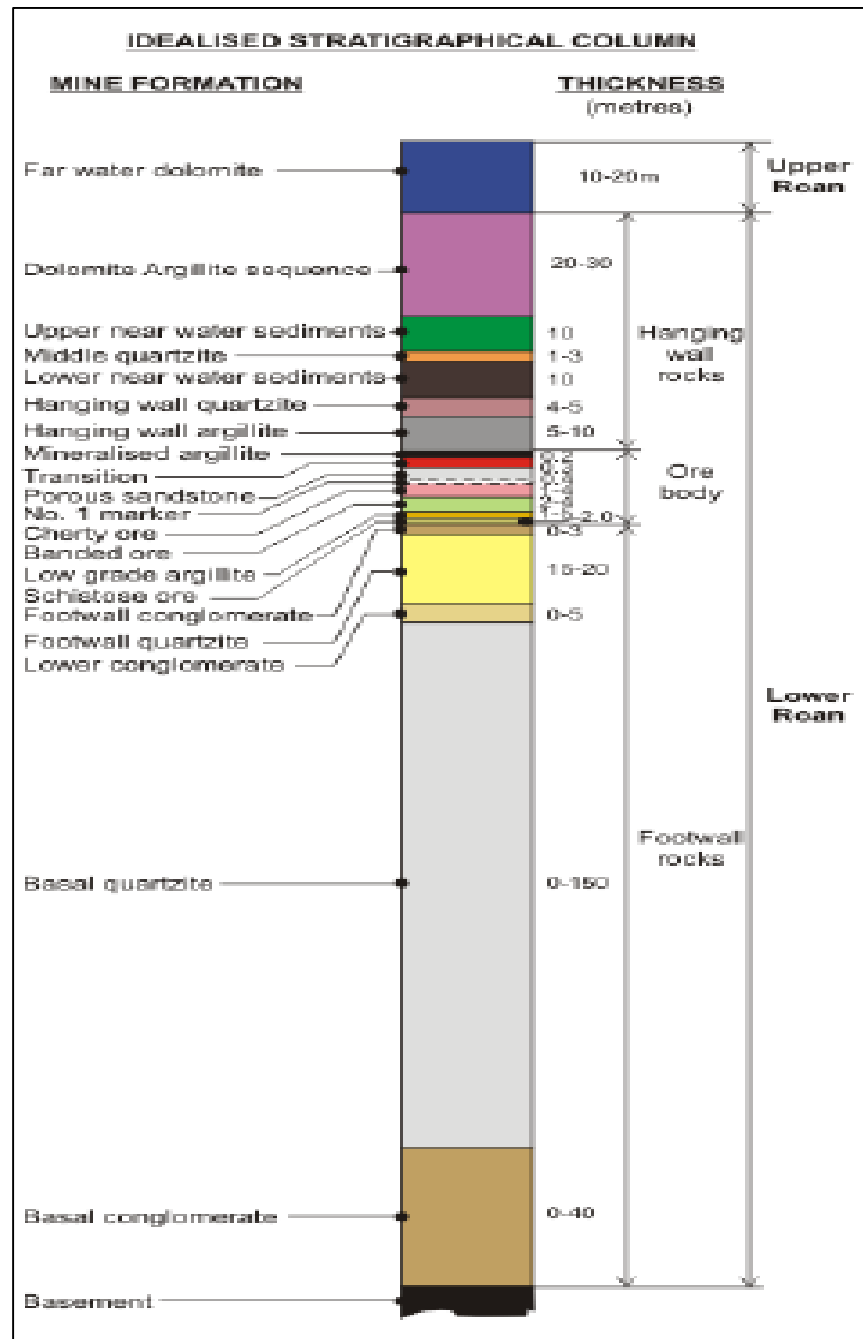


Figure 1.7 Mindola Stratigraphy (Mindola Technical Office, 2012)

The salient features of the members are described below;

The Schistose Ore: The Schistose Ore is two meters thick and forms the base of the Ore Formation. It consists of laminated white Dolomites and schistose Dolomitic Argillite, locally carrying blebs of Dolomite and Anhydrite.

The Low Grade Argillite: The Low Grade Argillite is two meters thick and is a massive, grey Dolomitic Mudstone with patches of purer Dolomite in places.

The Banded Ore: Banded ore is two to four meters thick Dolomite and Argillite, which locally exhibit small-scale slumping, load casting and washouts.

The Cherty Ore: The cherty ore is one to four meters thick. It is a tough, massive grey Argillite with sparse white Dolomite laminae near its base. In its upper portion Dolomite spots and shrinkages cracks are developed.

Number 1 Marker: The number 1 Marker is 0.5m thick and can be traced through much of the Mindola and Central shaft areas. It has not been recognized in Mindola open pit and parts of the North Shaft area underground. It comprises a laminated sequence of Dolomite and Argillite locally rich in anhydrite. Laterally it changes to a bedded Dolomite- Anhydrite rock.

Porous Sandstone: The Porous Sandstone is up to four meters thick but may be absent. The name is an old mining term and is lithologically incorrect. The member varies from a massive, khaki siliceous Dolomite through a Dolomite anhydrite rock to a massive algal dolomite with stromatolitic growth forms, which are well developed on the north side of Mindola. Desiccation cracks and anhydrite are common throughout the unit.

Mineralised Argillite: The Mineralized Argillite is up to 10 meters thick. It is generally a massive Argillite with Dolomite streaks and spots in places. Locally the member is a grey cherty Argillite with white Dolomite bands.

Hanging wall Argillite: The Hanging wall Argillite is 5 to 10 meters thick. It is not part of the Orebody, but marks the top of the Formation. The member comprises a grey Dolomitic-Argillite or siltstone, locally rich in Dolomite spots and Anhydrite blebs, which coarsen upwards towards the overlying hanging wall Quartzite.

1.3.5.3 Mineralization

In the underground workings, the main copper or minerals are chalcopyrite and bornite with subordinate chalcocite, oxidation occurs at North Shaft especially in the Porous Sandstone member and locally at the South end of the South Orebody. Elsewhere, it is absent at the depth of production, but minor malachite, pseudo malachite; chrysocolla, native copper, cuprite and libethenite are associated with localized leach zones. Carrollite and cobaltiferous pyrite are major cobalt bearing minerals. Minor amounts of cattierite are also present.

At the structurally simpler Mindola Mine, the minerals typically occur as a fine dissemination, commonly aggregated into clots and blebs in the richer units. In the structurally complex areas of Central and South ore body Shafts; the minerals occur predominately in the dolomite bands of the Contact Shale and South Ore Body Shale as large streaks, lenses and cross-cutting veins. Enrichment on the crests and in the troughs of folds is common. Migration of Mineralization below Geological Footwall into the Footwall Quartzite is not unusual, especially at South Ore Body Shaft.

1.3.5.4 Mineral Zoning

The sulphide minerals are zoned both stratigraphically and regionally. The stratigraphical zoning is well displayed at Mindola (Figures 1.8 and 1.9). Typically, the lower member, that is the Schistose Ore and the Low Grade Argillite, carry low-grade bornite and chalcopyrite mineralization. The Banded Ore and Cherty Ore contain similar mineralization of a higher grade, with chalcopyrite becoming predominant over bornite higher in the succession. The Number One Marker, Porous Sandstone and Mineralized Argillite contain almost exclusively chalcopyrite mineralization with minor pyrite. The one percent total copper assay Hanging wall usually occurs at the contact between the Mineralized Argillite and Hanging wall Argillite members. Above this contact, pyrite is the dominant mineral. Significant amounts of carrollite are normally confined to the Cherty Ore, Number 1 Marker and Porous Sandstone in areas of high copper/cobalt values. In areas of low cobalt values, the cobalt is present as cobaltiferous pyrite at the top of the ore Formation on either side of one percent total copper assay hanging wall.



Figure 1.8 Mineralised Argillite at Mindola Mine



Figure 1.9 Banded Ore, light whitish grey on the left in contact with Khaki brown Cherty Ore on the right

The South Orebody is characterized by chalcopyrite mineralization in Contact Shale and copper rich sections of the South Orebody Shale. Pyrite mineralization increases at the expense of chalcopyrite in the upper part of the South Orebody Shale, and a zone of exclusively pyrite mineralization occurs at the top. Bornite is typically absent from the Ore Formation, but minor occurrence appears on the fringes of the Barren Gaps, particularly in the Contact Shale. In order of importance, chalcopyrite, chalcocite and bornite are present in the mineralized footwall. Higher cobalt values are concentrated on either side of the geological footwall, in the lower part of the contact Shale and at the top of the Lower Footwall Formation, especially at the south side of the Central Shaft area.

1.3.5.5 Barren Gaps

There are three types of barren gaps at Nkana. In all three the normal Ore Formation lithology is absent.

- The Ore Formation may be replaced by an arenaceous facies. Replacement of this type results from a shallow water on-shore environment associated with palaeohills. The arenaceous material commonly rests directly on the Basement. The 3 Shaft Barren Gaps and 4 Shaft Barren Gap at Mindola is typical.
- The Ore Formation may be replaced by a normally bedded dolomitic facies. Under these conditions normal sedimentary influx was absent or minimal and dolomitic was deposited in its place. The Kitwe Barren Gap, some 600 to 1000 meters wide, lying between the Mindola and Central Ore Bodies, provides a large-scale example (see Figure 1.7).
- The Ore Formation may be replaced by a dolomitic facies represented by reefs, bio herms, etc. Such features developed in shallower and more oxygen-rich environments, such as over highs in the basement seabed. Algal bio herms established themselves in complex inter-fingering with the surrounding ore shales. The dolomitic Footwall and Ore body appear to develop in this way.

1.4 Problem Statement

Vertical Crater Retreat (VCR) mining method forms the backbone of Mindola mining operations. However, the mining method has posed stability challenges in the Deeps section, especially with the stability of Vertical Crater Retreat chambers and Ventilation drives. Mindola mining operations faces the challenge of premature failure of Vertical Crater Retreat chambers and Ventilation drives as evidenced from the frequent occurrence of rock falls from the roof and side walls (Mopani

Nkana North accident report, 2014). Rock falls vary in size and amount depending upon the state of stress condition around the openings, distribution of discontinuities, strength and condition of the rock mass and finally the dimensions of the excavations. These problems have caused unacceptable risks for safe mining operations to sustain the required levels of production (Figure 1.10).



Figure 1.10 Showing equipment damaged by a rock in the Vertical Crater Retreat chamber (2014)

1.5 Research Questions

- What is the maximum stable span for the Vertical Crater Retreat chambers in the Deeps section?
- What are the support requirements for Vertical Crater Retreat chambers?
- How far should the Ventilation drive be mined from the orebody?

- What is the suitable mining echelon for the Deeps section?

1.6 Research Objective

To improve the stability of Vertical Crater Retreat (VCR) chambers and Ventilation drives in the Deeps section.

1.7 Sub Objectives

- To analyse stress redistribution around stoping areas, with particular emphasis on the effect of stress loading on the footwall developments and on the stability of the stopes.
- To verify the effect of stress on short and long lead/lag distances between the adjacent upper and lower advancing stoping faces, on stress redistribution in areas adjacent to excavation boundaries.
- To come up with a suitable stoping echelon for the Deeps section.
- To come up with a stable span and appropriate support system for the Vertical Crater Retreat chambers.
- To come up with a suitable location of the Ventilation drive in relation to the orebody.

1.8 Methodology

The following was the approach in undertaking this research:

- Literature review of support system used globally
- Site investigations
- Geotechnical data collection
- Analysis of geotechnical data
- Geotechnical designs

- Conclusions and recommendations

1.9 Significance of the Research

This research is vital for the successful stabilisation of Vertical Crater Retreat chambers and Ventilation drives. Stabilisation of these excavations will bring about reduced operating costs for the company due to increased ore productivity and reduced support costs brought about by rehabilitating partially collapsed chambers and drives.

The successful stabilisation of Vertical Crater Retreat chambers and Ventilation drive will assist in combating some ventilation and waste rock handling problems. Fall of ground accidents will be reduced and hence the company's safety and environmental management policies will be achieved.

CHAPTER 2

LITERATURE REVIEW

2.1 Introduction

The potential for instability in the rock surrounding underground excavations is an ever-present threat to both the safety of men and equipment in the mine.

The profitability of the mining operation may also be reduced if failures are allowed to develop in the rock surrounding a stope. There are many factors that affect the overall stability of the mine and therefore to offset these threats, it is necessary to understand the causes of the instability and to design measures which will address these problems.

The contribution of this study lies in establishing the geometrical features of the rock mass of the study area, analyse stress distribution around stoping areas, come up with appropriate support system and to identify suitable location for the ventilation drive.

This is expected to enhance the safety of underground excavations and contribute to mine productivity.

2.2 Geotechnical designs

This involves establishment of loads to be induced on excavations/structures and determine support required to counter the loads to ensure stability of the excavations/structures.

2.2.1 Excavations and Structures

2.2.1.1 Excavations

The following are the types of excavations

- a. Service excavations include excavations like workshops and crusher chambers;
- b. Tunnels include excavations in primary and secondary development; and
- c. Stopes.

2.2.1.2 Structures

These include Pillars (Crown, Rib and Closure pillars)

The following are considered in the design of excavations and structures.

- a. Size/span
- b. Shape
- c. Orientation
- d. Location
- e. Induced loads

2.3 Design methods

There exists a wide range of support design methods that can be applied to improve the stability of underground excavations. Empirical, Numerical and Observational methods are some of them.

2.3.1 Empirical methods

These are methods that are derived from knowledge gained by various people in various locations during full scale “testing” of mine designs (case histories).

The development of empirical support design methods for the stability of underground project aim to include the experience gained from similar projects, in similar circumstances, in its construction.

The main characteristic of these methods is the breakdown of a wider range of rock mass quality by matching each of these categories with various support measures.

In order to estimate the geotechnical parameters of the rockmass, and the appropriate support measures, rock mass classification can be performed following the Rock Mass Rating or Geomechanics classification (RMR after Bieniawski) and the Rock Tunnelling Quality Index (Q after Barton - NGI).

These classification systems help in grouping the rock mass into sections with similar geomechanical behaviour based on qualitative and quantitative data measured on site. The analysis of these data leads to different classifications of each of the selected rock mass section, making possible to calibrate the final rock mass quality and the acquisition of the limits of variation of geomechanical parameters.

2.3.1.1 Bieniawski 1989 Method (Rock Mass Rating)

Bieniawski (1976) published the details of a rock mass classification called the Geomechanics Classification or the Rock Mass Rating (RMR) system. Over the years, this system has been successively refined as more case records have been examined, and Bieniawski has made significant changes in the ratings assigned to different parameters. The discussion which follows is based upon the 1989 version of the classification (Bieniawski, 1989). Both this version and the 1976 version deal with estimating the strength of rock masses and the evaluation of the necessary support measures. One of the main advantages of the Rock Mass Rating (RMR) classification system is the easy of data collection needed to classify the rock mass. The following six parameters are used to classify a rock mass using the Bieniawski Rock Mass Rating (RMR) system:

- a. Uniaxial compressive strength of rock material
- b. Rock Quality Designation (RQD)
- c. Spacing of discontinuities

- d. Condition of discontinuities
- e. Groundwater conditions
- f. Orientation of discontinuities

By applying this classification system, the rock mass is divided into a number of structural regions and each region is classified separately. The boundaries of the structural regions usually coincide with a major structural feature such as a fault or with a change in rock type. In some cases, significant changes in discontinuity spacing or characteristics, within the same rock type, may necessitate the division of the rock mass into a number of small structural regions.

The Rock Mass Rating (RMR) system is presented in Appendix D, giving the ratings for each of the six parameters listed above. These ratings are summed to give a value of the rock mass rating (RMR). It should be noted though, that when applying and evaluating rock mass rating (RMR) a range of values must be introduced rather than a single rock mass rating (RMR) value, corresponding to the expected range of the typical rock mass parameters (upper and lower bound values principle).

Using the basic rock mass rating (RMR) value, rock mass is classified into categories as depicted in Table 2.1. For each one of the categories Bieniawski proposed a range of values for friction angle and cohesion, as well as the average stand up time where unsupported excavation can withstand.

Table 2.1 Rock mass classifications, shear strength estimation and average stand - up time for unsupported excavation (after Bieniawski 1989, modified from Hutchison and Diederichs, 1996).

ROCK MASS CLASSES DETERMINED FROM TOTAL RATINGS					
Rating	100 - 81	80 - 61	60 - 41	40 - 21	< 20
Class number	I	II	III	IV	V
Description	Very good rock	Good rock	Fair rock	Poor rock	Very poor rock
MEANING OF ROCK CLASSES					
Class number	I	II	III	IV	V
Average stand-up time	20 years for 15m span	1 year for 10m span	1 week for 5m span	10 hours for 2.5m span	30 minutes for 1m span
Cohesion of rock mass (kPa)	> 400	300 - 400	200 - 300	100 - 200	< 100
Friction angle of rock mass (°)	> 45	35 - 45	25 - 35	15 - 25	< 15

2.3.1.2 NGI Method 1974 (Q Rock Tunnelling Quality Index)

By evaluating a large number of case histories of underground excavations, Barton et al (1974) of the Norwegian Geotechnical Institute proposed a Tunnelling Quality Index (Q) for the determination of rock mass characteristics and tunnel support requirements. The numerical value of the index Q varies on a logarithmic scale from 0.001 to a maximum of 1,000 and is defined by:

$$Q = \left(\frac{RQD}{J_n} \times \frac{J_n}{J_a} \times \frac{J_w}{SRF} \right) \quad \text{Equation 2.1}$$

Where:

RQD is the Rock Quality Designation

J_n is the Joint set number, ranging from 0.5 to 20

J_r is the Joint roughness number, ranging from 0.5 to 4

J_a is the Joint alteration number, ranging from 0.75 to 20

J_w is the Joint water reduction factor, ranging from 0.05 to 1

SRF is the Stress reduction factor, ranging from 0.5 to 400

In explaining the meaning of the parameters used to determine the value of Q , Barton et al (1974) offered the following comments:

- a. The first quotient (RQD/J_n), representing the structure of the rock mass, is a crude measure of the block or particle size.
- b. The second quotient (J_r/J_a) represents the roughness and frictional characteristics of the joint walls or filling materials.
- c. The third quotient (J_w/SRF) consists of two stress parameters describing the 'active stress'.

The rock tunnelling quality Q can be considered to be a function of only three parameters which are crude measures of:

- a. Block size (RQD/J_n)
- b. Inter-block shear strength (J_r/J_a)
- c. Active stress (J_w/SRF)

The source of identification of the necessary factor needed to evaluate Q is one field surveys. Moreover, in the extreme case where no borehole data are available, the range of RQD values can be estimated using the relationship introduced by Hudson - Priest ('79) and ISRM ('78), taking

into account the mean discontinuity span (x) and J_v (sum of discontinuities per cubic meter of rock).

$$RQD = 100 \times e^{-0.1\gamma} \times (0.1\gamma + 1) \quad \text{Equation 2.2}$$

$$RQD = 115 - 3.3J_v \quad (\text{Hudson/Priest ('79) where } \lambda=1/x, \text{ ISRM ('78)}) \quad \text{Equation 2.3}$$

Q values ranges from 0.001 to 1000 as are shown in Table 2.2. The rock mass is classified into several support categories as shown in Figure 2.1 (after Barton and Grimstad (1994)).

Table 2.2 Rock mass quality types after Q values (after Barton and Grimstad 1994, modified from Hutchison et al., 1996)

Q	Rock mass quality type
0.001 - 0.01	Exceptionally poor
0.01 - 0.1	Extremely poor
0.1 - 1	Very poor
1 - 4	Poor
4 - 10	Fair
10 - 40	Good
40 - 100	Very good
100 - 400	Extremely good
400 - 1000	Exceptionally good

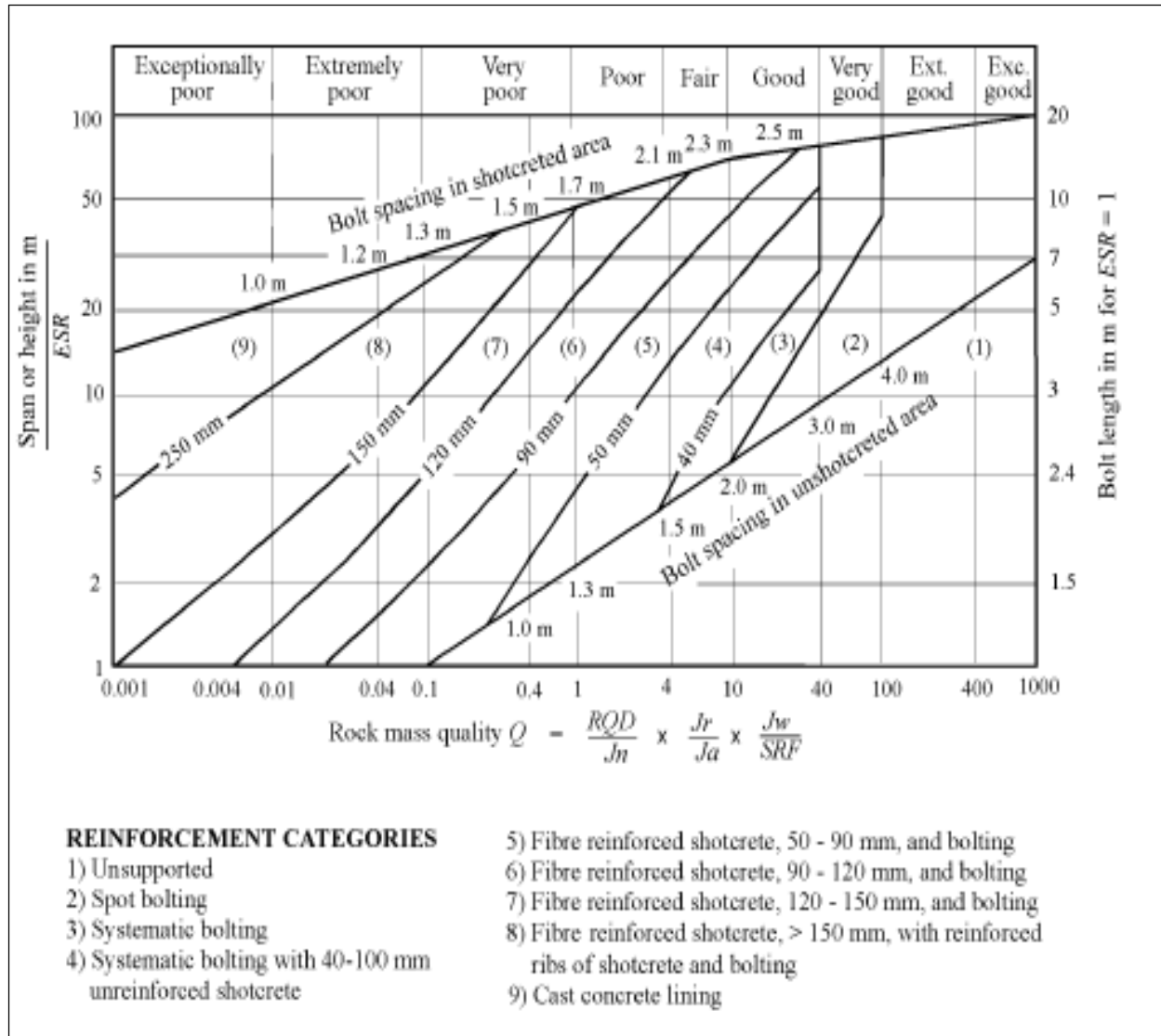


Figure 2.1 Estimated support categories based on the tunnelling quality index Q (after Grimstad and Barton, 1993, reproduced from Palmstrom and Broch, 2006)

2.3.1.3 Stability graph method

The empirical stability graph method was first proposed by Matthews et al in 1980 and was modified somewhat by Potvin in 1988 by incorporating the results of 175 case studies. Several other case studies and adjustments by Bawden (1992). Since its introduction, this design method has been used to design and evaluate geometry and ground support design for slopes in the

Zambian mining industry and it has proven to be a valuable design tool, particularly in larger mining blocks and with non-entry mining methods.

The graphs incorporate a 2 dimensional failure curve between a rock stability factor called “Modified Stability Number (N’)” and a shape factor called “Hydraulic Radius”. The stability number, N’ is similar to the value N proposed by Mathews et al. (1981) but has different factor weightings as it is a modification of the Q system. The parameter stress reduction factor (SRF) is not used and three specific multiplying factors are applied to take particular account of rock stress to strength effect, joint orientation and gravity. This method has been referred to as the Potvin method, the Mathews/Potvin method, the Modified Stability Graph method and the Stability Graph method.

N’ is based initially on Q’

Where;

$$Q' = \frac{RQD}{J_n} \times \frac{J_r}{J_a} \quad \text{Equation 2.4}$$

And

RQD/J_n is a measure of block size for a jointed rock mass

J_r/J_a is a measure of joint surface strength and stiffness

The modified stability number is calculated as:

$$N' = Q' \times A \times B \times C \quad \text{Equation 2.5}$$

Where;

A is a factor which allows for the strength to stress effect. 'A' is given by:

$$A = 1.125R - 0.125 \quad 1 > A > 0.1 \quad \text{Equation 2.6}$$

And

R is the ratio of the uniaxial compressive strength of the rock material to the

Maximum induced compressive stress. The latter is determined by stress analysis

$$R = \frac{\text{uniaxial compressive strength (UCS)}}{\text{Maximum induced stress}} \quad \text{Equation 2.7}$$

The rating of A can also be obtained from the Rock Stress Factor graph shown in figure 2.2.

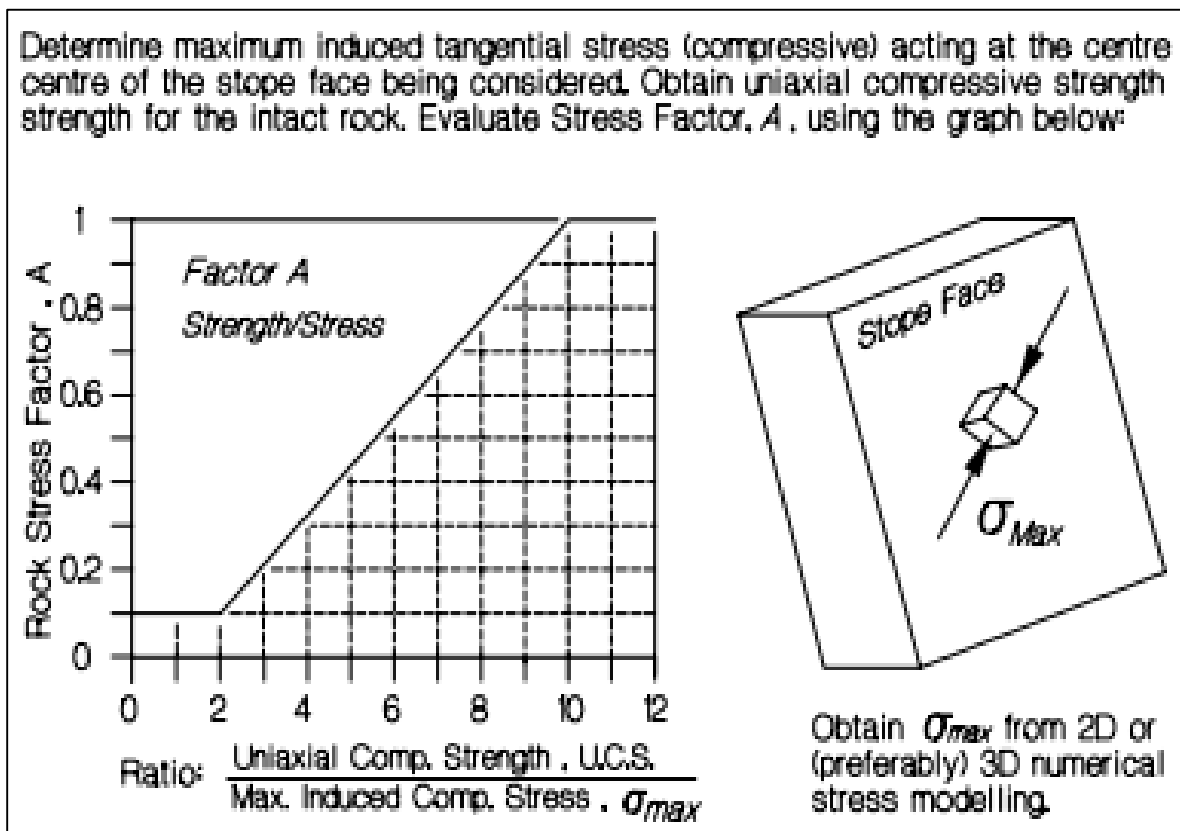


Figure 2.2 Rock Stress Factor 'A' (Potvin, 1988) for Stability Graph analysis (modified from Hutchison et al., 1996).

‘B’ is a factor which allows for the ease of block fall out effect. ‘B’ is given by the following equations:

$$B = 0.3 - 0.01\alpha < \alpha < 10 \quad \text{Equation 2.8}$$

$$B = 0.210 < \alpha < 30 \quad \text{Equation 2.9}$$

$$B = 0.02\alpha - 0.430 < \alpha < 60 \quad \text{Equation 2.10}$$

$$B = 0.0067\alpha + 0.460 < \alpha < 90 \quad \text{Equation 2.11}$$

Where α is the true angle between the hanging surface of the excavation and the joint plane. In the case of several joint planes, the smallest angle is applicable. The true angle can be determined by Stereo net or from the Joint Orientation Factor graph.

C is Gravity Adjustment Factor. In the case of gravity falls and slabbing, in which no sliding on the joints is involved, the factor is given by the following equation:

$$C = 8 - 6 \times \cos(\text{dip of stope face}) \quad \text{Equation 2.12}$$

When the sliding on joints is involved, the gravity adjustment factor is given by the following equations:

$$C = 8, \quad (\text{Dip of critical joint} < 30^\circ) \quad \text{Equation 2.13}$$

$$C = 11 - 0.1 \times \text{Dip of critical joint}, \quad (\text{Dip of critical joint} > 30^\circ) \quad \text{Equation 2.14}$$

Table 2.3 shows the range of values for the above three factors.

Table 2.3 Range of values (for hard rock mining) modified from Hutchison et al., 1996).

Range	RQD/ J_n	J_r/J_a	A	B	C	N'
Maximum	0.5 - 200	0.025 - 5	0.1 - 1	0.2 - 1	2 - 8	0.0005 - 8000
Typical	2.5 - 25	0.1 - 5	0.1 - 1	0.2 - 1	2 - 8	0.1 - 1000

Hydraulic Radius

The hydraulic radius is obtained from the Potvin's Stability graph shown in figure 2.3.

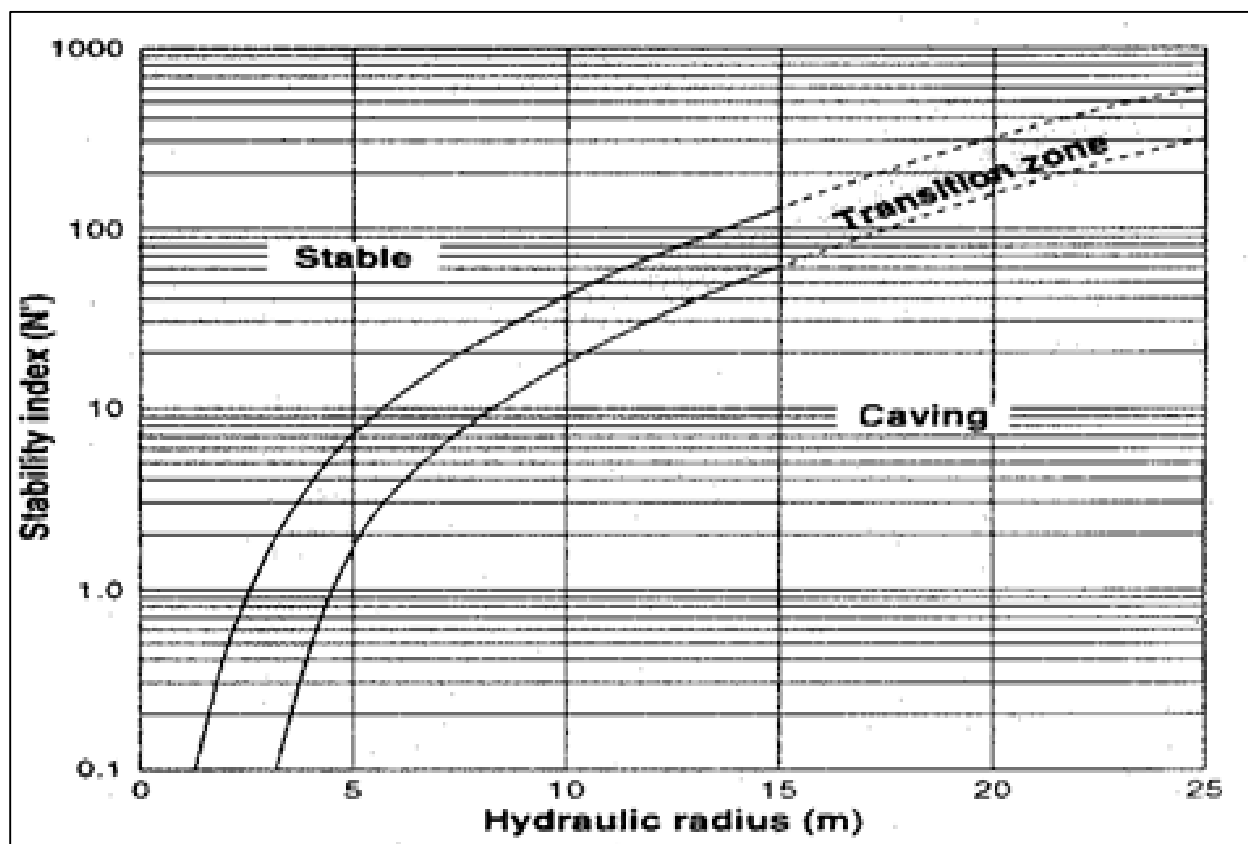


Figure 2.3 Stability graph showing zones of stable ground, caving ground and ground required support (After Potvin (1988), modified from Nickson (1992)).

The stability of the spans in the stopes is determined by the use of the Modified Stability Number (N'), together with the hydraulics radius. The hydraulic radius values are used to estimate

unsupported, transition and supported excavation/stope spans. It is calculated using the following equation:

$$\mathbf{HR} = \frac{\mathbf{Area\ (m^2)}}{\mathbf{Perimeter}} = \frac{\mathbf{w \times h}}{\mathbf{2(w+h)}} \quad (\text{units of m}) \quad \text{Equation 2.15}$$

Where:

HR is the Hydraulic Radius

w is the width

h is the height

2.3.2 Numerical support design methods

Numerical simulation and model testing are the main research methods of solving geo-technical and underground problems. Unwedge, Phase 2 and Examine^{tab} are some of them.

2.3.2.1 Unwedge

The size and shape of wedges formed in the rock mass surrounding a tunnel excavation depend upon geometry and orientation of the tunnel and also upon the orientation of the joint sets. The three dimensional geometry problems can be solved by computer programs such as Unwedge (Rocscience Inc.). Unwedge is a three dimensional stability analysis and visualization program for underground excavations in rock containing intersecting structural discontinuities. Unwedge provides enhanced support models for bolts, shotcrete and support pressures, the ability to optimize tunnel orientation and an option to look at different combinations of three joint sets based on a list of more than three joint sets. In Unwedge, safety factors are calculated for potentially unstable

wedges and support requirements can be modelled using various types of pattern and spot bolting and shotcrete. Figure 2.4 (A) presents a wedge formed by Unwedge on a horse-shoe shape tunnel and Figure 2.4 (B) support installed.

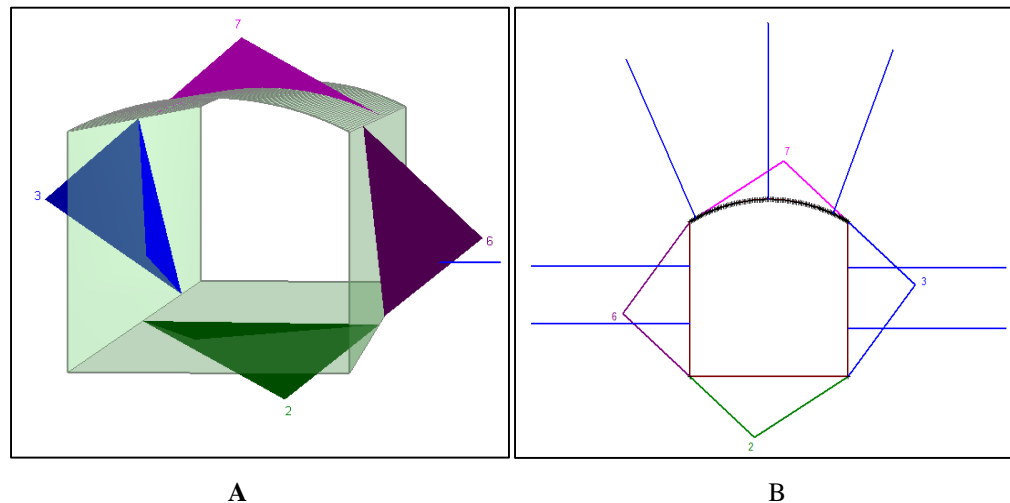


Figure 2.4 UNWEDGE Analysis: (A) Wedges formed surrounding a tunnel; (B) Support installation (results from 4716 FT L wedge analysis 2013, Mopani Rock mechanics office).

2.3.2.2 Phase 2

Phase 2 is a two dimensional plain strain plastic finite element program for calculating stresses and displacements around underground excavations. The plain is taken across the excavation in question. Progressive failure around the excavation, using stress, displacement or strength factors (ratio of rock strength/rock stress) is analysed.

2.3.2.3 Examine^{tab}

Examine^{tab} is a 3D displacement-discontinuity program for calculating stresses and displacements around tabular ore bodies. A model is generated by taking a dip plan of the excavation. Input data include modulus of elasticity of the host and ore body rock, unit weight, poissons ratio, depth,

thickness and dip of ore body. The results are in form of Normal Stress and Displacement in the rock surrounding the excavation in question.

CHAPTER 3

BASICS OF SUPPORT DESIGN

3.1 Introduction

Design of support is based on maximum loads that would occur on the system. Hence, it is critical that both ground demand and bolt capacities are well understood.

Understanding ground demand is the start of support design. Demand is brought about when the state of stress and gravity is disturbed in the rock mass and requires to be restored. At Mindola mine, rock mass demand or load is assessed using stress analysis, rock mass classification and wedge analysis. Once the potential unstable wedges or depth of rock failure is established, the length and spacing of bolts are then determined for acceptable safety factor. Lack of understanding demand would lead to poorly designed support system and can be a costly venture to the operation of the mine in terms of safety of employees, safety of equipment and economic extraction of ore. However the basic principle in support is that ground should be made to support itself through correct mine design, proper sequencing and good drilling and blasting practices.

In stress analysis, the level of induced stresses around the development is looked at and compared with the strength of the rock mass, and the effect of their interaction with other excavations. Using numerical analysis the extent of ground deformations/failure (loads) is then estimated. The other methods that are used to determine the load include, empirical support design based on RMR, wedge analysis and through observation in damaged/fallen areas.

The capacity of the support element is provided by the strength of the material and the surrounding grout in case of grouted bolts. Once the demand and bolt capacity are known, the primary or

secondary support system is designed in terms of length, orientation and spacing of bolts. Cable bolt length is the length of the individual cable bolt (minimum length) and cable bolt density represents the number of cable bolts per unit area of stope face. Based on the support systems designed, the support standards are developed as a guide in support installation in different ground conditions of the mine.

3.2 Empirical Cable Bolt Design

3.2.1 Cable bolt length

Classification systems serve to differentiate between different rock masses and to adjust design accordingly. Rules of thumb for support design have been developed for blocky to fractured ground. These are based on tunnels, caverns and mine openings and summarize current practice. Most of these guidelines are designed for rock bolting (mechanical or resin grouted) and as such can be used to select spacing for face support to supplement cable bolting in fractured ground. In many cases the recommended spacing are not economically practical for use directly with cable bolts. Figure 3.1 illustrates a data set of rock bolt lengths in existing tunnels and caverns.

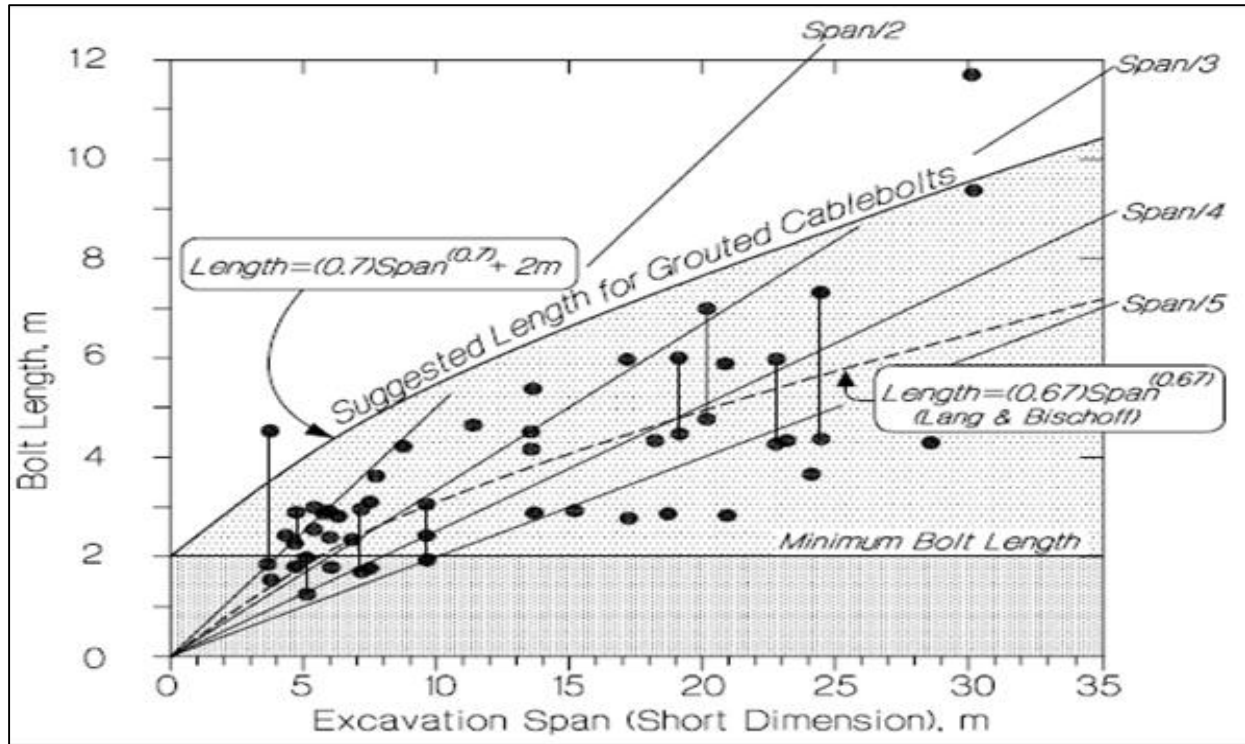


Figure 3.1 Bolt lengths in current practice (after Lang and Bischoff, 1984) with adjustment for cable bolt application (relationships are for S.I. units) (modified from Hutchison and Diederichs, 1996).

3.2.2 Cable bolt density (bolts/m² of face) and spacing.

Potvin (1988) plotted cable bolt densities used in case histories against $(RQD/J_n)/HR$ based on the assumption that relative block size was in principle the governing empirical parameter for stope face stability and support effectiveness. Nickson (1992), however, applied statistical techniques in an investigation of many possible parametric combinations. For the combined cable bolted stope database of Potvin and Nickson, $(RQD/J_n)/HR$ actually gave a very poor correlation to cable bolt density based on current practice. It is proposed here that the absolute block size represented by RQD/J_n should control local block fallout from the face and therefore should strongly influence ultimate stability of the stope. If cable bolts are spaced too far apart, unravelling will occur between bolts, progressively leading to more serious instability. The corresponding graph based on the Potvin/Nickson database is shown in Figure 3.2. The design zone plotted provides a crude

recommended design range for cable bolt density in open stope applications. This design zone should not be applied to permanent openings or in high traffic areas, where safety is a critical issue, unless accompanied by primary support such as rock bolts and screen.

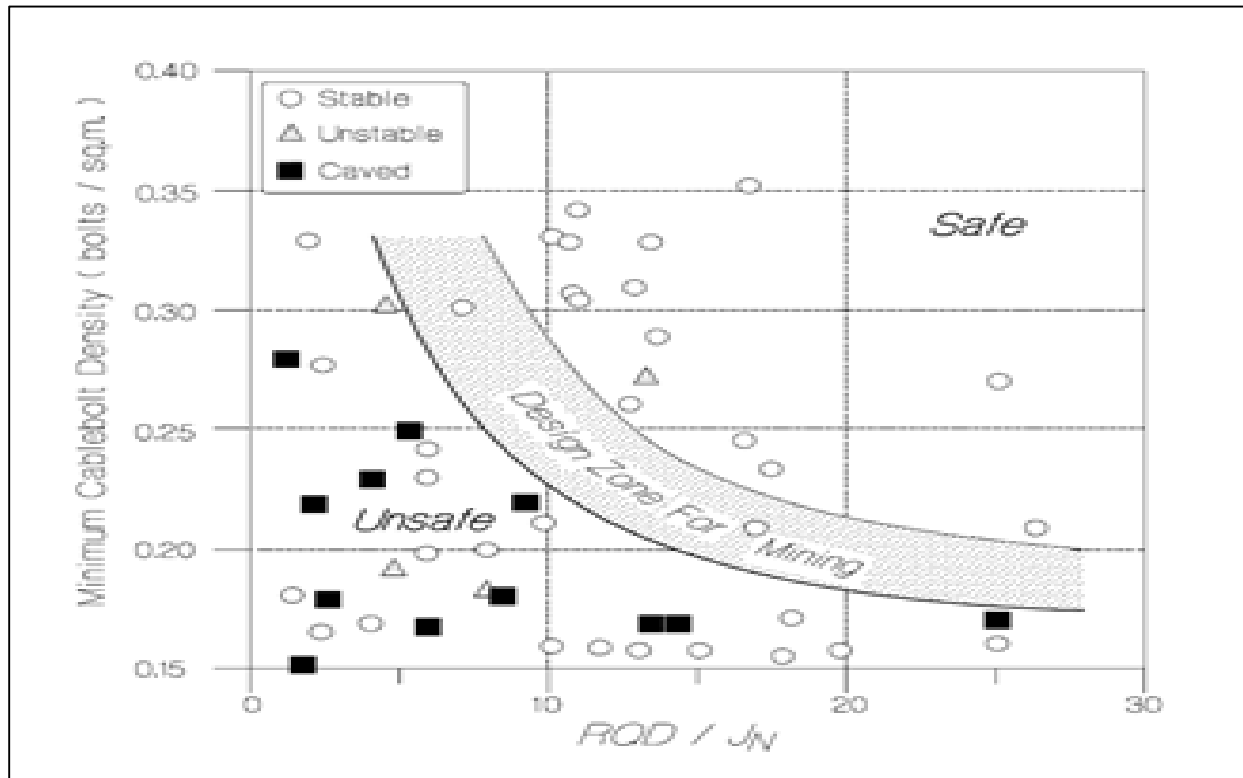


Figure 3.2 Potvin/Nickson guidelines for cable bolt density to control local unravelling (modified from Hutchison and Diederichs, 1996).

Nickson (1992) showed that the best empirical correlation with respect to cable bolt density was obtained by plotting density with respect to the parameter N'/HR . The logic here is similar to Potvin's usage of $(RQD/J_n)/HR$, except that N' contains additional information about stope inclination, stress related fracturing (parameter A) and favourable or unfavourable joint orientations. Nickson derived a relationship based on current practice without considering the degree of support effectiveness. The design zones proposed in Figure 3.3 do relate to this degree of success. While the data scatter is great due to the trial-and-error nature of present design

practice, there appears to be a reasonable limit to cable bolt effectiveness as delineated by the cluster of caved cases in the upper portion of this plot. The non-conservative zone can be used as a guide for non – entry conditions or where dilution is not critical. The conservative zone is applicable to stope backs above drilling horizons and other areas where entry is permitted. Note the two vertical scales used here. These illustrate the relationship between cable bolt density and the cable spacing of an equivalent square pattern.

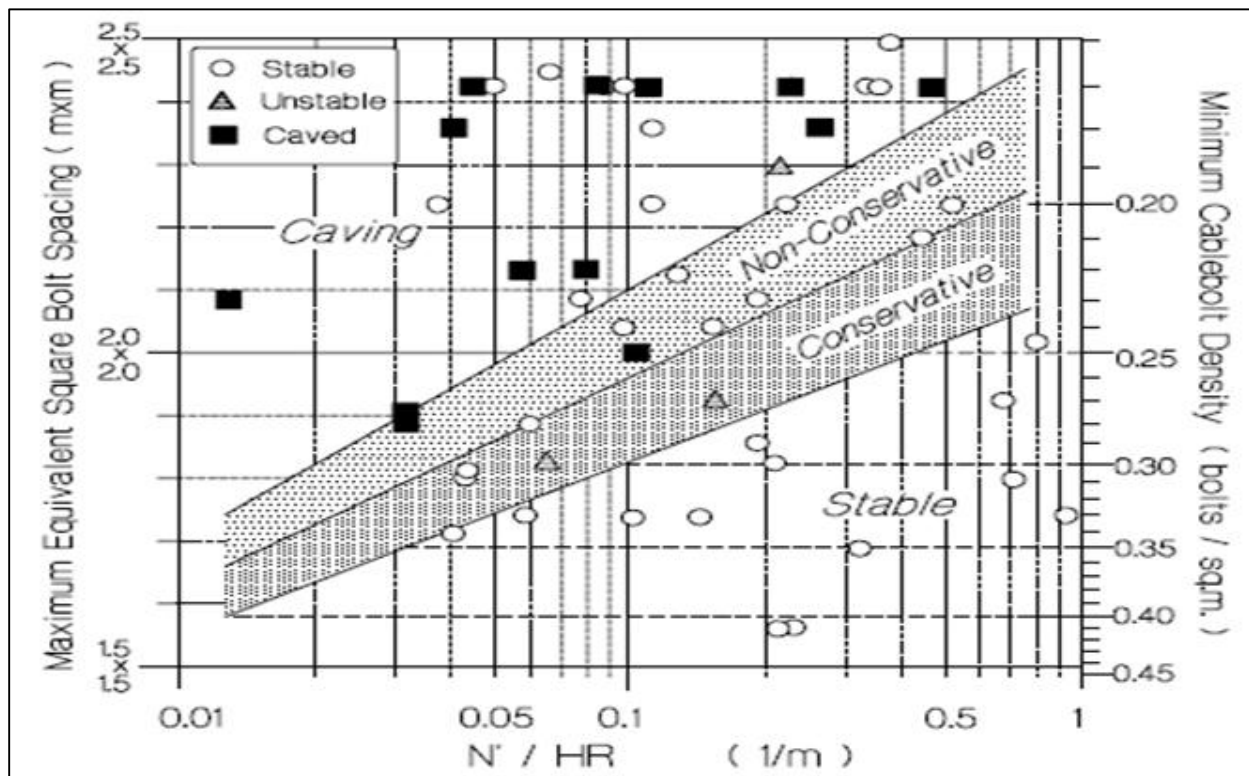


Figure 3.3 Guidelines for cable spacing and density - overall stope face stability (modified from Hutchison and Diederichs, 1996).

CHAPTER 4

GEOTECHNICAL DATA COLLECTION AND ANALYSIS

4.1 Geotechnical data acquisition

The following are the modes in which raw data was collected

4.1.1 Underground joint survey and Core logging

The geotechnical raw data collected during line mapping of joints and window mapping was entered into standard entry forms. The output of line mapping of joints and window mapping were joint spacing (J_s), joint orientation (J_o), joint condition (J_c), dip and dip direction of joints and rock samples. Joint condition (J_c) included the Aperture, Infill/gouge, Joint wall condition, Roughness and Persistence. The rock samples collected during mapping and logging were then tested for Point load Index (PLI) using Point Load Equipment for the calculation of Intact Rock Strength (IRS).

4.2 Analysis of Geotechnical data

The raw data was evaluated to obtain inputs into geotechnical designs.

4.2.1 Methods of Analysis

4.2.1.1 Joints Analysis

The dip and dip direction of joints from line or window mapping were entered into DIPS Program. The number of Joint Sets were determined and their dip and dip direction of each set was indicated. From stereo nets, it indicated that there are three joint sets over the Deeps section. Table 4.1 shows the summary of bedding and joint orientation.

Table 4.1 Summary of bedding and joint orientation

Joint Plane No.	Dip (°)	Direction (°)	Comments
1	66	213	Bedding
2	63	048	J1
3	72	002	J2
4	60	318	J3

4.2.1.2 Rock Mass Classification (RMC)

The rock mass at Mindola's Deeps section was classified using the Rock Tunnelling Quality Index (Q) and Rock Mass Rating (RMR) classification systems. These indices were calculated from domain logging undertaken on diamond drill cores and window mapping (the logging system format is shown in Appendix C).

4.2.1.2.1 Rock Mass Rating (RMR)

This was developed by Bieniawski, and Laubscher to determine the rock mass quality. The ratings for the intact rock strength, rock quality designation, joint spacing, joint orientation, joint condition and joint water obtained from standard tables were summed up to obtain the rock mass rating (RMR).

Based on core logging, underground mapping and point load test, the average results of the representative Rock Mass Classification data collected from the Deeps section are summarised in Table 4.2.

Table 4.2 Rock mass rating (RMR) for Mindola Deeps Rock units.

Rock Type	RQD		IRS		Spacing Rating (cm)	Joint Condition Rating	MRMR (%)	Class	Rock Mass Strength (MPa)	Descript ion
	Value (%)	Rating	Value (MPa)	Rating						
Basal Sandstone	89	13	129	13	17	27	70	2B	72	Good
Lower Conglomerate	83	13	145	14	16	27	70	2B	81	Good
Footwall Sandstone	96	14	180	17	16	26	73	2A	100	Good
Footwall Conglomerate	85	13	139	14	19	25	71	2A	78	Good
Schistose Ore	87	13	58	6	17	23	59	3A	31	Fair
Low Grade Argillite	96	14	108	11	18	25	68	2B	62	Good
Banded Ore	97	15	108	11	21	25	72	2A	66	Good
Cherty Ore	98	15	166	17	20	27	79	2A	102	Good
Porous Sandstone	97	15	140	14	20	26	75	2A	83	Good
Hanging wall Argillite	85	13	196	19	17	23	72	2A	103	Good

4.2.1.2.2 Q-System

The system was developed by the Norwegian Geotechnical Institute (NGI) for the determination of rock mass quality. The Q – value was calculated using the formula;

$$Q - \text{Value} = \text{RQD}/J_n \times J_r/J_a \times J_w/\text{SRF},$$

Where J_n is the rating for joint set number, J_r is the rating for joint roughness, J_a is the rating for the joint alteration, J_w is the rating for the Joint flow and SRF is the rating for the Stress Reduction Factor. All these parameters are empirical numbers and were obtained from standard table. Table 4.3 shows the geotechnical parameters collected from the Deeps section and their ratings. The ratings were used in the calculation of the Q value and the modified Q value (Q').

Table 4.3 Geotechnical parameters used in the calculation of the Q' value

Parameter	Description	Rating
Average width of the orebody	16m	
RQD	85%	
Joint set number (J_n)	2 joint sets plus random	6
Joint roughness number (J_r)	Slickensided	1.5
Joint alteration number (J_a)	low friction clay mineral coatings	4
Joint water reduction factor (J_w)	Moist	1
Stress reduction factor (SRF)	(109MPa/40MPa) = 2.725	
Q - value	Q - value	1.94
Q'	Modified Q - value	5.3

4.2.1.2.3 Rock Mass Stability Number (N)

The Rock Mass stability number (N) developed by Mathews and Potvin for stope span design was calculated using the formula;

$$N = Q' \times A \times B \times C$$

Where A is the stress factor, B is the joint orientation factor and C is surface orientation factors.

All these factors are empirical numbers obtained from standard tables. Table 4.4 shows the geotechnical data collected and their rating used in the calculation of the rock mass stability number.

Table 4.4 Geotechnical parameters used in the calculation of the modified stability number (N')

Parameter	Description	Rating
A	Rock Stress Factor	0.54
B	Rock Defect Orientation Factor	0.4
C	Design Surface Orientation Factor	6
Q'	Modified NGI Rock Mass Rating	5.3
N'	Modified Rockmass stability number	6.9

CHAPTER 5

GEOTECHNICAL DESIGNS

5.1 Stability of the Vertical Crater Retreat chamber

In order to improve the stability of Vertical Crater Retreat (VCR) chambers and Ventilation drives in the Deeps section, Potvin's stability graph method was applied.

Potvin's Stability Graph Method (1988), which was modified after Mathews et al (1980), has been used along with Laubscher's (1990) stable stope chart to estimate stable span of Vertical Crater Retreat (VCR) chambers. Laubscher's system is based predominantly on case histories of caving operations, thereby providing a good check against the caving spans predicted by Potvin's method, which is based purely on open stoping cases. Properties for the orebody have been used to calculate stable dimensions since this rock type is the predominant host for the Vertical Crater Retreat (VCR) chambers.

5.1.1 Stable span of the Vertical Crater Retreat chamber

$$N' - \text{Stability Number} = Q' \times A \times B \times C$$

$$A - \text{Rock Stress Factor} = 0.54$$

$$B - \text{Rock Defect Orientation Factor} = 0.4$$

$$C - \text{Design Surface Orientation Factor} = 6$$

$$Q' - \text{Modified NGI Rock Mass Rating} = 5.3$$

$$N' = 5.3 \times 0.54 \times 0.4 \times 6$$

$$= \underline{6.9}$$

The calculated modified stability number ($N' = 6.9$) is plotted on Mathews/Potvin stability graph so as to determine the Hydraulic radius (H), (Figure 5.1).

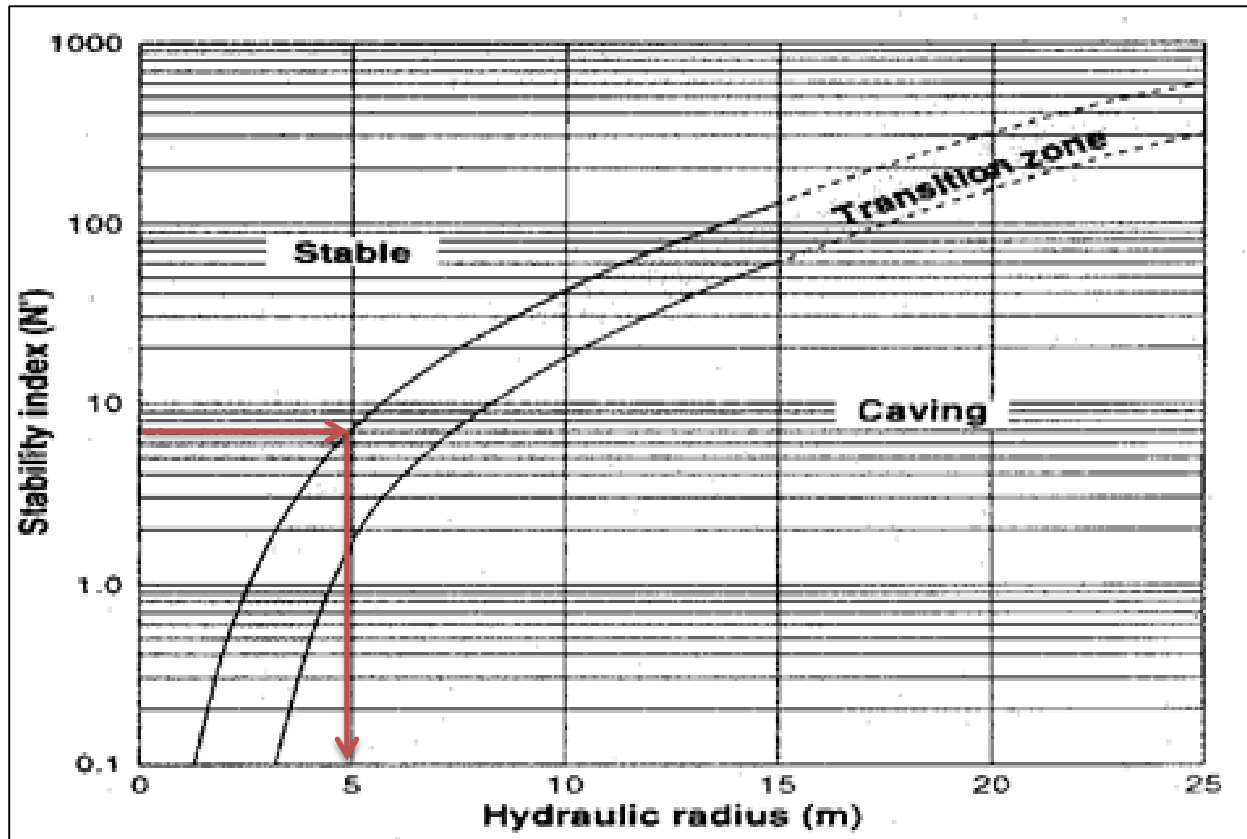


Figure 5.1 Mathews/Potvin stability graph

Hydraulic Radius, from Mathews/Potvin graph, is approximately 4.9m.

The length (L) is calculated by rearranging the formula for the Hydraulic radius (HR) given as;

$$HR = \frac{\text{Area}}{\text{perimeter}}$$

$$= \frac{\text{width X length}}{2(\text{width}+\text{length})} = \frac{W \times L}{2(W \times L)}$$

Rearranging this equation to make the length subject we get;

$$\text{Length (L)} = \frac{2 \times W \times HR}{W - 2HR} \quad \text{Equation 5.1}$$

$$=(2 \times 16 \times 4.9) / (16 - (2 \times 4.9))$$

$$= 25.29\text{m}$$

Therefore the length (L) (stope span) of the Vertical crater retreat chamber is 25.29m. This implies that the stable span length of a Vertical Crater Retreat (VCR) is 25.29m with a width of 16m.

5.1.2 Secondary support requirements

Support requirements were estimated using Grimstad and Barton's graph shown in Figure 5.2. In this chart, the Q – value was plotted against the equivalent excavation dimension (De) which was calculated by dividing the true excavation dimension by a factor termed Excavation Support Ratio (ESR).

$$Q - \text{Value} = 1.94$$

$$De = \frac{\text{Excavation width (W)}}{\text{Excavation support ratio (ESR)}} \quad \text{Equation 5.2}$$

Width of the Vertical crater retreat chamber = 16m

Excavation support Ratio (ESR) used for the Vertical Crater Retreat (VCR) chamber is 1.6 (for large excavation heading).

Equivalent excavation dimension (De) = 10.

Plotting the equivalent excavation dimension (De = 10) and the Q value (1.94) on Grimstad and Barton's graph gives the results shown in Figure 5.2.

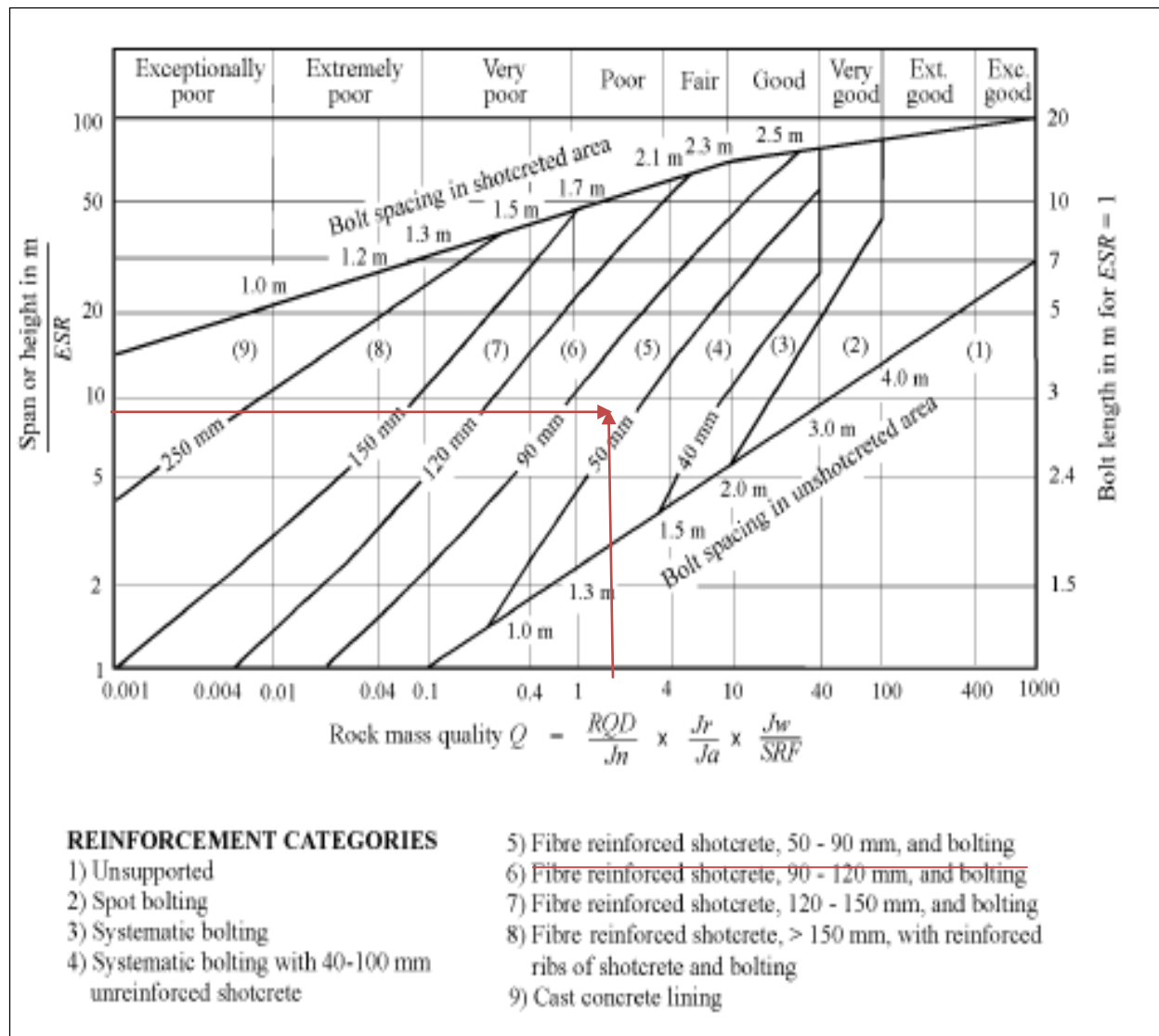


Figure 5.2 Grimstad and Barton's graph

Using Tunnel Support Guidelines (after Grimstad et al., 1993) shown in Figure 5.3, the recommended support for optimum 10m short span is 50mm to 90mm thickness of fibre or mesh reinforced shotcrete and cable bolts.

5.1.3 Cable bolt specification

5.1.3.1 Cable bolt length

$$\text{Cable bolt length} = 0.7 \times \text{Span}^{0.7} + 2 \quad \text{Equation 5.3}$$

$$= 0.7 \times (10)^{0.7} + 2$$

$$= 5.5\text{m (that is effective length)} - \text{Available 6m Cable suitable}$$

5.1.3.2 Bolt density

RQD is 85%

J_n is 6

$$\frac{\text{RQD}}{J_n} = 14.17$$

The calculated value of RQD/J_n is plotted on Potvin/Nickson cable bolting graph so as to determine the maximum cable bolt density (Figure 5.3).

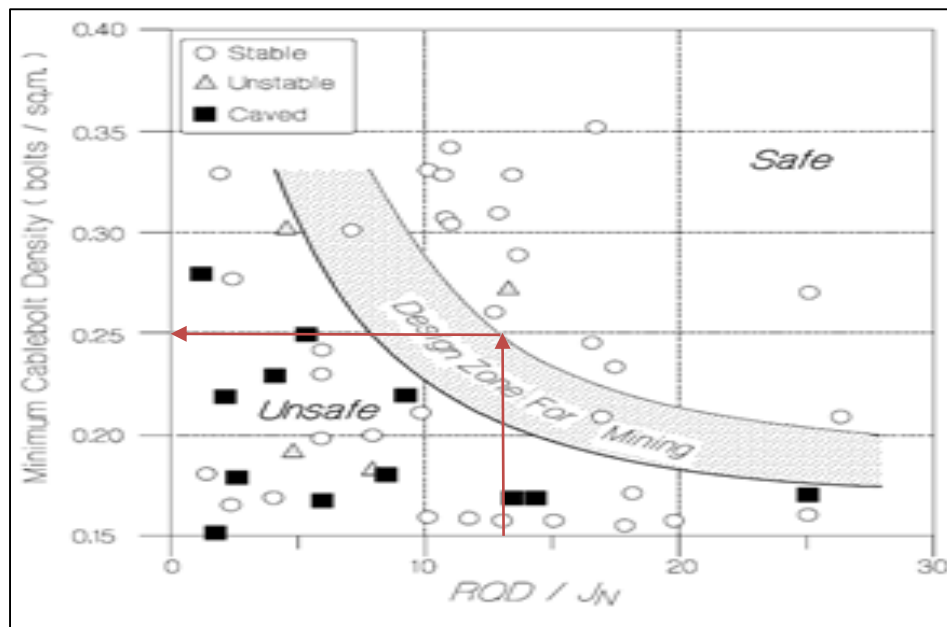


Figure 5.3 Potvin/Nickson cable bolting graph (Guidelines for cable bolt density to control local unravelling)

The maximum cable bolt density is 0.25 bolts/m²

100 bolts (for 25m x 16m roof – equivalent to 2.0m x 2.0m pattern)

5.1.3.3 Support Patterns and Cost Comparison

5.1.3.3.1 Support Patterns

A ring in the current cable bolt support pattern consists of 8 by 6m cable bolts and 6 by 15m cable bolts as shown in Figure 5.4.

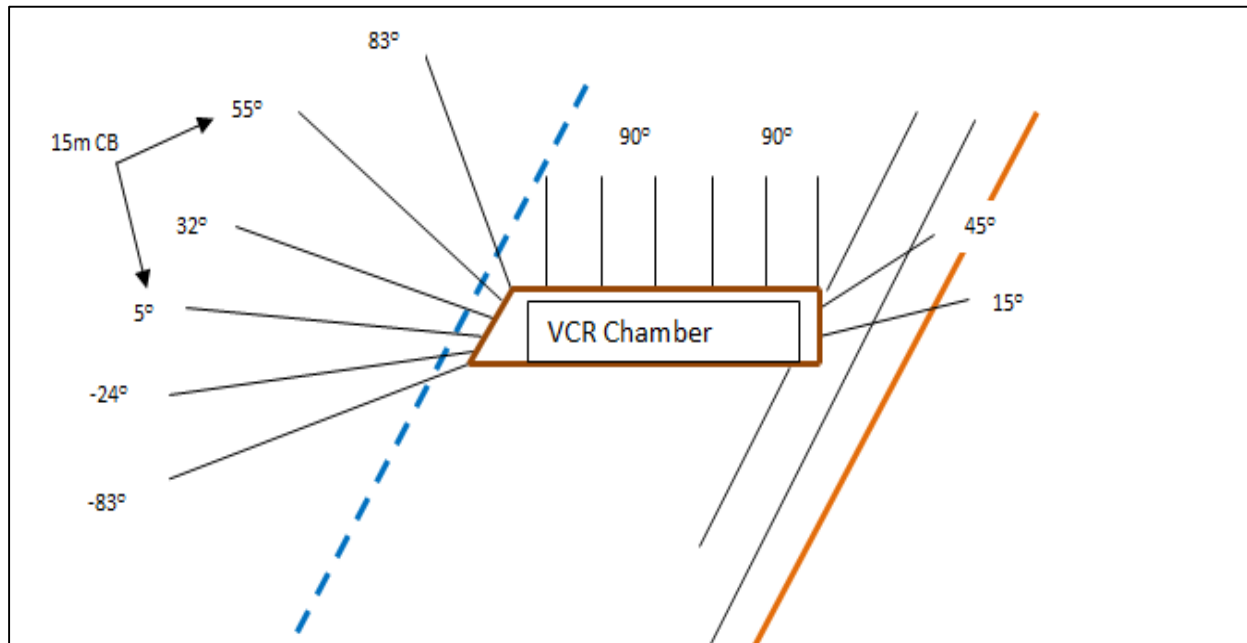


Figure 5.4 Section of a Vertical Crater Retreat chamber with cable bolts installed in a ring (Reproduced from Mindola Mine Support Standards Booklet, 2012).

The proposed cable bolt support pattern will consist of 11 by 6m cable bolts in a ring. The cable bolt spacing within the ring is 2.0m as shown in Figure 5.5.

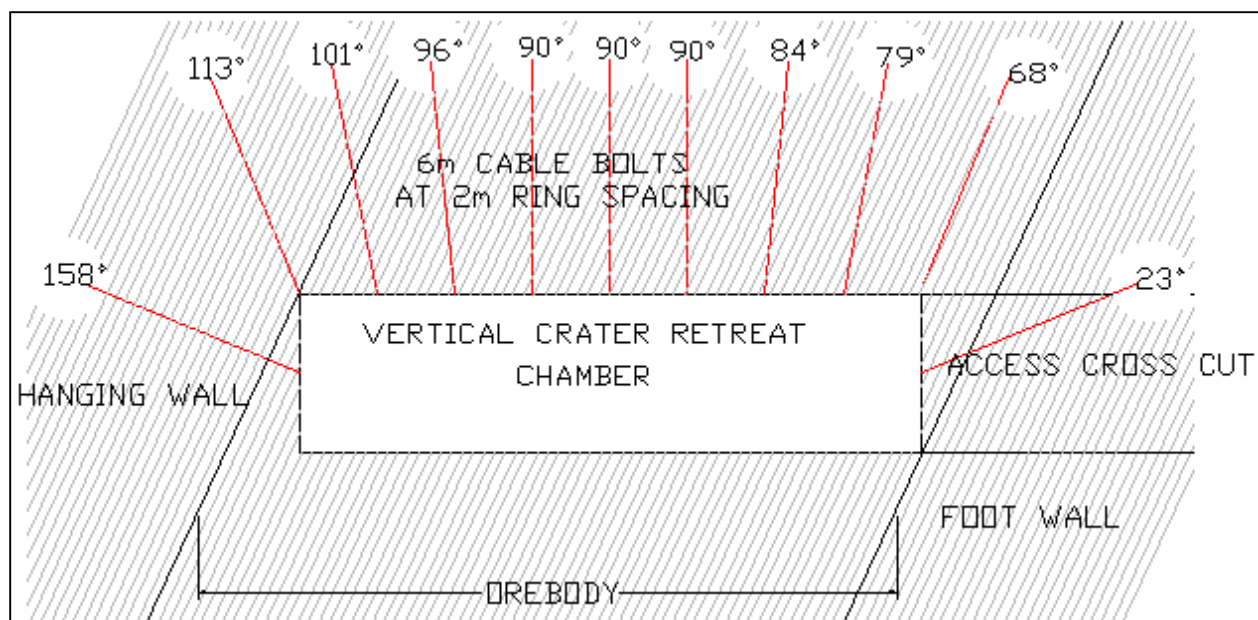


Figure 5.5 Section of the proposed cable bolt support pattern.

5.1.3.3.2 Cost comparison

Analysis of support cost per ring in the current cable bolt pattern (Table 5.1).

Table 5.1 Analysis of cable bolt support cost in a ring (Current cable bolt support pattern)

Support Material Description	Unit of measure	Unit Price (\$)	Quantity/Ring	Sub total
6m Cable Bolts	Each	26.16	8	209.28
15m Cable bolts	Each	42.1	6	252.60
50Kg Bags of Cement	Each	5.42	8	43.36
Breather tubes	Meter	0.79	145	114.55
Grand total				619.79

Analysis of support cost per ring in the proposed cable bolt pattern (Table 5.2).

Table 5.2 Analysis of cable bolt support cost in a ring (Proposed cable bolt support pattern)

Support Material Description	Unit of measure	Unit Price (\$)	Quantity/Ring	Sub total
6m Cable Bolts	Each	26.16	11	287.76
15m Cable bolts	Each	42.1	0	0
50Kg Bags of Cement	Each	5.42	4	21.68
Breather tubes	Meter	0.79	84.5	66.76
Grand total				376.2

In view of the above analysis, it can be seen that support costs reduces from \$619.79 to \$376.2.

5.2 Numerical Modelling

The purpose for running numerical models was to analyse stress redistribution around stoping areas in the Deeps section, with particular emphasis on the effect of stress loading on the footwall developments and on the stability of the stopes, to verify the effect of stress on short and long lead/lag distances between the adjacent upper and lower advancing stoping faces, on stress redistribution/ loading in areas adjacent to excavation boundaries – volume of stressed rock, to come up with a suitable stoping echelon for the Deeps section and to come up with a suitable location of the Ventilation drive in relation to the orebody.

Mining simulations using Phase 2 and Examine^{tab} numerical modelling programs were carried out.

Examine^{tab} is a 3D displacement-discontinuity program for calculating stresses and displacements around tabular ore bodies. A model is generated by taking a dip plan of the whole mine area. Input data include modulus of elasticity of the host and ore body rock, unit weight, poissons ratio, depth,

thickness and dip of ore body. The results are in form of Normal Stress and Displacement in the rock surrounding the excavation in question.

Phase 2 is a two dimensional plastic finite element program for calculating stresses and displacements around underground excavations such as Vertical Crater Retreat chambers. Progressive failure, support interaction and other problems can be analysed.

By necessity, models are incomplete representations of the real world. To generate the models, the following assumptions were made.

- a. Above 3400 level, the footwall and hanging walls have sufficiently closed up compressing the broken ground allowing stress transmission across stoped out areas. Studies conducted in early 1990 indicated that there was complete closure of hanging wall and footwall and this had occurred at three mining level blocks above current producing level.
- b. In the upper section of the mine, the caved rock that migrates down and fills the stope void after blasting the stopes, and the backfilled waste rock material in the Deeps section, will not transmit any significant stresses.
- c. Average rock mass properties for the ore body have been used other than properties of small individual rock units.
- d. Due to the slenderness of the rib pillars ($W/H = 0.55$) and the large expanse of mined out area in the deeps section, the pillars have yielded/fractured and do not transmit any stresses.

5.2.1 Location of the Ventilation drive in relation to the ore body (Phase 2 – stress analysis)

To analyse stresses and displacements around Vertical Crater Retreat (VCR) chambers and the Ventilation drives in the Deeps section, a Phase 2 model was generated. The section was taken across the orebody hanging wall to footwall. Progressive failure around the stope and immediate footwall excavations, using stress distribution was analysed.

The Phase 2 model in Figure 5.6 shows the mesh set up, location of the Ventilation drives in relation to the ore body on 4552, 4716, 4881, 5045 and 5220 feet levels.

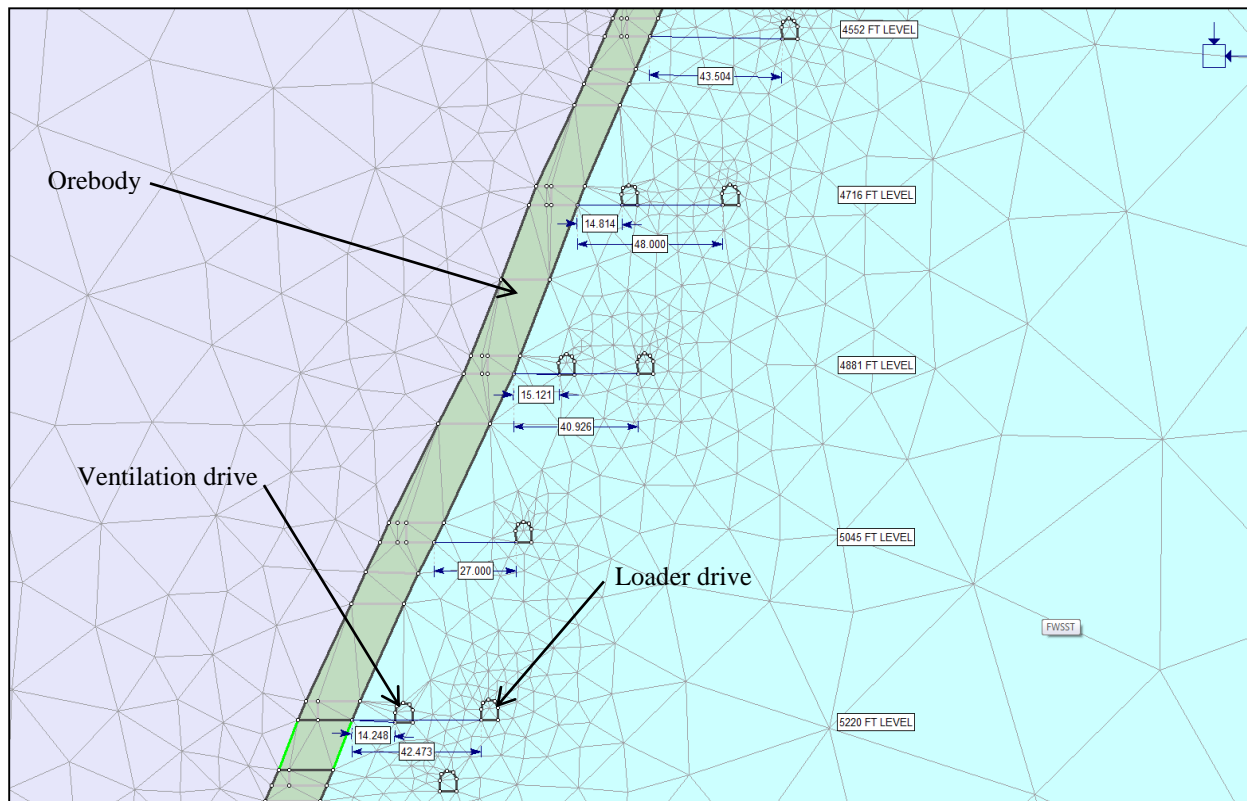


Figure 5.6 Model set up showing mesh, the orebody and location of foot wall developments on various levels. (Results from MSV DEEPS stress analysis - GRAVITY, 2015).

Phase 2 results in figure 5.7 shows variation of virgin stress levels before any mining takes place and the mining stages.

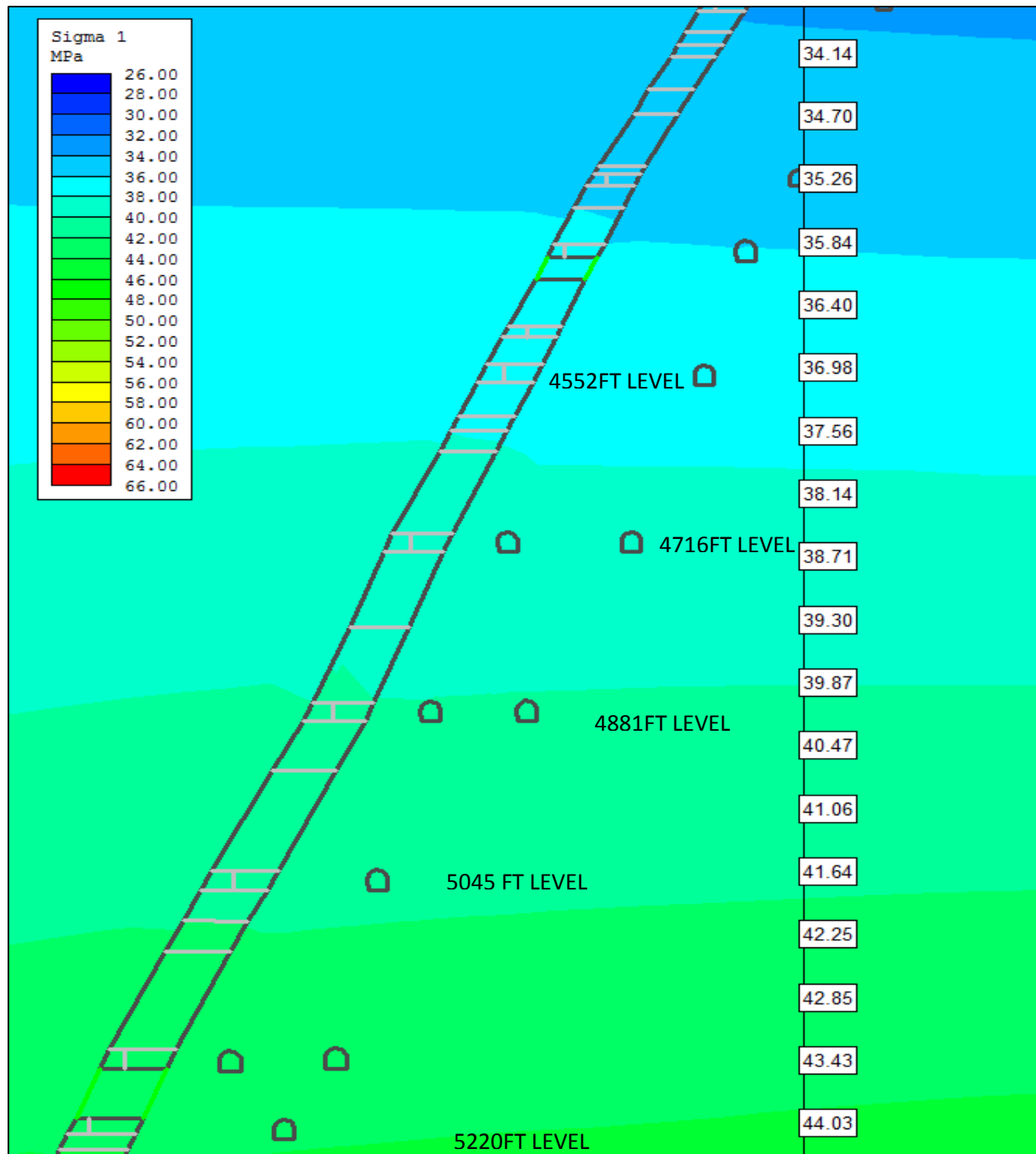


Figure 5.7 Phase2 results showing variation of virgin stress levels with depth (prior to mining out) (Results from MSV DEEPS stress analysis - GRAVITY, 2015).

Phase 2 results in figure 5.8 displays a section showing stress levels as Vertical Crater Retreat (VCR) stope blasting advances upward at early stages of up dip mining.

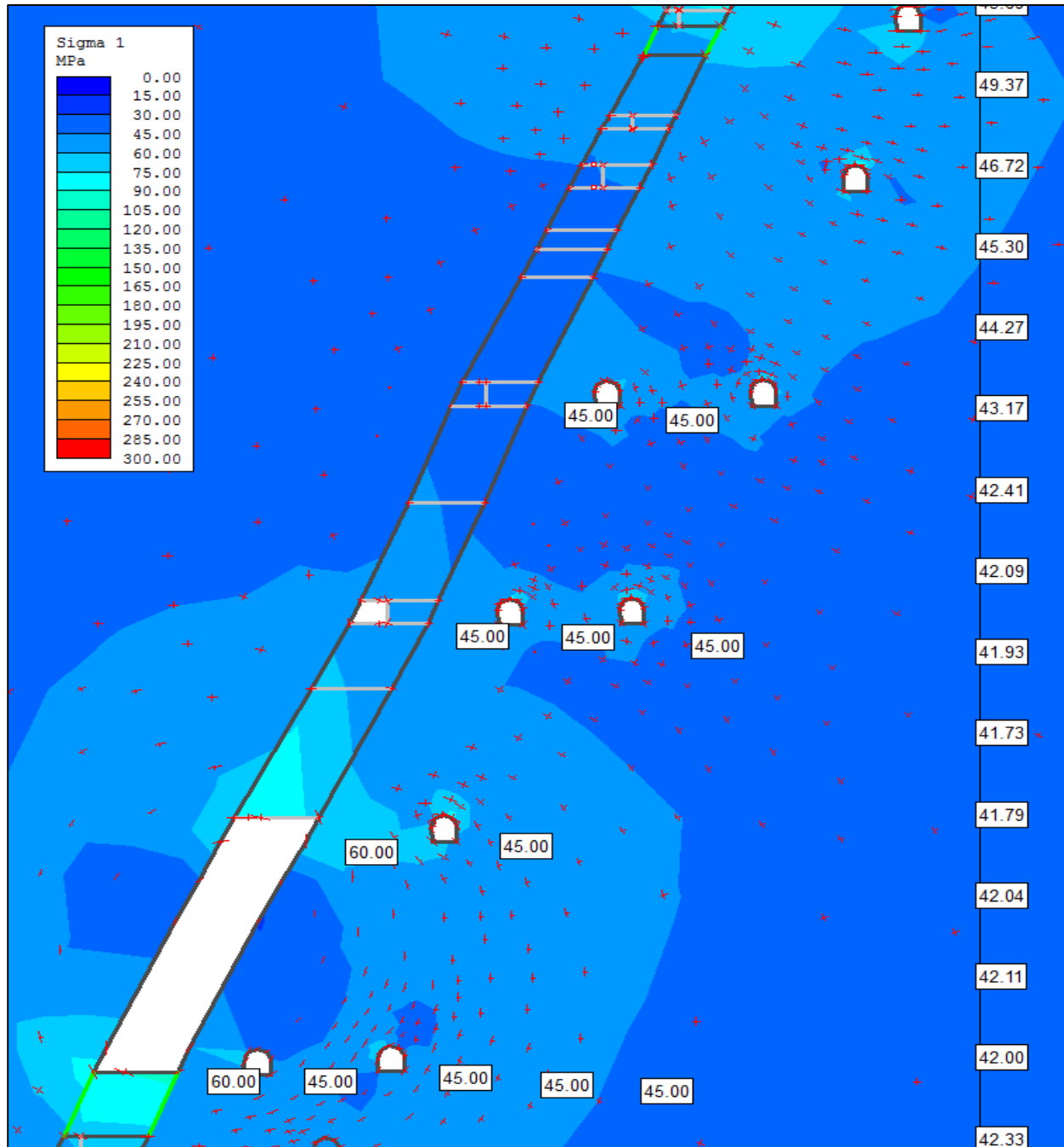


Figure 5.8 Section showing stress levels as VCR blasting advances upward at early stages of up dip mining (Results from MSV DEEPS stress analysis - GRAVITY, 2015).

Figure 5.9 shows excessive stress loading around the Ventilation drive as stope blasting progresses up dip. Note the stressing effect around the Ventilation drives on 4716 feet level and the distressing effect below 4881 feet level.

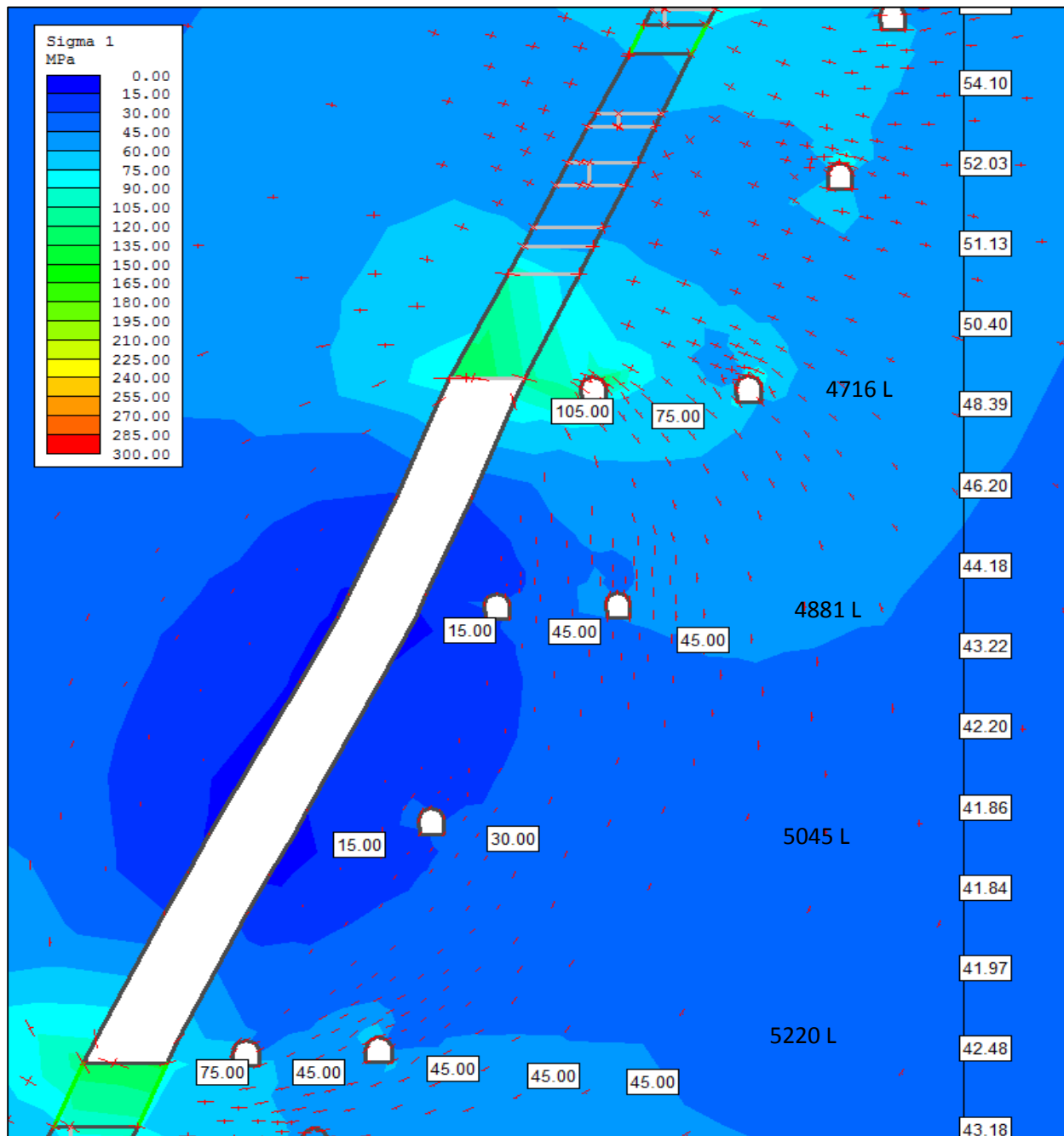


Figure 5.9 Excessive stress loading around the ventilation drive as stope blasting progresses up dip (Results from MSV DEEPS stress analysis - GRAVITY, 2015).

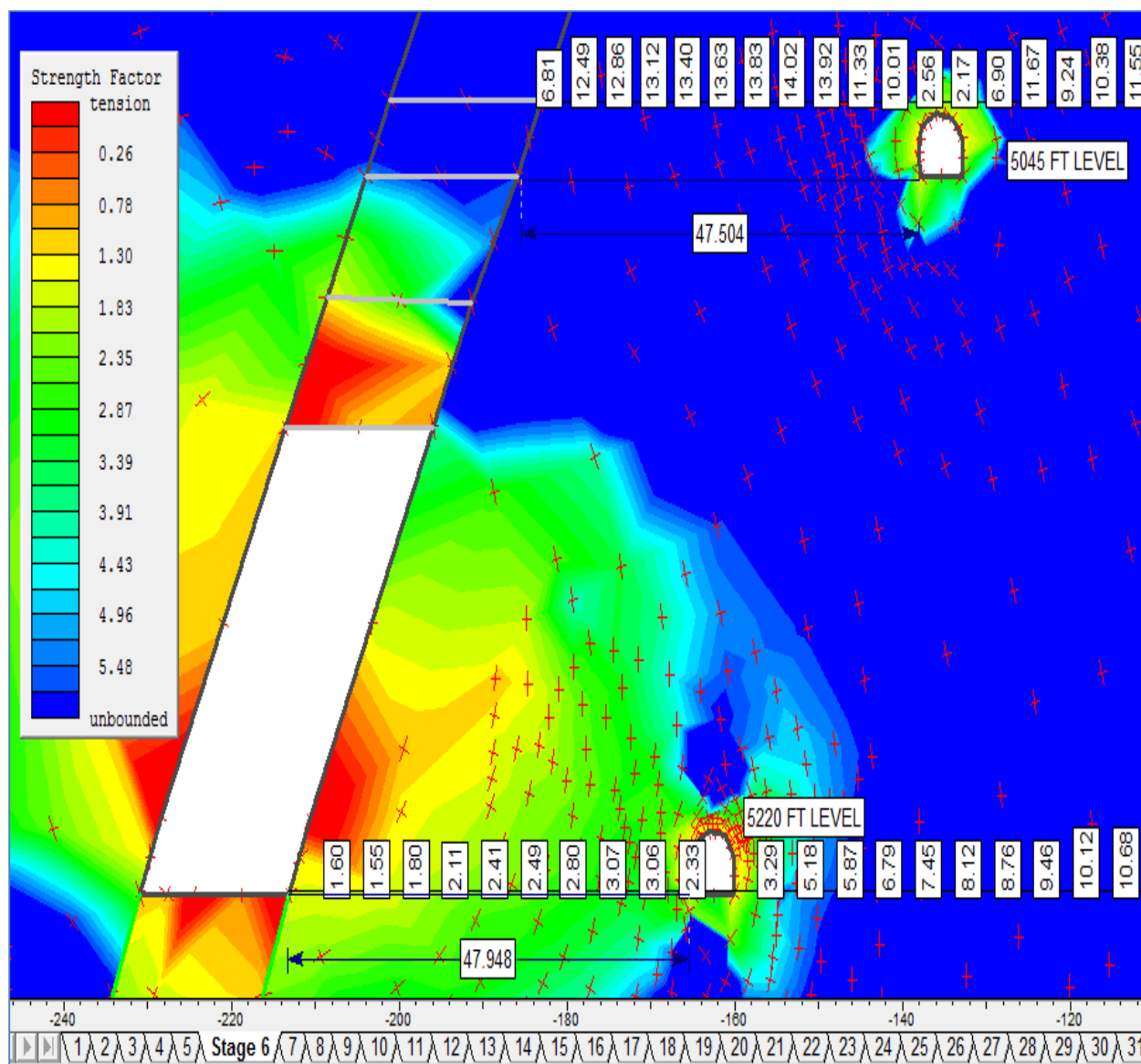


Figure 5.10 Levels of strength factors in the early stages of stoping between 5220 FT level and 5045 FT level (Results from Mindola Deeps Phase 2 stress analysis 2, 2016).

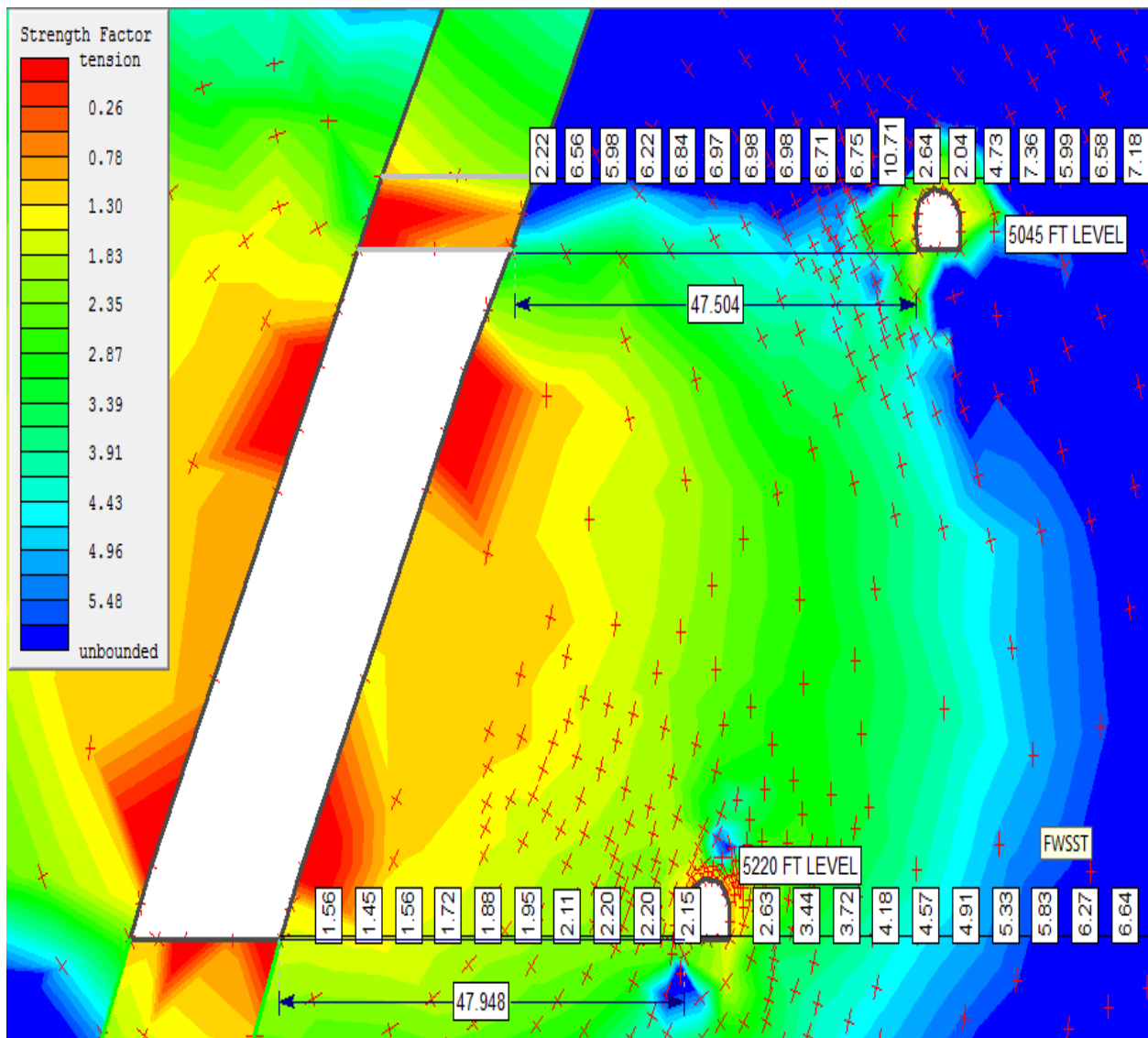


Figure 5.11 Strength factor levels in the late stages of stoping between 5220 FT level and 5045 FT level (Results from Mindola Deeps Phase 2 stress analysis 2, 2016).

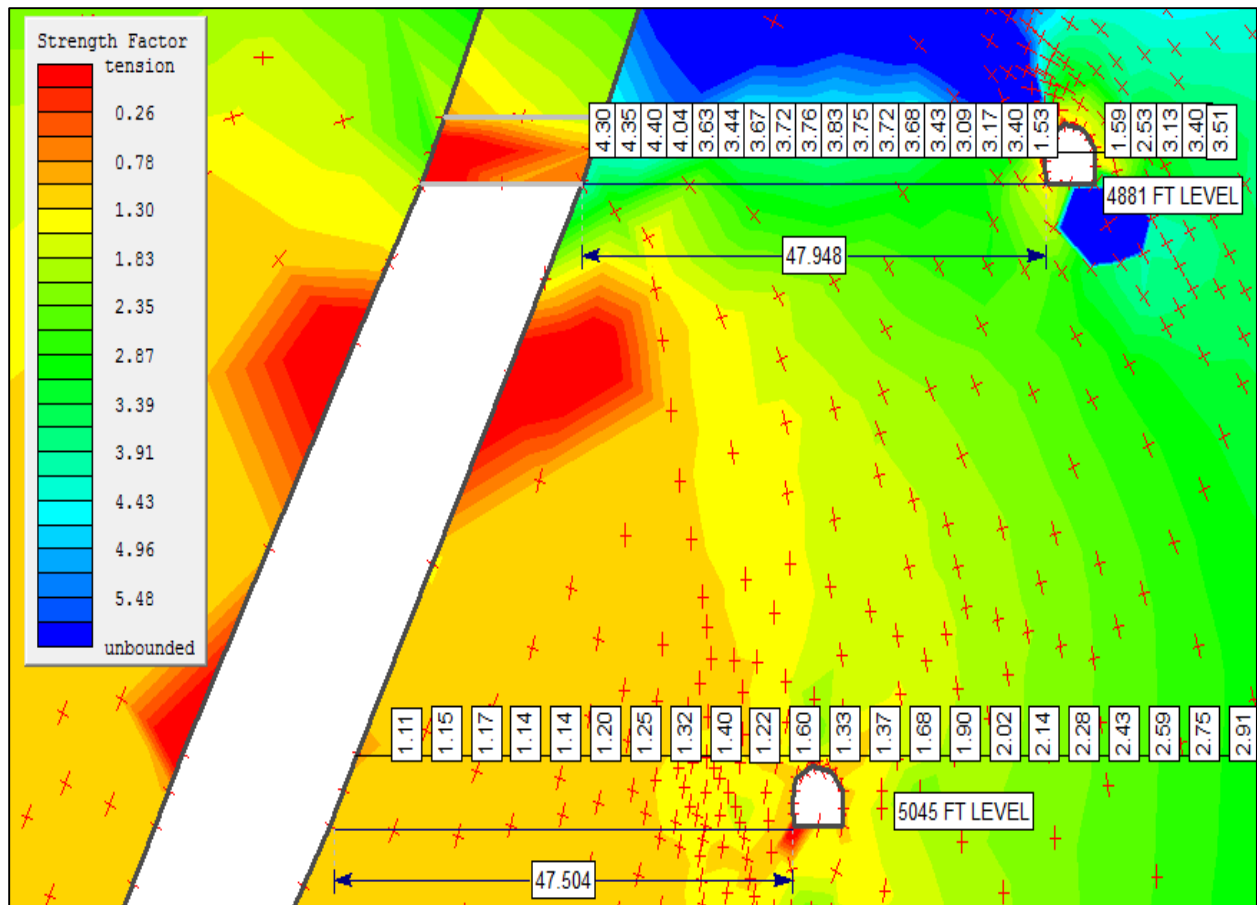


Figure 5.12 Levels of strength factors in the late stages of stoping on 5045 FT level (Results from Mindola Deeps Phase 2 stress analysis 2, 2016).

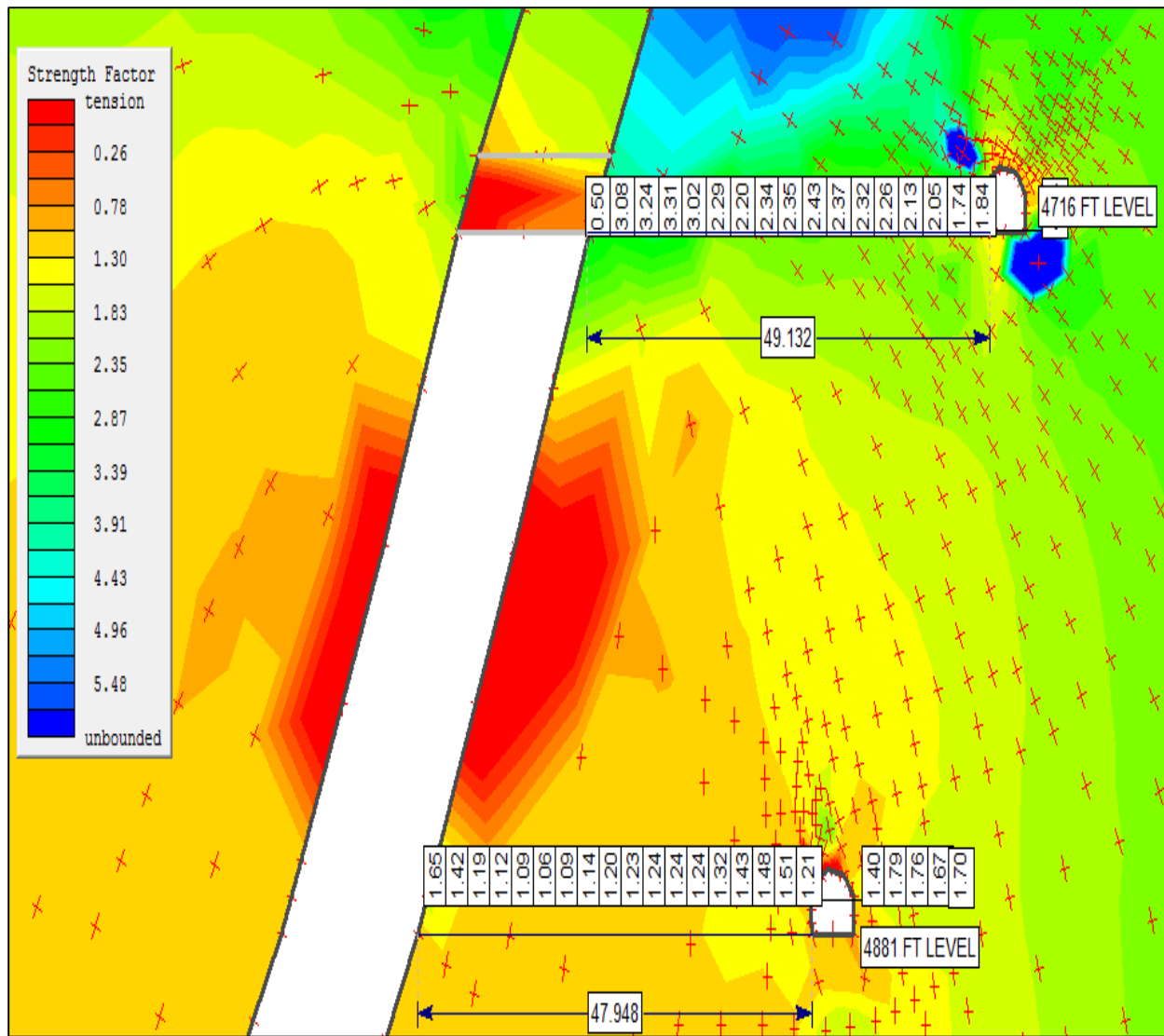


Figure 5.13 Strength factor levels in the late stages of stoping between 4881 FT level and 4716 Ft level (Results from Mindola Deeps Phase 2 stress analysis 2, 2016).

- a. Results of the numerical modelling in figure 5.8 indicate that stress conditions around the ventilation drives remains good in the early stages of mining.
- b. As the stopes are being extracted up dip, the ventilation drives and part of the cross cuts undergo stressing and distressing, of which both effects cause ground deterioration (see Figure 5.9).

- c. In the late stages of stoping from the draw level to the drilling level, the strength factor at the draw levels ranges from 1.5 to 1.6 at a distance between 47m and 49m (Figures 5.10, 5.11, 5.12 and 5.13).

5.2.2 Stopping echelon (Examine^{tab} – Stress analysis)

To determine a suitable stoping echelon for the Deeps section, Examine^{tab} a 3D displacement – discontinuity program for calculating stresses and displacements around tabular ore bodies was used. A model was generated by taking a dip plan of the whole mine area. Input data included modulus of elasticity of the orebody, unit weight, poissons ratio, depth, thickness and dip of the ore body. The results are in form of Normal Stress and Displacement in the rock surrounding the excavation in question.

5.2.2.1 Examine^{tab} Results at no lead/ lag distance

Figure 5.14 shows Examine^{tab} results displaying the effect of normal stress redistribution in areas adjacent to excavation boundaries on no lead/lag distance between the adjacent upper and lower advancing stoping faces.

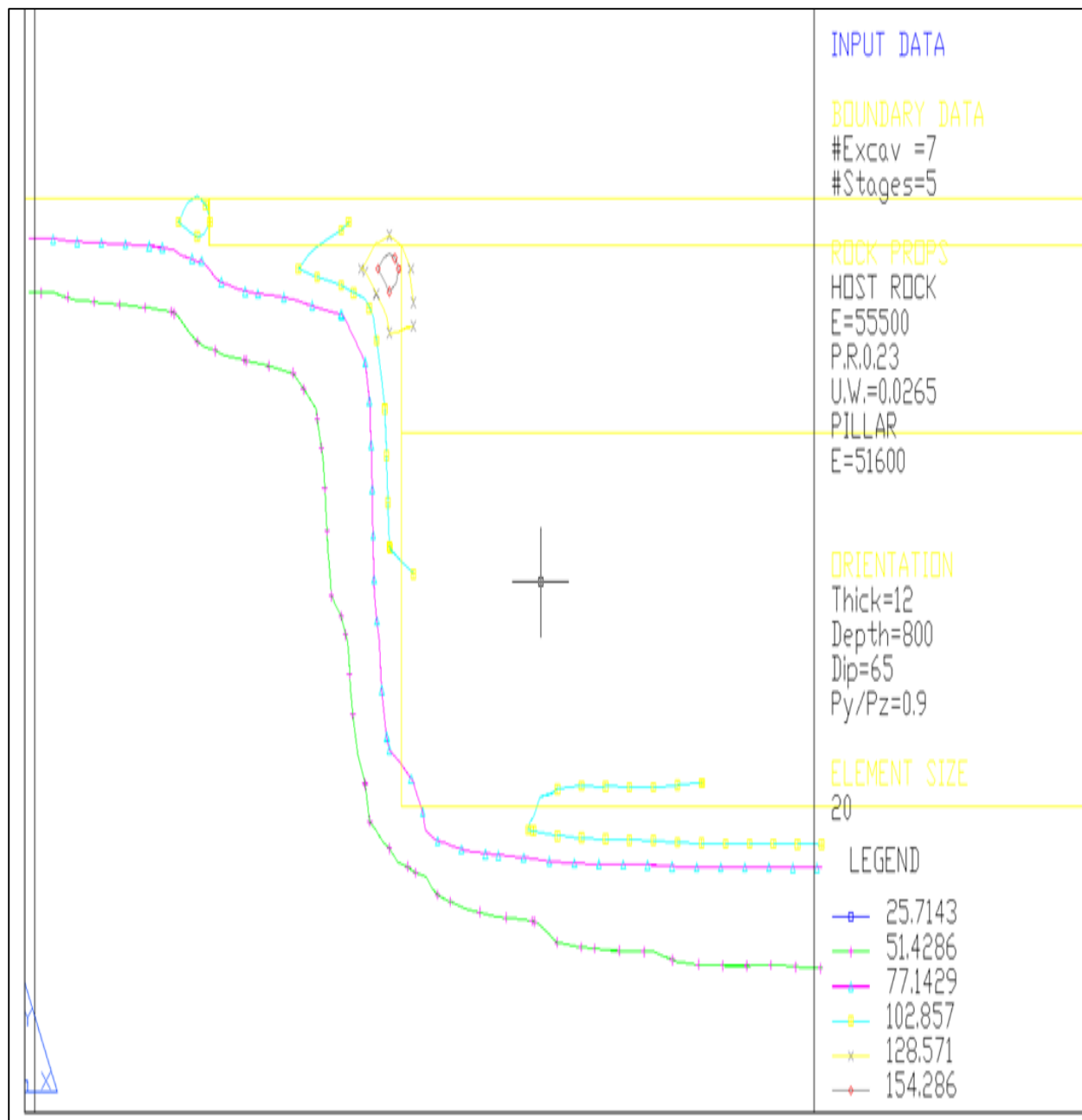
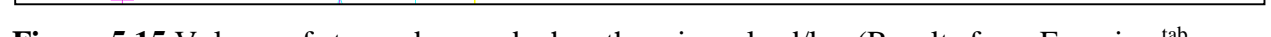


Figure 5.14 No lead/lag, contours of stress levels. Note very high stress levels in the corner of the block not mined (Results from Examine^{tab} MSV Stress analysis, 2015).

- a. The portion of rock in the corner of the block not mined is subjected to very high stress levels.



5.2.2.2 Examine^{tab} Results at 30m lead/ lag distance

Figure 5.16 shows the effect of normal stress redistribution in areas adjacent to excavation boundaries on 30m lead/lag distance between the adjacent upper and lower advancing stopping faces.

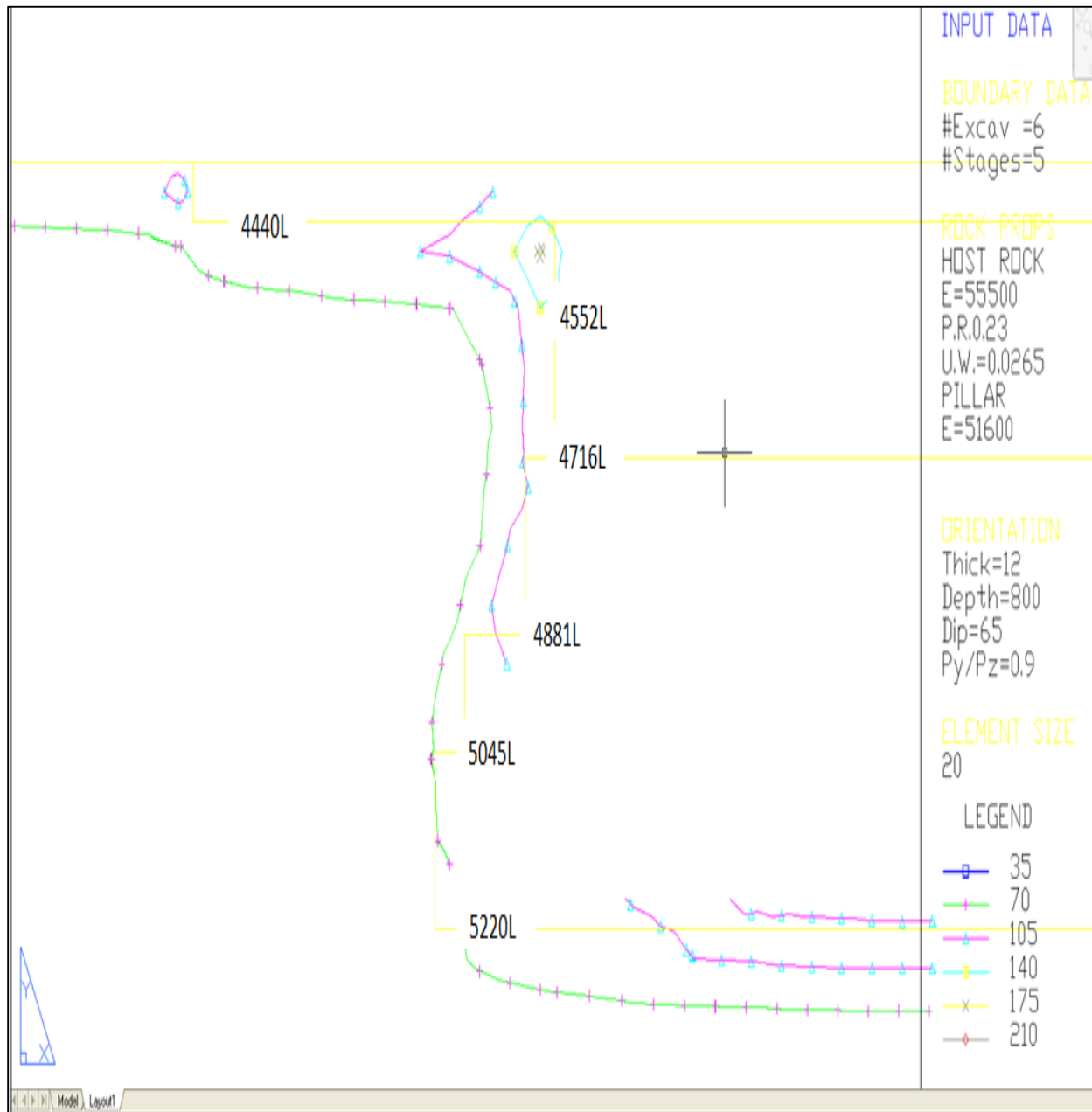


Figure 5.16 Contours of normal stress levels at 30m lead/lag (Results from Examine^{tab} MSV Stress analysis, 2015).

Figure 5.17 shows the volume of stressed rock in areas adjacent to excavation boundaries on 30m lead/lag distance between the adjacent upper and lower advancing stopping faces.

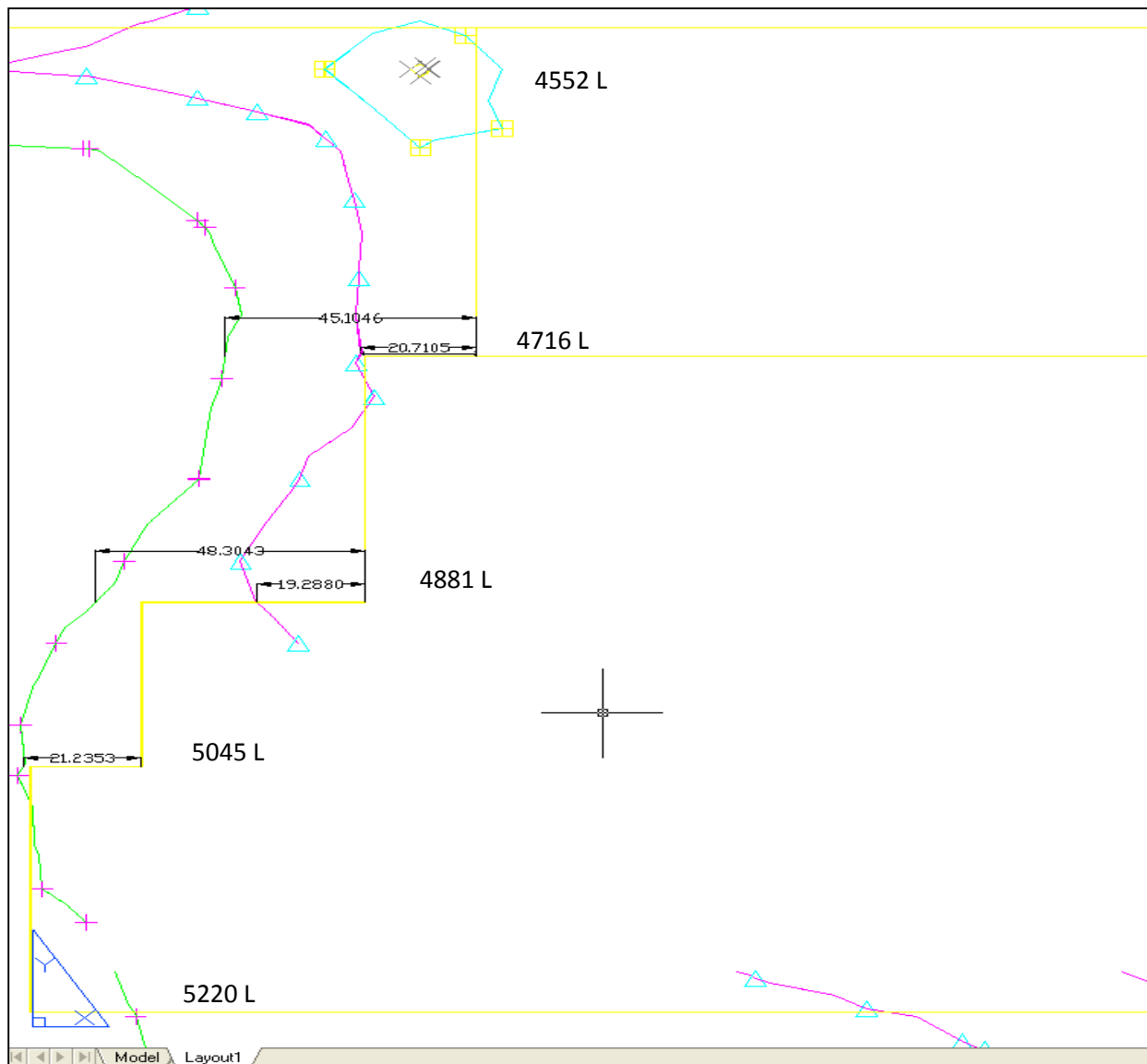


Figure 5.17 Volume of stressed ground with short lead/lag distance (30m) (Results from Examine^{tab} MSV Stress analysis, 2015).

a. 4716 feet level

From 45.1m to 20.7m, the normal stress levels range from 70MPa to 105MPa.

From 20.7m to the face, the normal stress levels range from 105MPa to 175MPa.

b. 4881 feet level

From 48.3m to 19.3m, the normal stress levels range from 70MPa to 105MPa.

From 19.3m to the face, the normal stress levels range from 105MPa to 175MPa.

c. 5045 feet level

From 21.2m to the face, the normal stress levels range from 70MPa to 105MPa.

d. 5220 feet level

From rock mass to the face, the normal stress levels range from 47MPa (Virgin Stress) to 70MPa.

5.2.2.3 Examine tab Results at 120m lead/ lag distance

Figure 5.18 shows the effect of normal stress redistribution in areas adjacent to excavation boundaries on 120m lead/lag distance between the adjacent upper and lower advancing stoping faces.

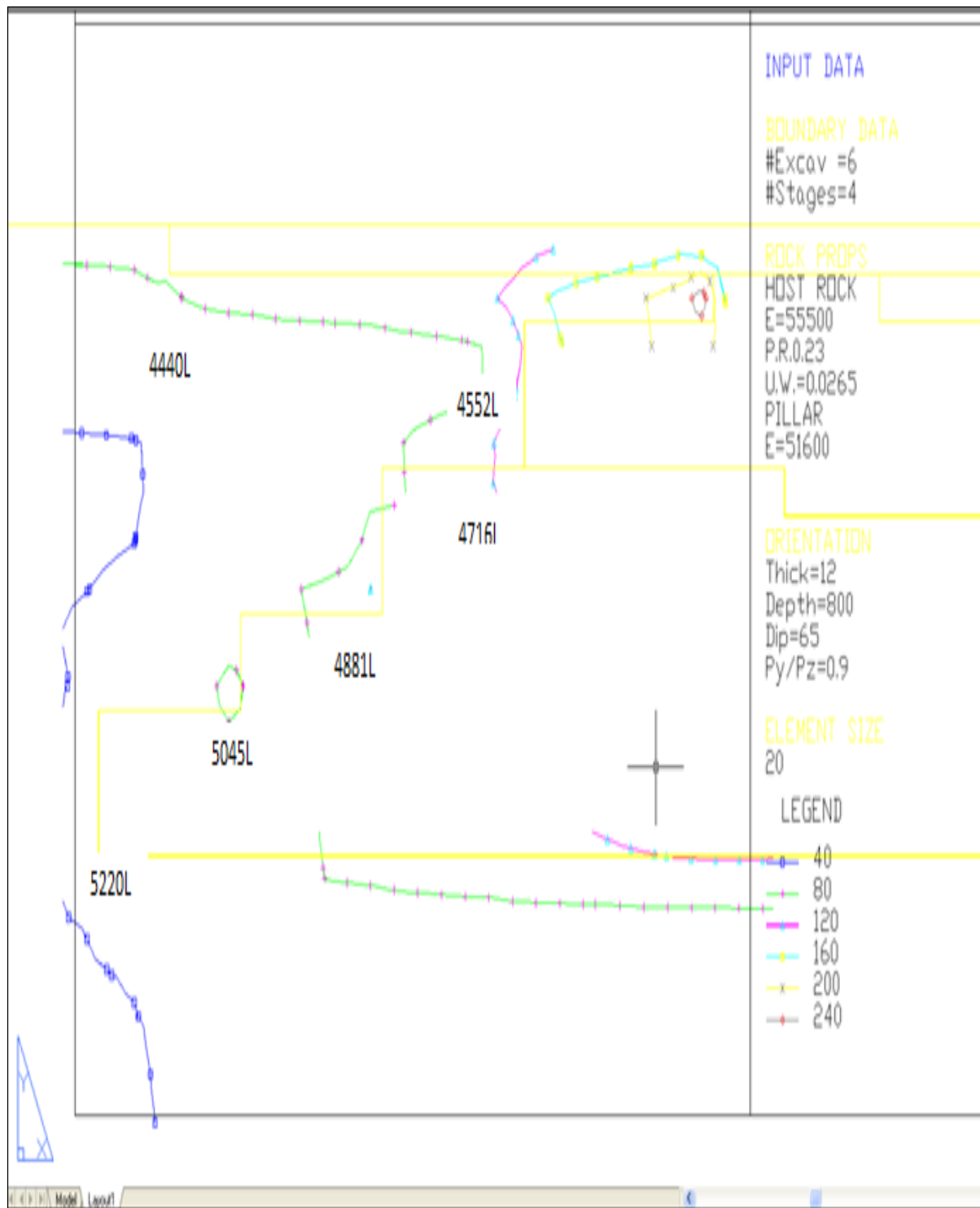


Figure 5.18 Contours of stress levels at 120m lead/lag (Results from Examine^{tab} MSV Stress analysis, 2015).

Figure 5.19 shows the volume of stressed rock in areas adjacent to excavation boundaries on 120m lead/lag distance between the adjacent upper and lower advancing stopping faces.

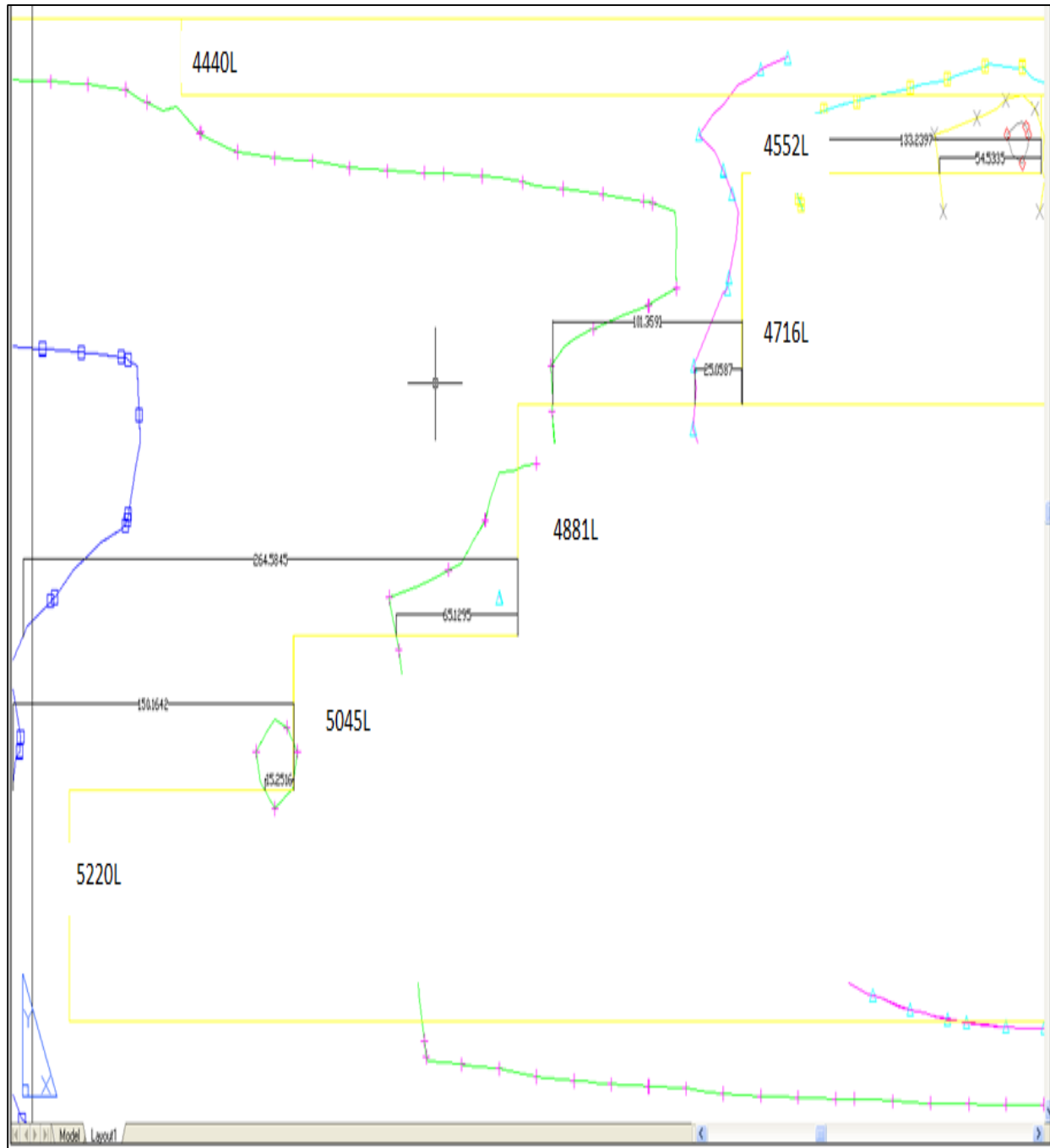


Figure 5.19 Volume of stressed ground with long lead/lag distance (120m) (Results from Examine^{tab} MSV Stress analysis, 2015).

a. 4552 feet level

From 133.24m to 54.53m (78.81m), the normal stress levels ranges from 160MPa to 200MPa. In this zone the rock is highly stressed and fracturing especially on excavation edges will take place.

From 54.53m to the face, the normal stress ranges from 200MPa to 240MPa. This zone is excessively stressed and crushing will take place.

b. 4716 feet level

From 101.36m to 25.05m (76.31m), the normal stress levels ranges from 80MPa to 120MPa. This zone is prone to fracturing.

From 25.05m to the face, the stress levels ranges from 120MPa to 160MPa. Fracturing especially on excavation edges is expected to takes place.

c. 4881 feet level

From 264.58m to 65.13m (199.45m), the stress levels ranges from 40MPa to 80MPa. The rock is partly in virgin stress.

From 65.13m to the face, the normal stress levels ranges from 80MPa to 120MPa. The rock in this zone is prone to fracturing.

d. 5045 feet level

From 150.16m to 15.25m (134.91m), the normal stress ranges from 40MPa to 80MPa.

From 15.25m to Face, the stress levels ranges from 80MPa to 120MPa. The rock in this zone is prone to fracturing.

e. 5220 feet level

From rock mass to the face, the normal stress levels ranges from 47MPa (Virgin Stress) to 80MPa.

CHAPTER 6

CONCLUSIONS AND RECOMMENDATIONS

6.1 Conclusions

Based on the main objective and sub objectives set in the study, the following conclusions have been drawn:

- a. From the stability graph method, it is indicated that a 16m wide Vertical Crater Retreat (VCR) chamber is stable if mined to a span length of 25m and supported with cable bolts and reinforced shotcrete. From the cost analysis done, it is evident that the proposed cable bolt support pattern will reduce support cost by 39.3% per ring. From the Phase 2 results, at a distance of about 48m from the ore body, the increase and decrease in stress levels as stoping advances up dip in the first three lifts, is not very significant and the safety factor is about 1.51, hence the stability of the excavation located at this distance and beyond is certain. High stress loading is experienced in the rock mass adjacent to the stoped out areas. Any excavation located within the zone of highly stressed rockmass may experience major instability before or during stope production.

The above conclusion meets the main objective of the research.

The following conclusion relates to the sub objectives of the research project.

- b. From the study of the Rock Mass Rating of the Deeps section, it is concluded that the mining rock mass rating (MRMR) of the rock varies from 59% to 79% corresponding to the ore bearing Schistose and Cherty Ore structures respectively. Both of these constitute the lower portion of the ore body. This range of results represents fair to good ground conditions across the Deeps section. The Schistose ore has a very low compressive

strength, its rock mass strength is half that of the next weakest rock, the Low Grade Argillite. From underground observations (VCR) failure in most cases is initiated in this zone, and then propagates to stronger units over time. The Hanging wall Argillite is one of the strongest rock types with a Mining Rock Mass Rating (MRMR) of 72% and Rock Mass Strength (RMS) of 103 MPa. The orebody has some of the weakest bands, while the hanging wall and footwall of the orebody are relatively stronger.

- c. From the examine ^{tab} results, it is concluded that the volume of stressed rock in short lead/lag distances between two vertically aligned adjacent stoping faces is less than in long lead/lag distances. A retreat with a single vertical face has much less volume of overstressed rock than multiple stoping faces with long lead/lag distances. However, from the point of view of mining very high stope faces are not practical, as a vertical rock face is more susceptible to instability than an incline one even in less stressed rock. Since ground deterioration due to stress loading is time dependent, a large volume of the rock mass will remain overstressed and deteriorated over a long period of time prior to development and production, as compared to small volume of the rock mass, making ground condition difficult during the time of development and production.

6.2 Recommendations

- a. The stability of a 16m wide Vertical Crater Retreat (VCR) chamber is recommended to be mined at 25m strike length and supported with 6.0m long Cable bolts (mechanical anchored pre-tensioned barrel and wedge or 500mm thread end) installed on Tendon straps at 2m by 2m grid pattern. It is also recommended that 50-90mm fibre or mesh reinforced shotcrete be applied on the rock surface within the chamber. At a distance of about 48m from the orebody the increase and decrease in stress levels, as stoping advances up dip in the first

three lifts, is not very significant. It is therefore recommended that the Ventilation drives below 4552 feet level be located at 48m from the orebody's geological footwall contact.

- b. To avoid a large volume of rock remaining stressed over a long period of time, which may affect quality of the rock mass prior to development and production, it is recommended to maintain short lead/lag distances between stoping faces. The ideal distance would be one stope length (32m) for a 48m equal stope height, resulting into 58⁰ echelons (See Appendix B).

REFERENCES

- Australian Mining Consultants. (July 2000). "Mindola Deeps Review" Mindola mine, Zambia.
- Aydan, O. (1989). "The stabilisation of rock engineering structures by rock bolts". Geotechnical Engineering. Thesis. Nagoya, Nagoya: 202.
- Azzoni, A., La Berbera, G. and Zaninetti, A. (1995). "Analysis and prediction of rock falls using a mathematical model". International Journal of Rock Mechanics and Mining Science and Geomechanics abstracts. Vol. 32, No. 7. Pp. 709 – 724.
- Barton, N. R. and Choubey, V. (1977). "The shear strength of rock joints in theory and practice". Rock Mech. 10:1-54
- Barton, N.R., Lien, R. and Lunde, J. (1974). "Engineering Classification of Rock Masses for the Design of Tunnel Support". Rock. Mech. 6, 189 – 239.
- Bawden, W.F., (1992). "The Use of Rock Mechanics Principles in Canadian Underground Hard Rock Mines". Queen's University Course Notes.
- Bieniawski, Z. T. (1989). "Engineering rock mass classification: a complete manual for engineers and geologists in mining, civil and petroleum engineering". John Wiley & Sons, p 51- 107.
- Brady, B. and Brown, E. (1985). "Rock Mechanics for Underground Mining". George Allen & Unwin Ltd. Herts HP2 4TE, UK.
- Curran, J.H., Hammah, R.E and Yacoub, T.E. (2003). "Can numerical modelling tools assist in mine design?" The case of Golden Giant Mine. ISRM News Journal, Vol. 7, No. 3.
- Goodman, R.E. (1989). "Introduction to Rock Mechanics" Second edition, John Wiley and sons
- Hendron, A. J. (1968). Dynamic behaviour of rock masses "Rock Mechanics Engineering Practice". London: Eds. K.G. Stagg and O.C. Zienkiewicz, Wiley and sons.

- Hoek, E. and Brown, T. (1980). “Underground Excavations in Rock”. The Institution of Mining and Metallurgy, 44 Portland Place, London W1, England
- Hutchinson, D.J. and Diederichs, M.S. (1996). “Cable bolting in Underground Mines”. Bitech Publishers Ltd., Richmond, BC, Canada, p 177 – 235.
- Jack de la Vergue. (2000). “Hard Rock Miner’s Handbook” First edition, McIntosh Redpath Engineering
- Jing, L. (2003). “A review of techniques, advances and outstanding issues in numerical modelling for rock mechanics and rock engineering”. International Journal of Rock Mechanics and Mining Sciences 40(3):283–353
- Lang, T. and Bischoff, J. (1984). “Stability of reinforced rock structures”. In: ISRM Symposium: Design and Performance of Underground Excavation, Cambridge, England, Code 7669, p 11–18.
- Lang, T. and Bischoff, J. A. (1982). “Stabilization of rock excavations using rock reinforcement”. In: Proceedings 23rd Symposium on Rock Mechanics, Berkeley, California, USA, Code 1727, p 935–944.
- Langford, C.J. (2016). “Revisiting support optimization at the Driskos tunnel using a quantitative risk approach”. Hatch Mott MacDonald, British Columbia, Canada.
- Laubscher, D. H. (1990). “A Geomechanics Classification System for the Rating of Rock Mass in Mine Design”. J. S. Afr. Inst. Min. Metall., Vol. 90, no. 10. pp. 257 – 273.
- Law, A. M. (2005). “How to build valid and credible simulation models”. Proceedings of the 2005 Winter Simulation Conference, Tucson, U.S.A.

- Mathews, K.E. (1980). "Prediction of stable excavations for mining at depth below 1000m in hard rock". CANMET report DSS serial no. OSQ80-00081, DSS file no. 17SQ.23440-0-9020 (Ottawa: Dept. of Energy, Mines and Resources), 39p.
- Nickson, S.D (1992). "Cable support guidelines for underground hard rock mine operations". Mining and mineral process engineering. Thesis. British Columbia: 87-106
- OHMS. (2014). Strata Control Preparation Notes. "Excavation Stability". Open House Management Solution (Pty), Klerksdorp, South Africa.
- Parker, H., Hargraves, R. P. N., Ramsell, R. and Hawkins, A. (1973). "Strata reinforcement using the technique of long hole resin dowelling". The Mining Engineer, .pp.519-532. (Cited in Dwight 1982).
- Pellet, F. (1994). "Strength and deformability of jointed rock masses reinforced by rock bolts". Civil Engineering. Thesis. Lausanne, Institute of Technology: 206.
- Potvin, Y. (2014 Newsletter). "Ground Support System Optimization Project". Australian Centre for Geomechanics (ACG) Unpublished Document.
- Potvin, Y. and Milne, D. (1992). "Empirical cable bolt support design". Rock Support, (eds. Kaiser and McCreath), Rotterdam: A.A. Balkema, 269 - 275.
- Potvin, Y. (1988). "Empirical open stope design in Canada". Ph.D. Thesis, Dept. Mining and Mineral Processing, University of British Columbia, 343 p.
- Potvin, Y., Hudyma, M.R. and Miller, H. D.S. (1989). "Design guidelines for open stope support". CIM Bulletin, 82, (926), 53 - 62.
- Priest, S.D. (1985). "Hemispherical projection methods in rock mechanics". London: George Allen and Unwin, 124 p.

- Priest, S.D. and Hudson, J. A. (1981). "Estimation of discontinuity spacing and trace length using scan line surveys". *Int. J. of Rock Mech. and Min. Sciences & Geomech. Abstracts*, 18, 183 - 197.
- Schach. R., Garshol, K. and Heltzen, A. M. (1979). "Rock bolting A practical handbook". Wheaton and Co. Ltd., Exeter.
- Schmuck, C.H. (1979). "Cable bolting at the Homestake gold mine". *Mining Engineering*, December, 31, (12), 1677 - 1681.
- Schubert, P (1984). "The bearing capacity of fully grouted rock bolts at shearing joints". Thesis. Leoben, Montan: 176.
- Starfield, A. M. and Cundall, P. A. (1988). "Towards a methodology for rock mechanics modelling". *Int. J. Rock Mech. Min. Sci. Geomech.* Vol. 25, No. 3, 99–106.
- St. John, C.M. and Van Dillen, D.E. (1983). "Rock bolts: a new numerical representation and its application in tunnel design". *Rock Mechanics - Theory - Experiment - Practice. Proc. of the 24th U.S. Symposium on Rock Mechanics.* A.E.G. New York, 13-26.
- Sweby, G. (2014 article). "The use of numerical models for ground support systems optimization: applications, methods and challenges". Australian Centre for Geomechanics, the University of Western Australia, Perth, Western Australia, Australia.
- Thirukumaran, S. (2016). "A review of shear strength models for rock joints subjected to constant normal stiffness". Research Centre for Geomechanics and Railway Engineering, Australia.
- Unal, E. (1983). "Design guidelines and roof control standards for coal mine roofs". Ph.D. Thesis, Pennsylvania State University, 355 p.
- Wickham, G. E., Tiedemann, H. R. and Skinner, E. H. (1972). "Support determination based on geologic predictions". *Proc. North American Rapid Excavation and Tunneling Conf.*,

- Chicago, New York: Soc. Min. Engrs., Am. Inst. Min. Metall. Petr. Engineers, (eds. K.S. Lane and L.A. Garfield), 43 - 64.
- Windsor, C. R., Thompson, A. G. and Choi, S. K. (1988). "Rock reinforcement research for hard rock mining". Proc. WASM Conference 1988 - R&D for the Minerals Industry, Kalgoorlie, Australia, 113 - 221.
- Vasarhelyi, B. and Kovács, D. (2017 article). "Empirical methods of calculating the mechanical parameters of the rock mass" Periodica Polytechnic Civil Engineering.
- Zhang, L. (2015) "Determination and applications of rock quality designation (RQD)". Department of Civil Engineering and Engineering Mechanics, University of Arizona, Tucson, AZ, USA.

APPENDICES

Appendix A: Proposed stoping echelon and mining sequence.

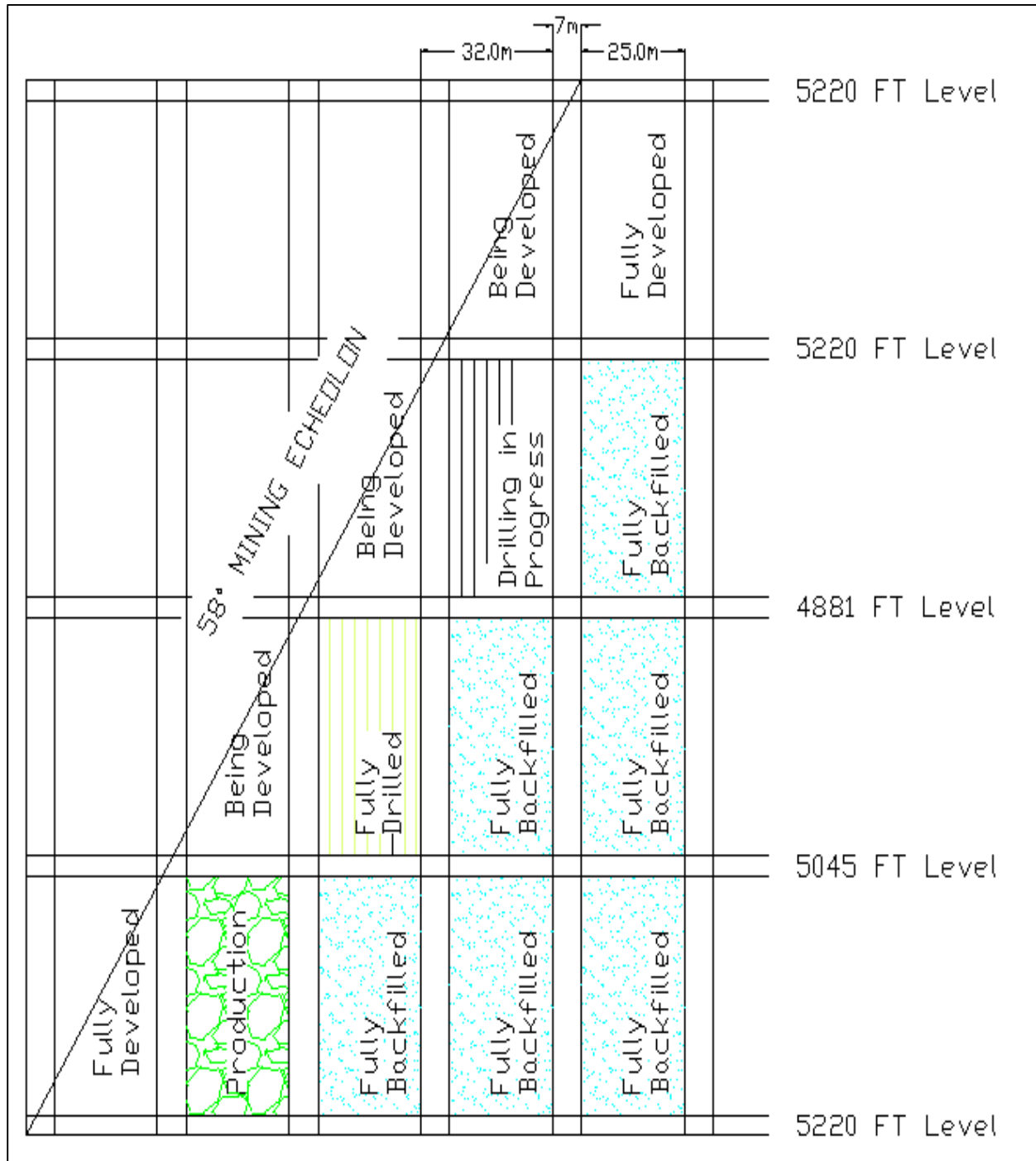


Figure 6.1 Proposed Stoping Echelon (58°) and Mining sequence.

Appendix B: Geotechnical and structural data collection log sheets.

The geotechnical core logging sheet for Nkana north.

															From	Hole Number:
															To	
															Rock Type	Domain Log
															Weathering (1-5)	
															Hardness (1-5)	page
															RQD	
															Jn	of
															Micro (1-9)	
															Macro (1-9)	
															Infill Type (1-9)	
															Structure Type	
															Total Fractures	
															Comments	

Figure 6.2 Geotechnical logging sheet (Mopani Nkana Rock Mechanics Office).

DESCRIPTION OF GEOTECHNICAL LOGGING CODES:

FROM – start of geotechnical domain

TO – end of geotechnical domain.

ROCK TYPE – as per Jundee terms

WEATHERING

1. Unweathered
2. Slightly
3. Moderately
4. Highly
5. Completely

HARDNESS

1. Very weak (0 – 5)
2. Weak (5 – 25)
3. Medium (25 – 50)
4. Strong (50 – 100)
5. Very Strong (100 – 250)

RQD

A standard value which is the sum of individual pieces of core greater than 100 mm divided by the length of the domain and expressed as a percentage.

NUMBER OF JOINT SETS

- 1 = 1 joint set
- 1+ = 1 set plus a random
- 2 = 2 joint sets

2+ = 2 joint sets plus a random

3 = 3 joint sets

3+ = 3 joint sets plus a random

4 = 4 joint sets

4+ = 4 joint sets plus a random

JOINT SURFACE

MICRO ROUGHNESS

1. Polished
2. Smooth planar
3. Rough planar
4. Slickensided undulating
5. Smooth undulating
6. Rough undulating
7. Slickensided stepped
8. Smooth stepped
9. Rough stepped/irregular

MACRO ROUGHNESS

1. Planar
2. Undulating
3. Curved
4. Irregular
5. Multi irregular

INFILLING TYPE

1. Gouge Thickness > Amplitude of Irregularities
2. Gouge thickness < Amplitude of Irregularities
3. Soft Sheared Material - Fine
4. Soft-Sheared Material - Medium
5. Soft-Sheared Material - Coarse
6. Non-Softening Material - Fine
7. Non-Softening Material - Medium
8. Non-Softening Material - Coarse
9. Clean

STRUCTURE TYPE

The most common or most unfavourable type of structure within the geotechnical domain, for example: Joint, Shear and Fault.

TOTAL FRACTURES

The number of natural breaks within the geotechnical domain.

CONVERSION TO Q TERMS

Jn (Joint Set Number)

If Number of Joint Sets = 1, Jn = 2

If Number of Joint Sets = 1+, Jn = 3

If Number of Joint Sets = 2, Jn = 4

If Number of Joint Sets = 2+, Jn = 6

If Number of Joint Sets = 3, Jn = 9

If Number of Joint Sets = 3, Jn = 9

If Number of Joint Sets = 3+, $J_n = 12$

If Number of Joint Sets = 4, $J_n = 15$

If Number of Joint Sets = 4 or more, $J_n = 15$

If the rock is crushed and/or earth like = $J_n = 20$

Jr (Joint Roughness)

If Micro = 1, then $J_r = 0.5$

If Micro > 1 -2, then $J_r = 1$ (for example, 1.5 or 2)

If Micro > 2 - 4, then $J_r = 1.5$ (for example, 2.5, 3, 3.5, 4)

If Micro >4-5, then $J_r = 2$

If Micro > 5-6, then $J_r = 3$

If Micro > 6-8, then $J_r=3.5$

If Micro > 8-9, then $J_r=4$

Ja (Joint Alteration)

If Infill Type = 1, then $J_a = 12$

If Infill Type = >1 - 2, then $J_a = 8$

If Infill Type = > 2 - 5, then $J_a = 4$

If Infill Type = > 5 - 8, then $J_a = 2$

If Infill Type = > 8-9, then $J_a =$

[illegible]

Appendix C: Rock Mass Rating System (After Bieniawski 1989).

Table 6.1 Rock Mass Rating System (After Bieniawski 1989), reproduced from Hoek, E. et al., 1995.

A. CLASSIFICATION PARAMETERS AND THEIR RATINGS									
Parameter			Range of values						
1	Strengt h of intact rock material	Point-load strength <small>index</small>	>10 MPa	4 - 10 MPa	2 - 4 MPa	1 - 2 MPa	For this low range - uniaxial compressive test is		
		Uniaxial comp. strength	>250 MPa	100 - 250 MPa	50 - 100 MPa	25 - 50 MPa	5 - 25 MPa	1 - 5 MPa	< 1 MPa
	Rating		15	12	7	4	2	1	0
2	Drill core <i>Quality RQD</i>		90% - 100%	75% - 90%	50% - 75%	25% - 50%	< 25%		
	Rating		20	17	13	8	3		
3	Spacing of discontinuities		> 2 m	0.6 - 2. m	200 - 600 mm	60 - 200 mm	< 60 mm		
	Rating		20	15	10	8	5		
4	Condition of discontinuities (See E)		Very rough surfaces Not continuous No separation Unweathered wall rock	Slightly rough surfaces Separation < 1 mm Slightly weathered walls	Slightly rough surfaces Separation < 1 mm Highly weathered walls	Slickensided surfaces or Gouge < 5 mm thick or Separation 1-5 mm Continuous	Soft gouge >5 mm thick or Separation > 5 mm Continuous		
	Rating		30	25	20	10	0		
5	Groun d water	Inflow per 10 m tunnel length (l/m)	None	< 10	10 - 25	25 - 125	> 125		
		(Joint water press)/ (Major principal □)	0	< 0.1	0.1, - 0.2	0.2 - 0.5	> 0.5		
		General conditions	Completely dry	Damp	Wet	Dripping	Flowing		
	Rating		15	10	7	4	0		
B. RATING ADJUSTMENT FOR DISCONTINUITY ORIENTATIONS (See F)									
Strike and dip orientations			Very favourable	Favourable	Fai r	Unfavourable	Very Unfavourable		
Ratings	Tunnels & mines		0	-2	-5	-10	-12		
	Foundations		0	-2	-7	-15	-25		

	Slopes	0	-5	-25	-50	
C. ROCK MASS CLASSES DETERMINED FROM TOTAL RATINGS						
Rating	100 □ 81	80 □ 61	60 □ 41	40 □ 21	< 21	
Class number	I	I I	II I	I V	V	
Description	Very good rock	Good rock	Fair rock	Poor rock	Very poor rock	
D. MEANING OF ROCK CLASSES						
Class number	I	I I	II I	I V	V	
Average stand-up time	20 yrs. for 15 m span	1 year for 10 m span	1 week for 5 m span	10 hrs. for 2.5 m span	30 min for 1 m span	
Cohesion of rock mass (kPa)	> 400	300 - 400	200 - 300	100 - 200	< 100	
Friction angle of rock mass (°)	> 45	35 - 45	25 - 35	15 - 25	< 15	
E. GUIDELINES FOR CLASSIFICATION OF DISCONTINUITY conditions						
Discontinuity length (persistence) Rating	< 1 m 6	1 - 3 m 4	3 - 10 m 2	10 - 20 m 1	> 20 m 0	
Separation (aperture) Rating	None 6	< 0.1 mm 5	0.1 - 1.0 mm 4	1 - 5 mm 1	> 5 mm 0	
Roughness Rating	Very rough 6	Rough 5	Slightly rough 3	Smooth 1	Slickensided 0	
Infilling (gouge) Rating	None 6	Hard filling < 5 mm 4	Hard filling > 5 mm 2	Soft filling < 5 mm 2	Soft filling > 5 mm 0	
Weathering Ratings	Unweathered 6	Slightly weathered 5	Moderately weathered 3	Highly weathered 1	Decomposed 0	
F. EFFECT OF DISCONTINUITY STRIKE AND DIP ORIENTATION IN TUNNELLING**						
Strike perpendicular to tunnel axis			Strike parallel to tunnel axis			
Drive with dip - Dip 45 - 90°	Drive with dip - Dip 20 - 45°		Dip 45 - 90°		Dip 20 - 45°	
Very favourable	Favourable		Very unfavourable		Fair	
Drive against dip - Dip 45-90°	Drive against dip - Dip 20-45°		Dip 0-20 - Irrespective of strike			
Fair	Unfavourable		Fair			

* Some conditions are mutually exclusive. For example, if infilling is present, the roughness of

the surface will be overshadowed by the influence of the gouge. In such cases use A.4 directly.

** Modified after Wickham et al (1972).

Appendix D: Phase 2 analysis information

Document Name

MSV DEEPS stress analysis 2015

Project Settings

General

Project Title: MSV DEEPS stress analysis - GRAVITY

Analysis: STRESS ANALYSIS

Comments: STRESS ANALYSIS GRAVITY METHOD DEEPS SECTION

Author: NOBLE CHIFWAILA

Company: MOPANI COPPER MINES PLC

Number of Stages: 40

Analysis Type: Plane Strain

Solver Type: Gaussian Elimination

Units: Metric, stress as MPa

Stress Analysis

Maximum Number of Iterations: 500

Tolerance: 0.001

Number of Load Steps: Automatic

Convergence Type: Absolute Energy

Tensile Failure: Reduces Shear Strength

Groundwater

Method: Piezometric Lines

Pore Fluid Unit Weight: 0.00981 MN/m³

Field Stress

Field stress: gravity

Ground surface elevation: 0 m

Unit weight of overburden: 0.027 MN/m³

Total stress ratio (horizontal/vertical in-plane): 1

Total stress ratio (horizontal/vertical out-of-plane): 1

Locked-in horizontal stress (in-plane): 0

Locked-in horizontal stress (out-of-plane): 0

Mesh

Mesh type: graded

Element type: 3 noded triangles

Number of elements on Stage 1: 3500

Number of nodes on Stage 1: 1766

Number of elements on Stage 2: 3471

Number of nodes on Stage 2: 1763

Number of elements on Stage 3: 3439

Number of nodes on Stage 3: 1759

Number of elements on Stage 4: 3423

Number of nodes on Stage 4: 1757

Number of elements on Stage 5: 3415

Number of nodes on Stage 5: 1755

Number of elements on Stage 6: 3405

Number of nodes on Stage 6: 1754

Material Properties

Material: HWA

Initial element loading: field stress & body force

Unit weight: 0.027 MN/m³

Elastic type: isotropic

Young's modulus: 55500 MPa

Poisson's ratio: 0.2

Failure criterion: Hoek-Brown

Material type: Elastic

Compressive strength 154 MPa

mb parameter: 11.562

s parameter: 0.1353

Piezo to use: None

Ru value: 0

Material: ORE SHALE

Initial element loading: field stress & body force

Unit weight: 0.027 MN/m³

Elastic type: isotropic

Young's modulus: 51600 MPa

Poisson's ratio: 0.2

Failure criterion: Hoek-Brown

Material type: Elastic

Compressive strength 109 MPa

mb parameter: 2.375

s parameter: 0.0229

Piezo to use: None

Ru value: 0

Material: FWSST

Initial element loading: field stress & body force

Unit weight: 0.027 MN/m³

Elastic type: isotropic

Young's modulus: 68750 MPa

Poisson's ratio: 0.3

Failure criterion: Hoek-Brown

Material type: Elastic

Compressive strength 183 MPa

mb parameter: 10.147

s parameter: 0.1211

Piezo to use: None

Ru value: 0

Appendix E: Mindola Sub Vertical Shaft Succession

Mopani Copper Mines Plc.

Nkana Mine Site

Mindola Sub Vertical Shaft Succession

Table 6.2 Geotechnical parameters of different rock formations at Mindola's Deeps section (Mopani Rock mechanics office)

Rock Type	Compressive Strength (MPa)	Rock Quality Designation (RQD)	Young Modules (MPa)	Poisson's Ratio	Specific Gravity For Ore
Lower Conglomerate	170	80-100	76000	0.25	
Basal Quartzite	190	-			
Basal Conglomerate	-	-	-	-	-
Basement	150	-	-	-	-
Footwall Quartzite	220	80- 100	66000	0.24	
Footwall Sandstone	190	75-100	70000	0.26	
Footwall Conglomerate	140	90-100	63000	0.19	
Footwall Quartzite	220	-	-	-	-
Schistose Ore	50	30-40	47000	0.38	2.56
Low Grade Argillite	110	15-70	61000	0.25	2.56
Banded Ore	105	25-100	53000	0.20	2.56
Cherty Ore	170	30-100	49000	0.18	2.56
No1 Marker	110	40	48000	0.25	2.56
Porous Sandstone	130	30-50	48000	0.25	2.56
Hanging wall Argillite	190	0-50	63000	0.21	2.56

Near Water Sediment	100	-	-	-	-
Mineralized Argillite	190	-	-	-	2.56
Pebble Marker	160	-	-	-	-

Appendix F: Procedure for Mining and Supporting the Vertical crater Retreat (VCR) chamber

Procedure for Mining and Supporting VCR drilling Chamber

1. Mine the two cross cuts up to the AHW and support with 2.4m roof bolts.
2. Mine the VCR hanging wall drive to connect the two cross cuts and support with 6m/10m cable bolts after 2.4m roof bolts.
3. After the cross cuts within the ore body and the hanging wall drive have been cable bolted, slyping to enlarge the chamber up to bull nose position can then commence with installation of 2.4m roof bolts close (1m) to the advancing face.
4. Install wire mesh and tendon straps and complete cable bolt installation in the slyped area.

Development: Vertical crater retreat hanging wall drive

Ground condition: some weak fissile rock units. Gradual stress build up (fracture) with time

Size: 4.0mH x 4.0-6mW

Support

1. Temporary Support (during support grouting and face charging) (J/H)
 - a. Wire mesh as safety net
 - b. Mechanical props (Minimum: 4 props Size H8)

2. Permanent Support (Sketch)

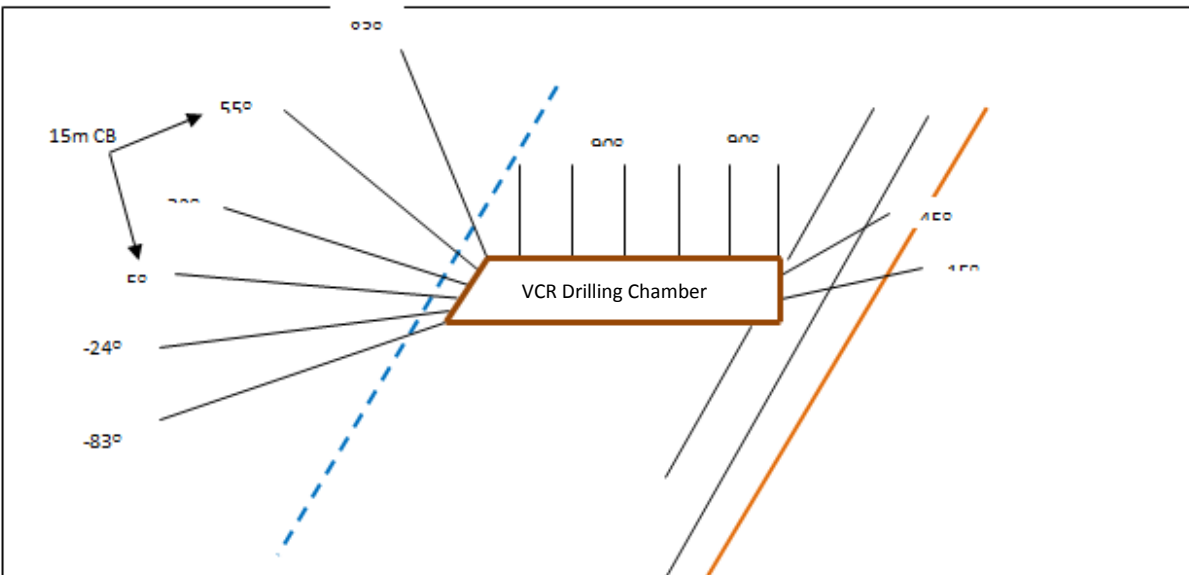


Figure 6.4 A ring of cable bolt support in a Vertical Crater Retreat (VCR) chamber (Mopani Nkana Rock Mechanics Office).

1. 2.4m long Split sets/grouted roof bolts with face plate and nut.
2. Rock bolts per ring = varying
3. Bolt spacing within ring = 1.0m
4. Ring spacing along strike = 1.0m

All holes **MUST** be drilled as much perpendicular to rock surface as possible

5. Maximum allowable unsupported span (during drilling and charging = 0.5m from the advancing face.
3. 25Ton x 6.5m long Cable bolts (mechanical anchored pre-tensioned barrel & wedge or 500mm thread end)
 - a. Number of 6.5m Cable bolts per ring 2
 - b. Bolt collar spacing within ring is 1.5m
 - c. Ring spacing is 2.0m

Compliance: Cable bolt installation prior to commencement of VCR slying.

Development: VCR Drilling Chamber (slyping)

Ground condition: Gradual stress build up with time

Size: 4.0mH – width varies

Support

1. Temporary Support (during support grouting and face charging) (J/H)
 - a. Wire mesh as safety net
 - b. Mechanical props (Minimum: 4 props Size H8)
2. Permanent Support (Sketch)

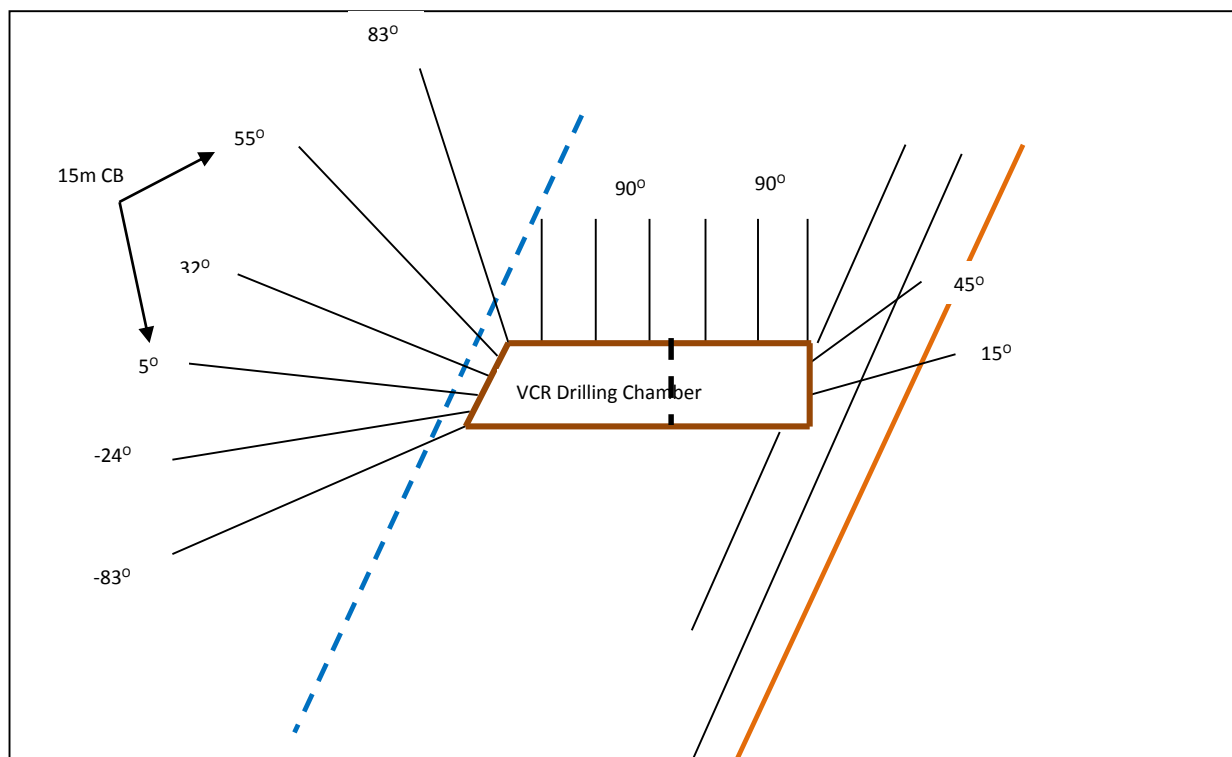


Figure 6.5 A ring of cable bolt support in a Vertical Crater Retreat (VCR) chamber (Mopani Nkana Rock Mechanics Office).

1. 2.4m Split sets/Long grouted roof bolts with face plate and nut.

2. Rock bolts per ring about 13(varies)
3. Bolt spacing within ring is 1.0m
4. Ring spacing along strike is 1.0m

All holes MUST be drilled as much perpendicular to rock surface as possible.

5. Maximum allowable unsupported span (during drilling and charging) = 0.5m from the advancing face.
3. 4mm x 1.8m wide x 15m long Diamond Wire mesh
Wire mesh to be installed tight against excavation surface along drive axis with 300mm overlap.
Maximum unsupported span for wire mesh –10m from the advancing face (or else in poor ground max. 5.0m from the advancing face).
4. Tendon Straps
2x6m tendon straps per ring every 2m, spaced across the axis of the drive, installed tight against excavation surface, on cable bolt ring.
Maximum unsupported span to be 10m from the advancing face (or else in poor ground to be 5.0m from the advancing face)
5. 25Ton x 6.5m long Cable bolts (mechanical anchored pre-tensioned barrel & wedge or 500mm thread end)
 - a. Cable bolts per ring to be 8(vary)
 - b. Bolt collar spacing within ring to be 2.0m
 - c. Ring spacing to be 2.0m

Compliance: Cable bolt installation to be installed in stages after slyping.

6. 25Ton x 15.5m long Hanging wall Cable bolts (mechanical anchored pre-tensioned barrel & wedge or 500mm thread end) installed on Tendon straps
 - a. Cable bolts per ring to be 6
 - b. Bolt collar spacing within ring to be 1.0m
 - c. Ring spacing to be 2.0m
7. 50mm Plain Shotcrete

To be applied as when required.

Appendix H: Joint Survey collected data

5220 level 1610 Chamber Cross Cut 1 side

Dip(°)	Dip direction (°)	Spacing, m	Type	Shape	aperture
80	256	1.23	Joint	SP	Closed
34	213	1.05	Bedding	RP	Closed
60	312	1.25	bedding	SP	Open
55	310	0.55	Joint	SP	Open
60	278	1.89	bedding	SP	Closed
68	065	2.69	bedding	SP	Closed
55	197	1.58	bedding	SP	Open
55	187	0.98	bedding	SP	Open
60	220	0.99	Joint	SP	Open
60	215	1.00	Joint	RP	Closed
65	214	0.56	bedding	RP	Closed
60	204	0.68	bedding	RP	Closed

56	213	0.65	bedding	RP	Closed
67	187	1.58	Joint	RP	Open
70	312	1.50	bedding	RP	Open
55	220	1.90	bedding	RP	Closed
35	245	2.00	Joint	RP	Closed
55	149	1.05	Joint	RP	Open
55	234	1.10	bedding	RP	Open
57	237	0.23	bedding	RP	Open
58	311	0.65	bedding	SP	Open
60	259	0.99	bedding	SP	Open
60	260	1.70	bedding	SP	Open
60	300	1.70	Joint	SP	Closed
70	200	1.42	Joint	SP	Closed
70	190	1.55	Joint	RP	Closed
70	165	1.23	Joint	RP	Closed
45	256	2.22	Joint	RP	Open
54	256	1.88	Joint	RP	Open
56	256	0.56	Joint	RP	Closed
65	234	0.47	Joint	RP	Closed
65	245	0.45	bedding	RP	Closed
65	217	0.32	bedding	RP	Closed
65	218	0.65	Joint	RP	Open
68	211	0.78	Joint	RP	Open

55	251	0.50	Joint	RP	Closed
----	-----	------	-------	----	--------

5220 level, 1750 Chamber Cross Cut 2 side

Dip(°)	Dip direction (°)	Spacing, m	Type	Shape	aperture
55	222	1.23	Joint	SP	Closed
60	208	1.05	Bedding	RP	Closed
80	234	1.25	bedding	SP	Open
78	234	0.55	Joint	SP	Open
45	213	1.89	bedding	SP	Closed
65	213	2.69	bedding	SP	Closed
65	216	1.58	bedding	SP	Open
65	217	0.98	bedding	SP	Open
86	256	0.99	Joint	SP	Open
73	311	1.00	Joint	RP	Closed
45	312	0.56	bedding	RP	Closed
76	324	0.68	bedding	RP	Closed
67	300	0.65	bedding	RP	Closed
67	309	1.58	Joint	RP	Open
67	320	1.50	bedding	RP	Open
55	326	1.90	bedding	RP	Closed
55	176	2.00	Joint	RP	Closed
60	197	1.05	Joint	RP	Open
60	187	1.10	bedding	RP	Open

60	194	0.23	bedding	RP	Open
65	234	0.65	bedding	SP	Open
65	287	0.99	bedding	SP	Open
65	298	1.70	bedding	SP	Open
60	256	1.70	Joint	SP	Closed
45	211	1.42	Joint	SP	Closed
54	100	1.55	Joint	RP	Closed
53	200	1.23	Joint	RP	Closed
53	209	2.22	Joint	RP	Open
45	223	1.88	Joint	RP	Open
59	226	0.56	Joint	RP	Closed
50	109	0.47	Joint	RP	Closed
54	112	0.45	bedding	RP	Closed
44	234	0.32	bedding	RP	Closed
66	158	0.65	Joint	RP	Open
45	254	0.78	Joint	RP	Open
87	233	0.50	Joint	RP	Closed

5045 level, 1380 chamber Cross Cut 1 side from the geological footwall contact

Dip(°)	Dip direction (°)	Spacing, m	Type	Shape	aperture
55	176	1.23	Joint	SP	Closed
60	197	1.05	Bedding	RP	Closed
60	187	1.25	bedding	SP	Open

60	194	0.55	Joint	SP	Open
65	234	1.89	bedding	SP	Closed
65	287	2.69	bedding	SP	Closed
65	298	1.58	bedding	SP	Open
60	256	0.98	bedding	SP	Open
45	211	0.99	Joint	SP	Open
54	100	1.00	Joint	RP	Closed
53	200	0.56	bedding	RP	Closed
53	209	0.68	bedding	RP	Closed
45	223	0.65	bedding	RP	Closed
59	226	1.58	Joint	RP	Open
50	109	1.50	bedding	RP	Open
54	112	1.90	bedding	RP	Closed
44	234	2.00	Joint	RP	Closed
66	158	1.05	Joint	RP	Open
45	254	1.10	bedding	RP	Open
87	233	0.23	bedding	RP	Open
55	176	0.65	bedding	SP	Open
60	197	0.99	bedding	SP	Open
60	187	1.70	bedding	SP	Open
60	194	1.70	Joint	SP	Closed
65	234	1.42	Joint	SP	Closed
65	287	1.55	Joint	RP	Closed

65	298	1.23	Joint	RP	Closed
60	256	2.22	Joint	RP	Open
45	211	1.88	Joint	RP	Open
54	100	0.56	Joint	RP	Closed
53	200	0.47	Joint	RP	Closed
53	209	0.45	bedding	RP	Closed
45	223	0.32	bedding	RP	Closed
59	226	0.65	Joint	RP	Open
50	109	0.78	Joint	RP	Open
54	112	0.50	Joint	RP	Closed

4881 level, 1270 chamber Cross Cut 2 side

Dip(°)	Dip direction (°)	Spacing, m	Type	Shape	aperture
67	187	1.23	Joint	SP	Closed
70	312	1.05	Bedding	RP	Closed
55	220	1.25	bedding	SP	Open
35	245	0.55	Joint	SP	Open
55	149	1.89	bedding	SP	Closed
55	234	2.69	bedding	SP	Closed
57	237	1.58	bedding	SP	Open
58	311	0.98	bedding	SP	Open
60	259	0.99	Joint	SP	Open
60	260	1.00	Joint	RP	Closed

60	300	0.56	bedding	RP	Closed
70	200	0.68	bedding	RP	Closed
70	190	0.65	bedding	RP	Closed
70	165	1.58	Joint	RP	Open
45	256	1.50	bedding	RP	Open
54	256	1.90	bedding	RP	Closed
56	256	2.00	Joint	RP	Closed
65	234	1.05	Joint	RP	Open
65	245	1.10	bedding	RP	Open
65	217	0.23	bedding	RP	Open
65	218	0.65	bedding	SP	Open
68	211	0.99	bedding	SP	Open
55	251	1.70	bedding	SP	Open
67	187	1.70	Joint	SP	Closed
70	312	1.42	Joint	SP	Closed
55	220	1.55	Joint	RP	Closed
35	245	1.23	Joint	RP	Closed
55	149	2.22	Joint	RP	Open
55	234	1.88	Joint	RP	Open
57	237	0.56	Joint	RP	Closed
58	311	0.47	Joint	RP	Closed
60	259	0.45	bedding	RP	Closed
60	260	0.32	bedding	RP	Closed

60	300	0.65	Joint	RP	Open
70	200	0.78	Joint	RP	Open
70	190	0.50	Joint	RP	Closed